Targeting alarmins to accelerate healing

Dr Geoffrey Lee

Christ Church

Supervisors

Professor Jagdeep Nanchahal

Professor Nicole Horwood

Dr James Chan

Trinity 2017

Thesis submitted for the degree of

Doctor of Philosophy in Molecular and Cellular Medicine

Acknowledgements

This four year DPhil program has been an epic experience and I am indebted to all those who have made it possible. It is the culmination of a seven year journey which has been full of serendipity, and positivity. Back in January 2012, I had just finished a wonderful medical elective term in balmy Darwin and outback Nhulunbuy, and was beginning to wonder why I had scheduled my second elective term to be in London, a city on the other side of the world, which was reportedly going through one of its harshest winters ever. Yet it was on this term that I happened to attend a conference at the Royal College of Surgeons, and in a side-corridor there was a poster by Dr James Chan detailing his double-life as a surgical registrar and as a basic scientist studying immunology and tissue regeneration. With his generous spirit, James met with me, took me up to Oxford to attend some student presentations, and shared his own clinician-scientist journey. I have him to thank for awakening my own nascent interest in this unique career path, and for all the ensuing years of guidance he has provided.

Despite the distance, Australia is evidently a popular business destination, because I subsequently met Sir Prof Marc Feldmann, and Prof Jagdeep Nanchahal when they were in Sydney attending meetings. I am ever grateful for Marc's support in helping me to attain the funding for this DPhil, and for his insightful reviews of my work throughout this DPhil. To be supervised by Jagdeep has been a true privilege, and I am fortunate to have a mentor who has the ambitious attitude of always striving for more. We have passionate, animated, and thought provoking discussions, and he has given me the opportunity to be embedded in all the aspects of a modern basic science laboratory, from the design, execution, and analyses of experiments, to grant writing, rebuttal, and administration, to human and animal ethical applications, to national and international presentations, to involvement in institutional scientific board reviews, and the exceptional freedom to initiate collaborations. He has provided me with the tools and broad scientific foundations needed to become an independent investigator and I look forward to fulfilling this potential in the future.

Efficiency and good teamwork are paramount for achieving the high amount of quality output that is necessary for a modern basic science project to be successful. To that end I am fortunate to have had the support of our post-doctoral scholar Dr Ana Espirito Santo. Her encouragement and wide experimental knowledge has allowed me to push through times of disappointment, exhaustion, and frustration, and has demonstrated how when two people have synergistic workflow they can produce much more than the sum of their parts. I have also been fortunate to be supported by the bone group, including Adel, Franzi, Lynette, Carlotta, and Houfu, and led by Prof Nicole Horwood. Nikki has been invaluable as a supervisor who has given me a thorough grounding in musculoskeletal biology, experimental design, and empirical scientific methodology.

Whilst at Oxford I have also been fortunate to meet some of the kindest, brightest, and industrious individuals, Anand, Phil, and Pradeep. From our shared DPhil trials and tribulations, and deliberations over grilled meats, lamb biryani, ice cream, and a trip to the Lake District, we have forged lasting friendships, and they have opened my eyes to the wonders and intellectual rigour of basic science. They have instilled in me a mindset that with effort and planning everything is possible, including servicing the community as a competent clinician and making a lasting advancement to science and patient care.

Lastly, I would like to thank my mum, dad, and brother for their unwavering support in this DPhil endeavour, and my wife, Linda, who was the most definite advocate of me embarking on this journey and who also always kept me focussed on the timely completion of these studies. I thank you whole heartedly and look forward to returning home and continuing our lives together.

Abstract

Promoting tissue repair in adults represents a major unmet medical need. Tissue regeneration relies on the activation of quiescent endogenous stem cells and whilst considerable progress has been made, novel therapies based on stem cells have thus far failed to translate to routine clinical practice. Much attention has focussed on administrating exogenous stem cells expanded or altered *in vitro*. However, this approach faces several major limitations, including poor engraftment, high cost and importantly, the necessity for immunosuppression for allogenic cells. An alternative strategy that overcomes these shortcomings is to promote repair by harnessing the regenerative potential of endogenous stem cells. This thesis focussed on the role of alarmins, the upstream group of mediators released immediately following injury, in promoting tissue regeneration. I show that the alarmin HMGB1 accelerates tissue regeneration in various systems by transitioning multiple stem cell types from the quiescent G_0 to the G_{Alert} state. Firstly, *in vitro* screening of candidate alarmins with human bone marrow-derived mesenchymal stromal cells showed that only pre-treatment with HMGB1 improved osteogenic differentiation. Using an optimised murine fracture model, I found that local administration of HMGB1 accelerated bone regeneration via the CXCL12-CXCR4 axis, whilst healing was impaired in inducible *Hmgb1*$^{-/-}$ animals. Cell cycle analyses revealed that HMGB1 transitioned the skeletal stem cell from G_0 to G_{Alert}. In this intermediate phase, the cell is more metabolically active and efficiently enters the cell cycle when exposed to activating factors. This effect also extended to other types of stem cells, including murine haematopoietic and muscle stem cells, as well as human haematopoietic stem and progenitor cells, and MSCs. Using murine models, HMGB1 accelerated recovery from injury to these tissues. Finally, treatment with a single systemic dose of HMGB1 two weeks before injury also accelerated bone, haematopoietic, and muscle regeneration, which was indicative of an acquired pro-regenerative signature. These findings document that the HMGB1-G_{Alert} pathway results in a dynamic and adaptive multi-tissue regenerative response, and suggest that exogenous HMGB1 may be of therapeutic benefit in diverse clinical contexts, including trauma, chemotherapy, and elective surgery.

Statement of originality

I hereby declare that this submission is my own work and to the best of my knowledge contains no materials previously published or written by another person, or which have been accepted for the award of any other degree or diploma at the University of Oxford or any other educational institution. Any contribution made to the research by others, with whom I have worked, is explicitly acknowledged in this thesis.

Table of Contents

Chapter 1. Introduction

1.1. Regenerative medicine

1.1.1. General clinical context

Regenerative therapeutics endeavour to restore healthy physiology by either replacing diseased tissues with those grown and engineered in the laboratory, or by stimulating the repair of damaged tissues by resident cells. This is markedly different from the vast majority of existing medicines which act by blocking pathological processes, and do not enhance endogenous repair pathways. Indeed the top ten most prescribed drugs in the USA are all '*anti*-pathology' medications[1], and the modern pharmacopoeia[2] is littered with their nomenclature, from the older *anti*biotics, and non-steroidal *anti*-inflammatories, to more recent *anti*virals and *anti*body based biologics. Yet treatments which make use of regenerative principles do already exist and are well-established in the domains of surgery and oncology[3]. These include partial liver living-donor transplants, which rely on partially resected livers regenerating in both the donor and recipient, autologous bone grafts which promote the formation of new bone, and haematopoietic stem cell transplants which replenish the entire haematopoietic system. Unfortunately the wide-use of these treatments is limited due to factors such as a lack of donors, finite amounts of autologous tissue, and donor-site morbidity. Regenerative medicine has the potential to free clinicians from these constraints which is of paramount importance due to the increasing prevalence of age-related degenerative diseases and disabilities. Fortunately we are beginning to see regenerative therapeutics enter the market, Table 1.1 and 1.2, many others are in clinical trials, and hopefully as their efficacy is demonstrated they will become standard of care.

Table 1.1 FDA approved molecular regenerative medicine products.

Therapeutic	Clinical specialty	Brand name	Biological agent	Approved use
Molecular	Haematology	Romiplostim	Thrombopoietin analogue	Immune thrombocytopenic purpura[4]
	Haematology	Eltrombopag	Small molecule thrombopoietin receptor agonist	Immune thrombocytopenic purpura, and aplastic anaemia[5]
	Haematology and nephrology	Atgam	Anti-thymocyte globulin	Aplastic anaemia, and renal transplant rejection[6]
	Haematology and oncology	Leukine	GM-CSF (sargramostim)	Acceleration of monocyte and neutrophil recovery following chemotherapy or radiotherapy[7], and as an anti-fungal[8]
	Haematology and oncology	Neupogen, Zarxio, Neulasta, Granocyte	G-CSF (filgrastim, PEG-filgrastim, lenograstim)	Acceleration of neutrophil recovery[9] following chemotherapy or radiotherapy, and for peripheral mobilisation of haematopoietic stem cells for haematopoietic stem cell transplants[10]
	Haematology and oncology	Plerixafor	AMD3100 (CXCL12-CXCR4 antagonist)	Peripheral mobilisation of haematopoietic stem cells for haematopoietic stem cell transplants[11]
	Dental surgery	GEM 21S	PDGF-BB and tricalcium phosphate	Periodontal defects[12]
	Plastic surgery	Regranex	PDGF-BB in becaplermin gel	Lower extremity diabetic ulcers[13]
	Orthopaedic surgery	INFUSE bone graft/InductOs	BMP2 in collagen sponge	Open tibial shaft fractures[14], and lower spine fusion[15]
	Orthopaedic surgery	OP-1	BMP7 and collagen mixture	Recalcitrant long bone non-union[16], and lower spine fusion[17]

Table 1.2 FDA approved cellular regenerative medicine products.

Therapeutic	Clinical specialty	Brand name	Biological agent	Approved use
Cellular	Haematology and oncology	Allocord, Clevecord, Ducord, Hemacord	Allogeneic cord blood haematopoietic stem and progenitor cells	Haematopoietic stem cells transplants[18–20]
	Dental surgery	Gintuit	Allogeneic cultured keratinocytes and fibroblasts in bovine collagen scaffold	Oral soft tissue substitute[21]
	Plastic surgery	Apligraf	Allogeneic cultured keratinocytes and fibroblasts in bovine collagen scaffold	Skin substitute for diabetic foot and venous leg foot ulcers[22]
	Plastic surgery	Celution	Adipose-derived regenerative cells	Enrichment of fat grafts for breast, face, and buttock augmentation[23]
	Plastic surgery	Dermagraft	Allogenic fibroblasts in a polyglactin mesh scaffold	Diabetic foot ulcer[24]
	Plastic surgery	Laviv	Autologous fibroblasts	Improving nasolabial fold (smile wrinkles) appearance[25]
	Orthopaedic surgery	Carticel	Autologous chondrocytes	Cartilage defects from trauma, not osteoarthritis[26]

1.1.2. Orthopaedic context

Orthopaedics is a surgical specialty that focuses on injuries and diseases of the musculoskeletal system. It is a large specialty with 1 in 2 people suffering from musculoskeletal disorders during their lifetime[27]. This is twice the rate of chronic heart and lung conditions, and numbers are increasing due to the aging population. Currently most orthopaedic conditions are managed through the use of surgical fixation, excision, implants, splints and/or physiotherapy. Therefore it follows that the majority of advances in orthopaedic practice have stemmed from clinical research, or basic physical science research in the disciplines of materials, mechanics, and engineering. Yet orthopaedic conditions are well-suited to molecular and cellular regenerative therapies[28] because many orthopaedic treatments already utilise the 'regrow' or 'replace' principles of regenerative medicine, such as with the distraction osteogenesis technique for skeletal deformities, and joint replacements for osteoarthritis respectively. By directly studying and targeting the biology of orthopaedic conditions we would be adding a major therapeutic adjunct to the predominantly physical treatment modalities currently available to orthopaedic surgeons.

1.2. Fractures

1.2.1. Clinical need

Fractures constitute a major public health problem. Each year 3.6% of the UK population sustain a fracture, with hip fractures alone costing the NHS £1.7billion[29]. Whilst most fractures heal uneventfully, certain sub-types are associated with excessive morbidity and mortality and would therefore benefit from accelerated fracture healing. These include high-energy open fractures which may be complicated by delayed and non-union[30], and fractures in osteoporotic bone, which represent the greatest unmet clinical need because rates of recovery and mobilisation are limited by the time required for fracture healing as premature loading can lead to implant failure (Figure 1.1).

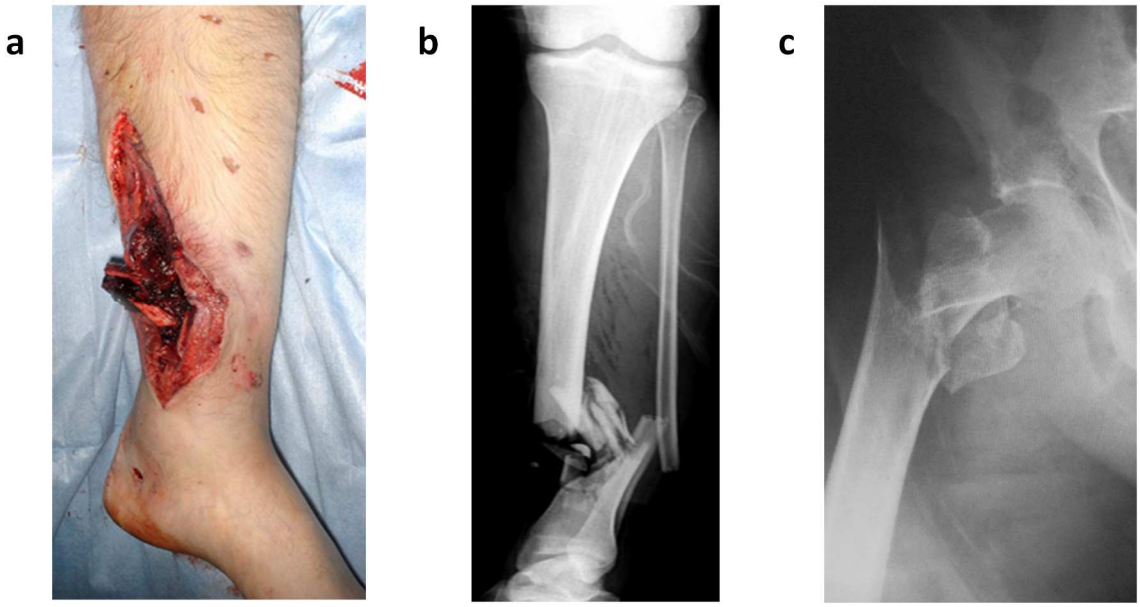

Figure 1.1 (a) Clinical photograph of high energy open tibia-fibula fracture with (b) corresponding anterior-posterior (AP) radiograph. (c) AP radiograph of an intertrochanteric hip fragility fracture.

Severe open fractures (Figure 1.1 a and b), Gustilo grades IIIB/C, are limb-threatening injuries associated with considerable morbidity. They largely affect young men and often occur as a result of motor vehicle accidents[31,32]. The rate of delayed or non-union is 10-31%[33], with the average time to union for an open tibial fracture being 41 to 43 weeks[34,35]. One third will require multiple surgical

interventions, and more than half will not have regained employment four years post-injury[35]. In 2007, each non-union which healed under 'best case scenario' conditions cost the NHS a minimum of £15,000[36]. Hence acceleration of fracture healing would dramatically improve the quality of life of these patients and reduce the socio-economic burden on the wider community.

Worldwide 9 million fractures in osteoporotic bone, commonly known as fragility fractures, occur every year[27]. Fragility fractures of the hip are associated with a mortality rate of 30% within the first year of injury[37], and it is estimated that 1 in 6 women will sustain a hip fracture within their lifetime, which is higher than the lifetime risk of developing breast cancer (1 in 9)[38]. The high mortality rate is in part attributed to prolonged bed-rest following fracture fixation[39] which is sometimes necessary as premature weight bearing can lead to implant 'cut-out' and failure[40]. Accelerated fracture healing would allow for earlier mobilisation which would avoid the major complications of prolonged bed-rest, including venous thromboembolism, hospital acquired pneumonia, urinary tract infections, and pressure ulcers[41,42].

There is currently no approved therapy for accelerating healing of high-energy or fragility fractures, and the number of fragility fractures continues to increase with the ageing population (Figure 1.2). Bone morphogenetic proteins (BMPs) are clinically approved for the treatment of spinal fusions, and established tibial non-unions. However they have failed to achieve the efficacy anticipated from preclinical studies[43], and there is insufficient clinical evidence to support their routine use[44]. Therefore, there is an urgent unmet need to develop therapeutic strategies to accelerate bone regeneration and the healing of fragility and high-energy fractures.

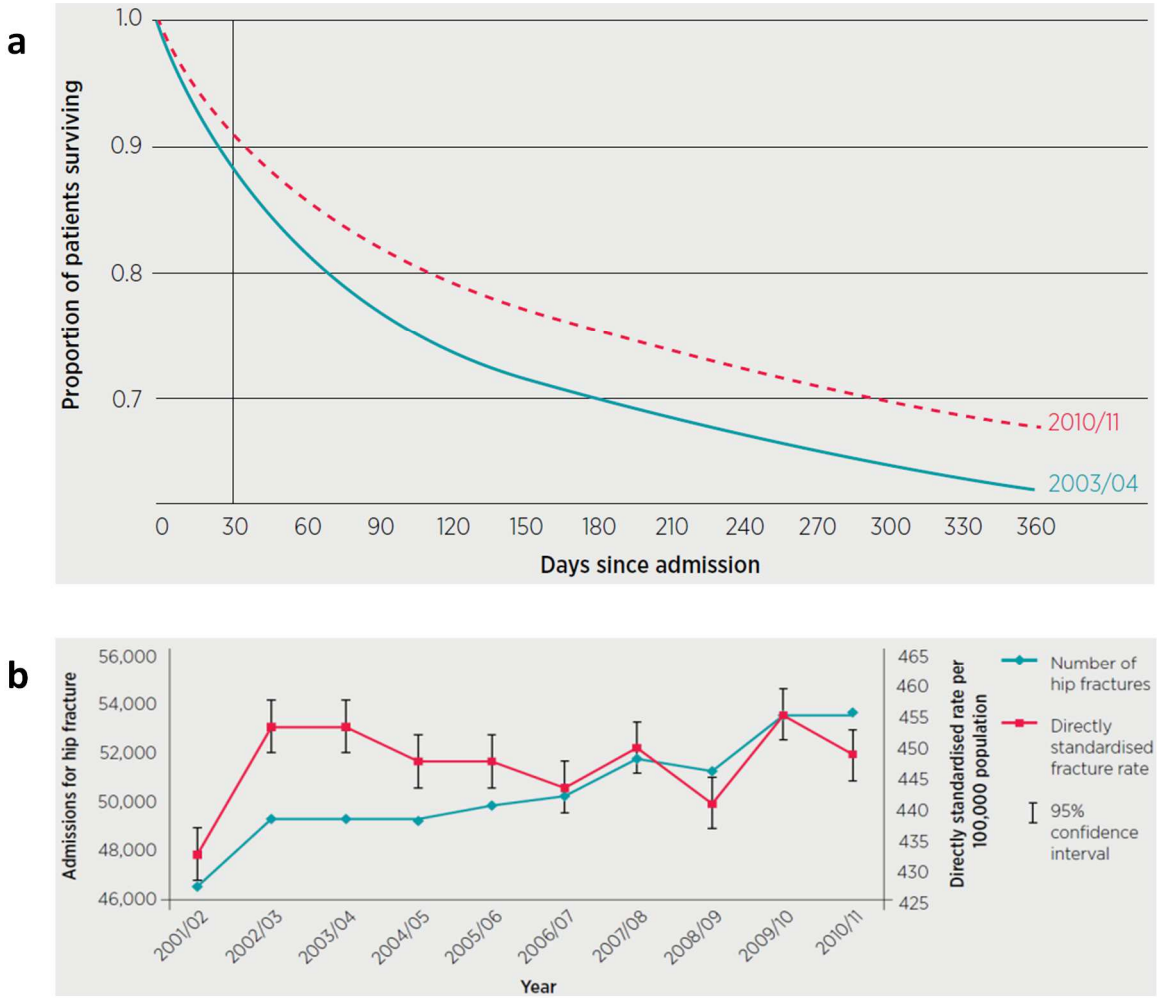

Figure 1.2 (a) Kaplan-Meier curve showing 30-day and one-year mortality following hip fracture admission for 2003/04 and 2010/11 for patients over the age of 65 in NHS hospitals in England. (b) Total annual admissions for hip fracture, and age- and sex-standardised hip fracture admission rates per 100,000. Adapted from Smith et al., 2013.

1.2.2. Fracture biology

Bone is one of the few adult human tissues that is capable of regenerating completely following injury. Fracture healing in both mice and humans involves a spatially and temporally regulated cascade of events with interactions between many cell types, cytokines, chemokines and growth factors[45]. It comprises three overlapping phases: inflammation, bone formation, and coupled remodelling (Figure 1.3).

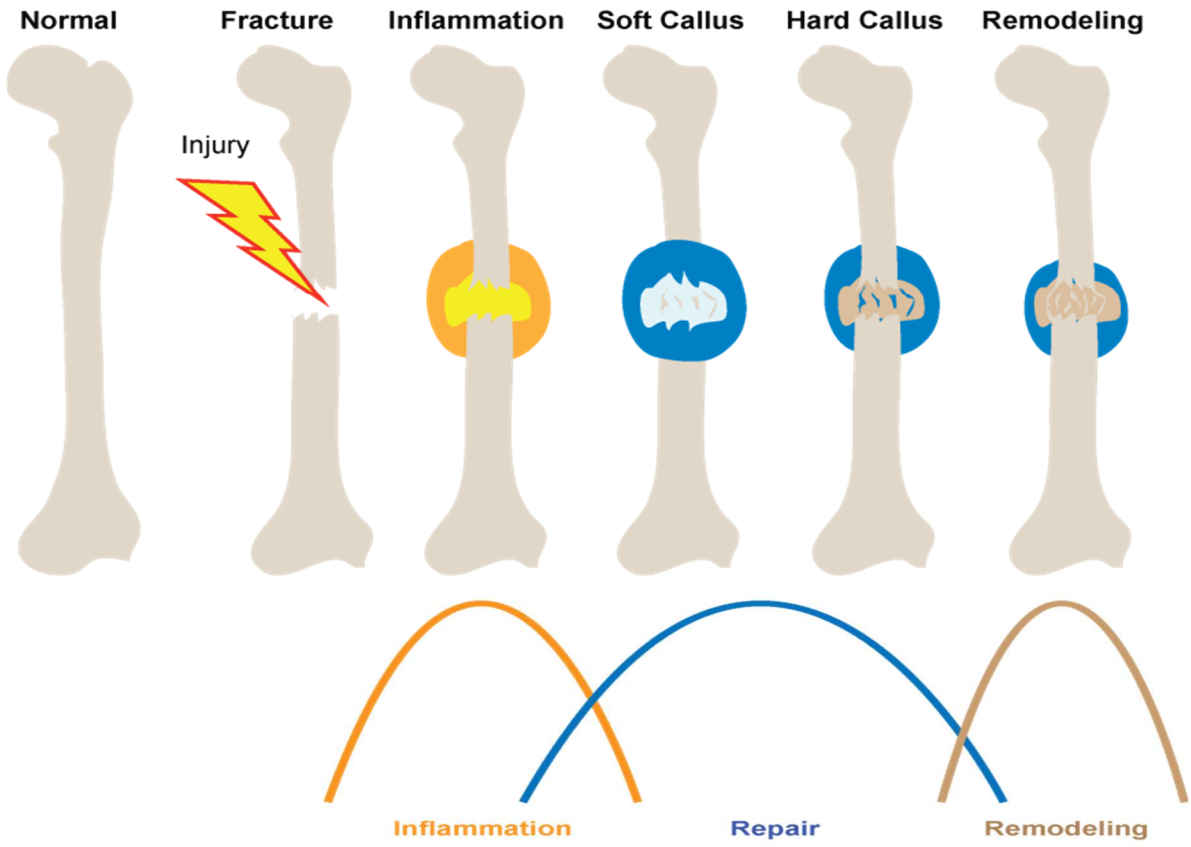

Figure 1.3 Schematic of the three major biological phases of fracture healing: inflammation, repair/bone formation, and coupled remodelling. In the murine diaphyseal fracture model the inflammatory phase typically lasts approximately 1 week, the repair/bone formation phase starts during week 1 and lasts until week 3, and remodelling is usually evident during week 3[45].

In the initial inflammatory phase, a haematoma forms around the fractured bone ends, and it is characterised by hypoxia, low pH, and the presence of necrotic and inflammatory cells[46], and

inflammatory cytokines[47]. Polymorphonuclear neutrophils (PMNs) are chemoattracted by the presence of necrotic cells[48] and are the first cells to invade the haematoma. They are critical to normal fracture healing[49], and secrete chemokines, including CCL2 and IL-6, which in turn attract monocytes/macrophages. Monocytes/macrophages are necessary for optimal fracture healing although their role is incompletely defined[50,51]. Our group previously observed that monocytes[52,53], M-CSF differentiated macrophages (M0), and M-CSF differentiated macrophages polarised with IL-4 (M2) promoted the *in vitro* osteogenic differentiation of human bone marrow derived mesenchymal stromal/stem cells (MSCs)[54]. These results established a role for monocyte/macrophages as critical regulators of osteogenic differentiation via oncostatin M production and the induction of STAT3 signaling in hMSCs[53]. However the role of monocytes/macrophages in bone regeneration *in vivo* is yet to be fully understood.

The inflammatory phase also sees the beginning of the recruitment and differentiation of osteoprogenitor cells[45] which contribute to the second phase of fracture healing, the formation of bone. Primary healing occurs when there is direct bone contact and absolute rigid stability. There is no callus, instead cutting-cones, which consist of bone-resorbing osteoclasts at the front and a trail of osteoid-depositing osteoblasts, directly create new osteons. Osteons are the fundamental functional unit of compact bone and consist of concentric layers (lamellae) of bone surrounding a central vascular (Haversian) canal. Most fractures are only relatively stable and therefore heal by secondary intent. This process involves the formation of a soft callus, which is a heterogeneous mixture of fibrous and cartilaginous tissue that is gradually mineralised to form a hard callus. The extramedullary callus undergoes endochondral ossification where chondroprogenitors differentiate into chondrocytes which lay down a hyaline cartilage template that is later invaded and replaced by capillaries and osteoprogenitors, which differentiate into osteoblasts to form bone. In contrast, the intramedullary callus undergoes intramembranous ossification where there is no cartilage intermediary, and osteoprogenitors differentiate into bone forming osteoblasts which proliferate and deposit new bone matrix.

The final phase of callus remodelling returns the macro and microarchitecture of the bone, and thereby the functional strength of the bone, to its pre-injury state. This is evident on plain radiographs as a reduction in callus volume. Remodelling is a dynamic process which involves osteocytes sensing load and co-ordinating coupled interactions between the bone-resorbing osteoclasts and the osteoid-depositing osteoblasts to adapt to these stressors. As per Wolff's law, bone is reinforced at sites of stress, and conversely undergoes resorption at sites that are not loaded. This phase is often prolonged and it may take years to restore the pre-injury bone strength and structure.

1.3. Alarmins

The term 'alarmins' was first coined in 2006[55] to describe endogenous molecules that are constitutively available, and when released upon cellular damage, activate the immune system (Figure 1.4). They are released from necrotic cells upon infection or tissue injury, or are rapidly secreted by stimulated leukocytes and fibroblasts. In the absence of injury or infection, they play important intracellular roles. However, once released, they serve to signal tissue and cell damage and initiate a host immune response[56] by promoting the activation of innate immune cells and recruitment and activation of antigen-presenting cells. Together with exogenous pathogen associated molecular pattern molecules (PAMPs), such as LPS, they comprise the larger family of danger associated molecular pattern molecules (DAMPs)[57–59]. The classical characteristics of alarmins include rapid release following necrosis but not apoptosis, active secretion by immune cells without cell death, and recruitment and activation of immune cells[55].

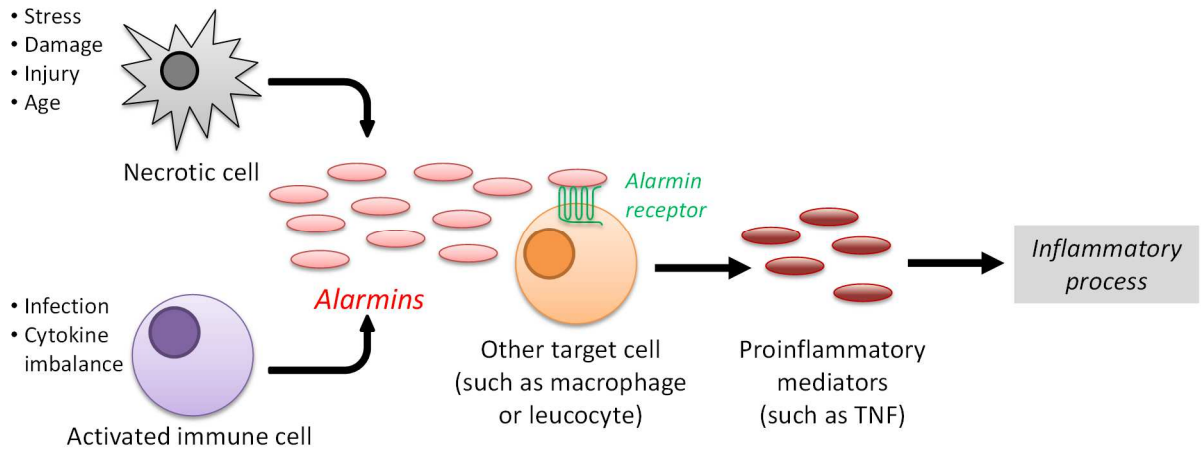

Figure 1.4 Schematic of overview of alarmins. In the steady state, alarmins have important intracellular roles. However, they can be passively released from cells undergoing necrosis or actively secreted by activated immune cells. Once extracellular, alarmins can then bind to specific receptors on the surface of target cells, such as monocytes/macrophages or leucocytes, to stimulate the production of proinflammatory mediators, such as TNF, thereby leading to an inflammatory cascade.

While there is a lack of investigative focus on the role of alarmins in tissue regeneration and bone biology, there is circumstantial evidence that two of the best characterised alarmins, S100A8/A9 and HMGB1, are involved in bone healing. S100A8, S100A9, and the S100A8/A9 dimer are members of the family of S100 calcium-binding cytosolic proteins. They are present within monocytes, dendritic cells[60], and constitute 45% of cytosolic proteins in the neutrophil[61], and the group has shown previously that neutrophils, by releasing monocytic mediators, are critical for optimal fracture healing. S100A8/A9 has also been associated with regulating hypertrophic chondrocytes, osteoblast differentiation[62], and enhanced osteoclast function[63].

HMGB1 is a chromatin protein that bends DNA, is released during cell necrosis but is bound firmly to chromatin during apoptosis[64], and can be secreted in an acetylated form by activated immune cells[65–67]. It has been implicated in tissue and bone regeneration[68–73], angiogenesis[74–78], neurogenesis[79,80], endochondral ossification[81], osteoclastogenesis[82,83], and is reported to aid in the migration and osteogenic differentiation of human bone marrow derived mesenchymal stromal cells *in vitro*[84]. The various roles of HMGB1[85] have been attributed to its different redox states[86], which *in vivo* is determined by the form of cell activation or cell death[87], and interactions with reactive oxygen species (ROS) in the acute inflammatory microenvironment[86] (Figure 1.5). Fully reduced (FR) all-thiol HMGB1 exerts chemoattractant effects on immune cells by first forming a heterocomplex with free CXCL12 (SDF-1), or with CXCL12 that has been released from cells where FR-HMGB1 engaged the RAGE receptor. This HMGB1-CXCL12 heterocomplex then signals via the receptor CXCR4[88]. In contrast, partially oxidised HMGB1 with a disulfide (DS) bond stimulates the release of pro-inflammatory cytokines by binding to the TLR4-MD2 receptor complex. Fully oxidised (FOX) all-sulfonyl HMGB1 is inert, as is the HMGB1 which is released from apoptotic cells because it is tightly bound with chromatin. With such pleiotropic effects it is possible for HMGB1 to promote osteogenesis through a variety of mechanisms, and the recently developed recombinant chemotactic non-oxidisable all-serine (3S) form of HMGB1 would be a useful tool to help delineate the contributions of each redox form.

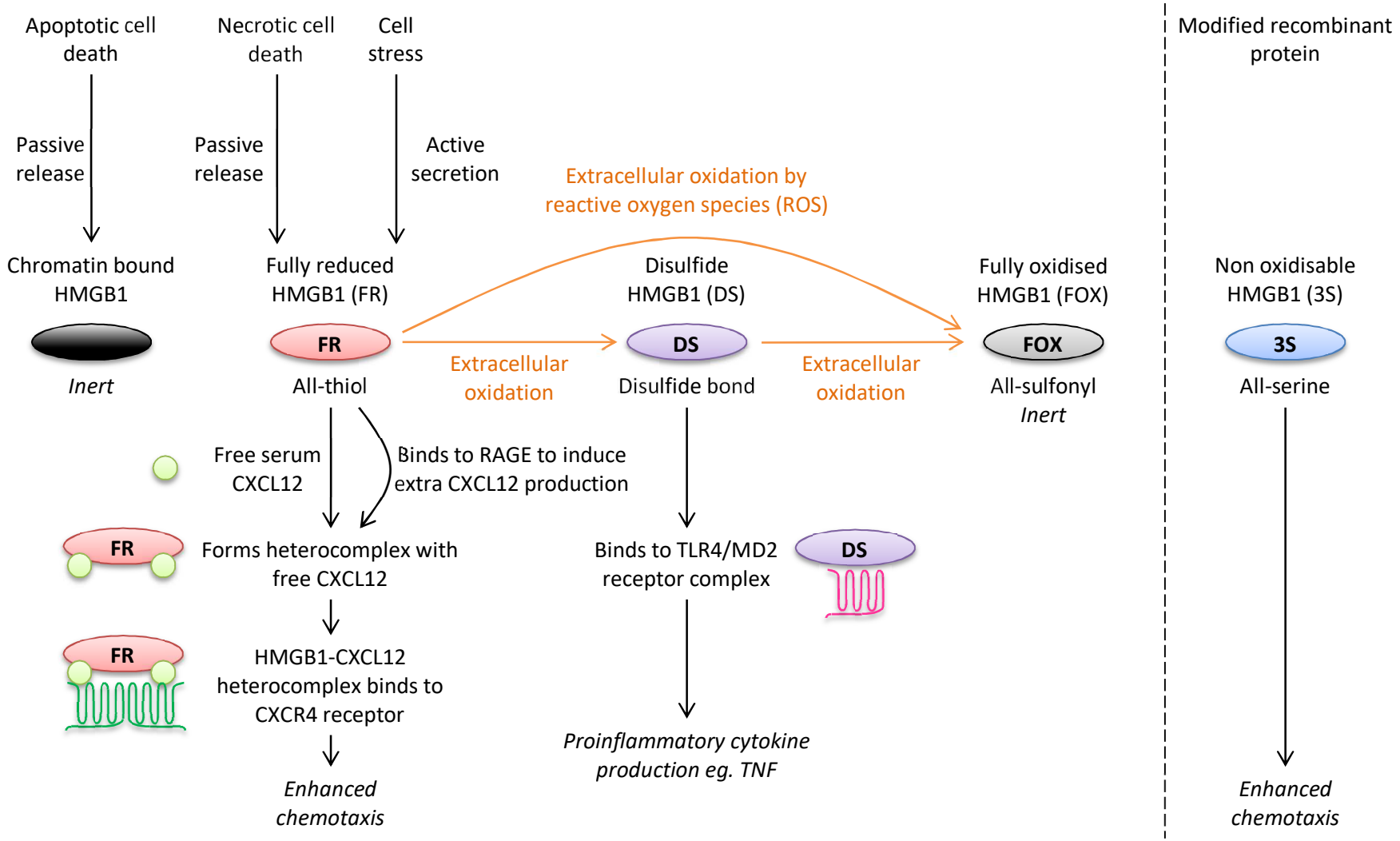

Figure 1.5 Schematic of the release, oxidative states and cellular effects of HMGB1. Apoptotic cells passively release chromatin bound and functionally inert HMGB1. Necrotic cells and activated immune cells passively release and actively secrete fully reduced (FR) HMGB1 respectively. This forms a heterocomplex with free CXCL12 which then binds to CXCR4 and enhances chemotaxis. When partially oxidised in the extracellular environment to the disulfide form it engages with the TLR4-MD2 receptor complex to induce the release of proinflammatory cytokines. Once fully oxidised, HMGB1 is functionally inert. As an investigative tool, a recombinant non-oxidizable all-serine form (3S) of HMGB1 has also been recently developed.

1.4. Stem cells

Stem cells can differentiate into more specialised cells and are also capable of self-renewal, thereby giving rise to more cells of the same type indefinitely. Progenitor cells can also differentiate into more specialised cells but they lack the capability of indefinite self-renewal[89]. Many precursor cell populations from various surrounding tissue sources are capable of contributing to the fracture callus. In simple fractures the majority of the osteoprogenitor cells arise from the periosteum and endosteum. However when these sources are disrupted, then stromal cells from the bone marrow, vasculature, muscle, and fat can also make a significant contribution. Due to their relative ease of access, being named 'stem' cells, and well-established *in vitro* tri-lineage differentiation into osteoblasts, chondrocytes, and adipocytes, human bone marrow derived mesenchymal stromal/stem cells (hMSCs) have been studied for decades for their potential to improve fracture healing. Unfortunately there is doubt on their likely direct clinical utility due to all studies showing that hMSCs do not self-renew for long periods *in vivo*[90], the defining characteristic of a stem cell. In addition, there are conflicting pre-clinical studies on their effectiveness, engraftment, and relative contribution to the callus when administered locally at the fracture site[91–93], and strong evidence that systemic administration of hMSCs would be at best futile, with up to 99% being entrapped in the lungs[94,95], and at worst clinically dangerous, due to a large bolus of hMSCs possibly causing a cellular pulmonary embolism. Interestingly positive pre-clinical results were reported with repurposing hMSCs as a delivery vehicle for drugs to the lung itself[96], and this has progressed to the TACTICAL/MSCTRAIL clinical trial[97], which further reinforces the poor ability of systemically administered hMSCs to home to the site of limb injuries.

The reason why hMSCs appear capable of long term self-renewal *in vitro*, but not *in vivo*, appears to be related to the well-known genetic, transcriptional and protein perturbations[98–100] that can occur when cells are taken out of their native microenvironments and cultured on plastic. These perturbations typically impede the self-renewal of endogenous stem cell populations, but in this

instance conversely promote the self-renewal of this cell population. Therefore the current prevailing opinion is that hMSCs may behave as stem cells but only in the *in vitro* setting. Whilst this may limit their direct clinical application, if combined with suitable *in vivo* validation they remain a valuable *in vitro* tool to investigate aspects of stem cell behaviour. In addition hMSCs are valuable as a readily available primary cell for studying human osteogenic, chondrogenic, and adipogenic pathways.

Of great interest in the musculoskeletal field is the recent identification and specification of the murine skeletal stem cell (mSSC) (Figure 1.5). Using leading genetic lineage tracing techniques, the Longaker and Weissman group defined the mSSC according to immunophenotypic cell surface markers[101] and the Mukherjee and Wang group defined it according to expression of the Gremlin1 gene[102]. There was a high degree of overlap in their populations, and they were unified in showing that mSSCs only give rise to bone, cartilage, and haematopoietic supportive stroma, and not fat[103]. They proved that mSSCs are particularly concentrated in the diaphysis and epiphyseal plates of long bones, contribute to the fracture callus, and further studies have demonstrated that mSSCs can be targeted to improve the healing of diabetic fractures *in vivo*[104]. Of note, it was also shown that mSSCs and bone, cartilage, and stromal progenitors (BCSPs) isolated from the fracture callus displayed enhanced osteogenic capacity *in vitro* and *in vivo*[101,105,106]. It is possible that the injury niche, which in this context is the fracture microenvironment, may be mediating this cellular enhancement through molecular signals, including alarmins. With the myriad of advances that have been made in the field of haematology and oncology since the identification of the haematopoietic stem cell almost 30 years ago, one would envision that similar progress will be made with the treatment of musculoskeletal disorders now that the skeletal stem cell has also been identified in mice, and hopefully its human counterpart soon to follow.

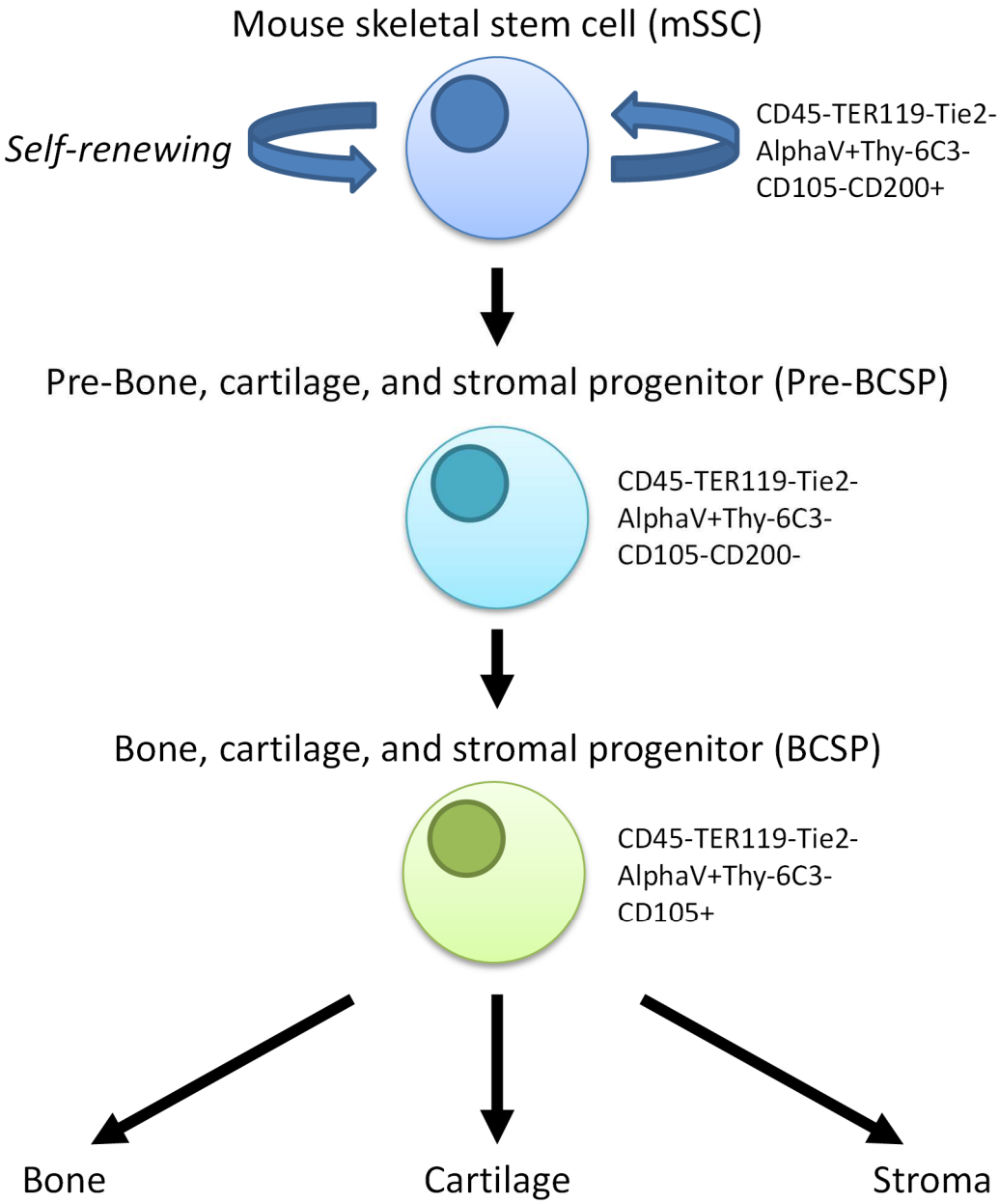

Figure 1.6 Schematic of the murine skeletal stem cell (mSSC) lineage tree with immunophenotype definitions of each stage. The mSSC occupies the apex of the hierarchy, is multipotent, and self-renews long term *in vivo*. It differentiates into more lineage-restricted progenitor cells, namely pre-bone cartilage and stromal progenitors (pre-BCSPs) and bone cartilage and stromal progenitors (BCSPs). These stem and progenitor cells only contribute to bone, cartilage, and bone marrow hematopoietic stroma.

1.5. Research hypothesis

Alarmins are released post-fracture and may be targeted to accelerate tissue regeneration *in vivo*, using a murine model of fracture healing.

1.6. Research aims

1. To measure if alarmins are released post-fracture in humans and mice, and to determine their effects on the osteogenic differentiation of primary human cells.

2. To assess if modulation of alarmins accelerates tissue regeneration *in vivo*, by developing a murine model of fracture healing that is conducive to serial *in vivo* measurements over a time course.

3. To investigate the *in vivo* molecular and cellular pathways by which alarmins modulate tissue regeneration, with an initial focus on the murine skeletal stem cell, and then to assess if these pathways pertain to the regeneration of other tissues.

Chapter 2. Materials and methods

2.1. Human and murine plasma

Plasma samples from patients who had sustained femoral fractures and from healthy unfractured controls were obtained from the John Radcliffe Hospital (REC: 16/SW/0263, PID: 12229, IRAS: 213014). The human plasma samples were from the patient's first in-hospital blood sampling, typically within 4 hours post-fracture. Murine plasma was collected 3 hours post-femoral fracture via cardiac puncture from 12 week old female C57Bl6/J wild type, *Hmgb1*$^{fl/fl}$, *Hmgb1*$^{-/-}$ mice, and from healthy unfractured controls. All human and murine samples were aliquoted, frozen, and stored at -80^{o}C before being thawed and assayed.

2.2. Mice

All animal procedures were approved by the institutional ethics committee and the United Kingdom Home Office (PLL 71/7161, and PLL 30/3330), and were performed on skeletally mature 12-14 week old female C57BL/6J (Charles River), and transgenic mice. *Hmgb1*$^{-/-}$ mice were generated by crossing *Hmgb1*$^{fl/fl}$ (Riken) with Rosa-CreER^{T2} mice (Jackson Laboratory), and at 10 weeks of age administering 3 intraperitoneal (i.p.) injections of 1.5mg tamoxifen (Sigma, T5648) in a mixture of sunflower seed oil (Sigma, 88921) and 10% ethanol (VWR, 437433T) on alternate days over a 6 day period,. Mice were used 7 days after the last tamoxifen injection. *Hmgb1*$^{-/-}$ mice were obtained at the expected Mendelian ratio with no adverse phenotypic side effects, and *Hmgb1*$^{fl/fl}$ mice injected with tamoxifen were used as controls. Animals were genotyped by PCR of earclip DNA, with the primer sequences in Table 2.1, using the HotStart Mouse Genotyping Kit (Kapa Biosystems, KK7352).

Table 2.1 Primers for genotyping of mice and q-PCR experiments

	Hmgb1$^{fl/fl}$		*Rosa-CreER*^{T2}
HMGB1 forward	TGTCATGCCACCCTGAGCAGTT	Common forward	AAGGGAGCTGCAGTGGAGTA
HMGB1 reverse	TGTGCTCCTCCCGGCAAGTT	Wild type reverse	CCGAAAATCTGTGGGAAGTC
		Mutant reverse	CGGTTATTCAACTTGCACCA

2.3. Fracture Model

The greatest clinical need for accelerating fracture healing is in patients with osteoporosis who suffer fragility fractures, or those who develop delayed or non-union, such as when an open fracture with periosteal stripping has been sustained. In an attempt to faithfully reproduce each of these clinical scenarios, murine fracture healing studies have been performed in bone stripped of periosteum[107,108], and osteoporosis has been induced by ovariectomy[109]. The existing method of stripping the periosteum simply involves abrading the bone surface, however it is very difficult to confirm the amount of stripping that has been performed because the 1-2 cell layer thick murine periosteum is not visible upon gross inspection. Therefore it is likely that a variable amount of periosteum would remain and this would affect the healing process, increase variability, and reduce internal validity. Ovariectomy adds an additional injury insult with its own subsequent molecular and cellular healing processes that could potentially interact with pathways I was analysing, and thereby confound my results. Thus I decided to pursue my fracture healing studies in a steady state mouse model, with the possibility of future work that would incorporate additional complexities to more faithfully reproduce the clinical scenarios of greatest need.

Mice were anesthetised by aerosolised 2 % isoflurane, given subcutaneous (s.c.) 0.125 mg/kg buprenorphine for analgesia and transferred to a warming pad. The right upper hind limb was shaved and skin prepared with povidone iodine solution. After incising the skin, the femur was exposed by blunt dissecting through the fascia lata between the biceps femoris and gluteus superficialis muscles. A commercial external fixator jig was fitted[110,111] (RISystem, RIS.611) and a 0.5 mm osteotomy created in the femoral diaphysis with a Gigli wire. The wound was closed with interrupted non-absorbable 6/0 Prolene sutures (Ethicon, W8005T). Immediately postoperatively all mice were given s.c. hydration, 0.125 mg/kg buprenorphine for analgesia and allowed to mobilise freely. They were given further postoperative s.c. 0.125 mg/kg buprenorphine analgesia daily for 3 days. Mice were treated locally at the time of injury with an injection into the tissue pocket surrounding the osteotomy of 0.75 mg/kg FR-HMGB1 (HMGBiotech, HM-114), 0.075 mg/kg, 0.75

mg/kg, or 7.75 mg/kg 3S-HMGB1 (HMGBiotech, HM-130), 75 µg/kg CXCL12 (R&D, 350-NS-050), or 50 µl PBS vehicle control; 50 mg/kg glycyrrhizin (Sigma, 50531), or 50 µl DMSO:PBS 1:1 vehicle control; 3 mg/kg AMD3100 (Abcam, ab120718), or 50 µl PBS vehicle control; 4mg/kg rapamycin (LC Laboratories, R-5000), or 50 µl DMSO:PBS 1:1 vehicle control. For priming experiments, mice were treated systemically 2 weeks prior to injury with an intravenous (i.v.) injection of 0.75 mg/kg FR-HMGB1, 0.75 mg/kg 3S-HMGB1, or 50 µl PBS vehicle control.

2.4. Enzyme-linked immunosorbent assay (ELISA)

ELISA assays were used to measure levels of TNF, S100A8/A9 (R&D, DS8900), HMGB1 (IBL International, ST51011), and HMGB1-CXCL12 heterocomplex (R&D, DY350; IBL International, ST51011) in human monocyte supernatant, and human and murine plasma samples. These were 'sandwich' ELISAs where the antigen of interest was quantified between two layers of antibodies, the capture and the detection antibody. For S100A8/A9 and HMGB1, commercial kits were used according to manufacturer's instructions. For HMGB1-CXCL12, we used the heterocomplex hybrid ELISA[86,88]. The reagents for the TNF and HMGB1-CXCL12 ELISA are listed in Table 2.2.

Table 2.2 Reagents for TNF ELISA and HMGB1-CXCL12 hybrid ELISA.

	TNF	HMGB1-CXCL12 heterocomplex
Capture antibody	Mouse anti-human TNF (BD Bioscience, 551220)	Mouse anti-human CXCL12 (R&D, DY350)
Protein standard	Human TNF (R&D, 210-TA)	FR-HMGB1 (HMGBiotech, HM-114) and human CXCL12 (R&D, 350-NS-050), in a 1:2 ratio.
Detect antibody	Biotin mouse anti-human TNF (BD Bioscience, 554511)	anti-HMGB1 (IBL International, ST51011)
Substrate	Streptavidin-HRP (R&D, DY 998), TMB Microwell Peroxidase Substrate Kit (KPL, 507603)	Substrate A and Substrate B (IBL International, ST51011)
Stop	Sulfuric Acid (Sigma, 320501)	Stop Solution (IBL International, ST51011)
Read	Mithras Multimode Microplate Reader LB 940 (Berthold Techologies) 450nm	Mithras Multimode Microplate Reader LB 940 (Berthold Techologies) 450nm

2.5. Human MSC osteogenesis screen

Human MSCs (hMSC) (Lonza, PT-2501) were maintained in DMEM (Gibco, 32430-027) supplemented with 10% FBS (Gibco, 10270-106), 1% L-Glutamine (GE, M11-004), and 1% penicillin/streptomycin (GE, P11-010), in standard tissue culture conditions (37^{o}C; 5% CO_2) and used between passages 3-5. hMSCs were commercially verified for their *in vitro* plastic adherence, tri-lineage differentiation capacity to osteogenic, chondrogenic, and adipogenic cells when cultured in standard differentiation cocktails, cell surface expression of CD29, CD44, CD73, CD90, and CD105, and absence of CD14, CD19, CD34, CD45, and HLA-DR. Human monocytes were isolated from human peripheral blood leucocyte cones (John Radcliffe Hospital, NHS Blood and Transplant) by positive selection with CD14 MACS microbeads (Miltenyi Biotech, 130-050-201) and an autoMACS machine. To determine the direct effect of the alarmins, S100A8, S100A9 (gifted by T.Vogl, Münster), FR-HMGB1, DS-HMGB1 (HMGBiotech, HM-120), 3S-HMGB1, or LPS (ALEXIS Biochemicals, 581-010) on hMSC osteogenesis, 10^4 hMSCs were plated in triplicate into wells of a 96 well plate with various concentration of alarmins or LPS in 200µl of osteogenic media. The latter consisted of maintenance media supplemented with 100 nM dexamethasone (Sigma, D2915), 50 µg/ml ascorbic acid 2-phosphate (Sigma, L8960), and 10 mM β-glycerophosphate (Sigma, G9422). Treatment with oncostatin M 10 ng/ml (Peprotech, 300-10T 209 a.a.) was used as a positive control. To determine the effects of alarmins on hMSC osteogenesis in the presence of monocytes or their products, monocytes were co-cultured with hMSCs in a ratio of 10:1 (10^5 monocytes: 10^4 hMSCs) in osteogenic media with various concentrations of alarmins or LPS, and monocytes were incubated with various concentrations of alarmins or LPS for 16 hours, and the resulting supernatant was subsequently applied onto hMSCs. To determine the effects of priming hMSC with alarmins, hMSCs were plated in maintenance media with various concentrations of alarmins; after 16 hours this was changed to osteogenic media alone. For all permutations, the respective medium was replaced at day 3, and at day 7 the media was removed, cells lysed in 20µl NP-40 lysis buffer and alkaline phosphatase (ALP) activity, which is a

marker of osteogenic differentiation, was quantified using a commercial kit (WAKO Chemicals, 291-58601) as per manufacturer's instructions.

2.6. In vivo micro computed tomography (CT) setup and analyses

MicroCT imaging was performed using a high-speed rotating gantry based system (PerkinElmer, Quantum FX). Animals were anaesthetised briefly with aerosolised isofluorane 2% for each 3 minute scan. The X-ray source was set to a current of 200 µA, voltage of 90 kVp and a field of view of 5 mm to encompass the two fixator pins closest to the osteotomy gap, for a voxel resolution of 10 µm. After the scans, mice were revived in a heated box and returned to their cages. Scans were analysed using a commercially available microCT software package Analyze12 (AnalyzeDirect), which permitted co-registration of scans acquired over a time course. The region of interest was defined as the bridging callus, which included only the tissue that formed in the osteotomy gap (Figure 2.1). Global thresholding[112,113] was performed to distinguish between mineralised (hard callus), poorly mineralised (soft callus) and non-mineralised (fibrous) tissue. The thresholds for mineralised, poorly mineralised and non-mineralised tissues were set at the grey values of femoral diaphyseal bone, epiphyseal cartilage plates, and bone marrow cavity, respectively. Callus volume included the volumes of both hard and soft callus. Callus bone mineral density was the density of hard mineralised tissue, otherwise previously known as tissue mineral density[112,113], and was calibrated by means of phantoms with known densities of calcium hydroxyapatite.

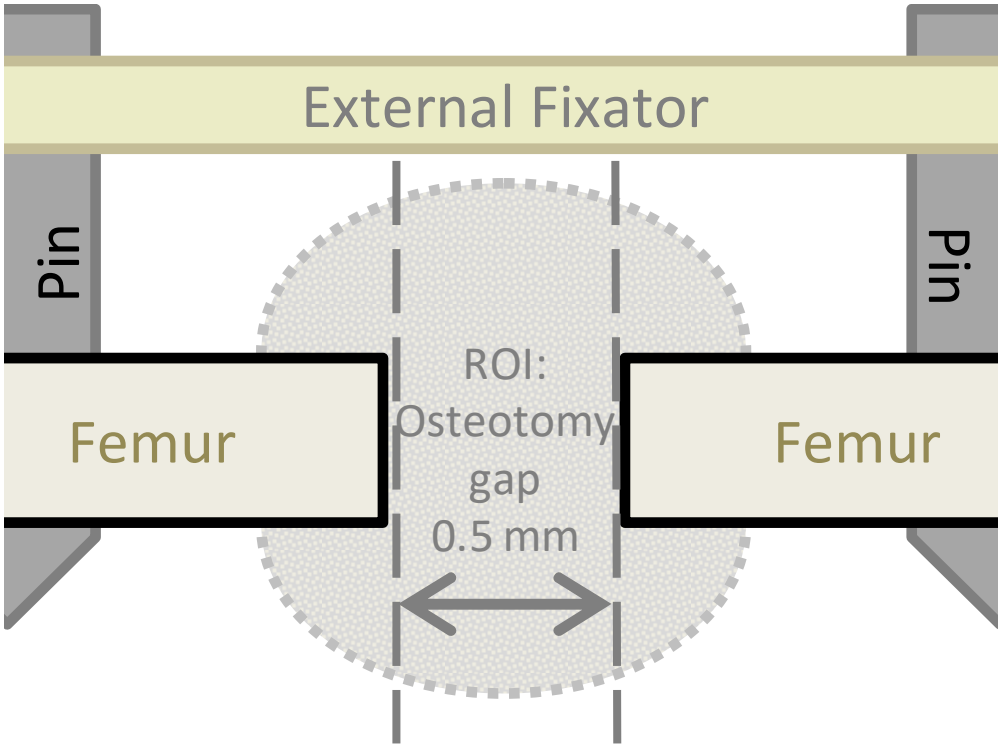

Figure 2.1 Region of interest schematic for microCT evaluation. It included only the tissue that formed at the osteotomy gap, otherwise known as the bridging callus.

2.7. Mechanical strength testing

Both hind limbs were harvested after the final microCT scan, immediately dehydrated and fixed in 70% ethanol for at least 24 hours. Prior to 3-point bend testing (Figure 2.2), all soft tissues overlying the femurs and the external fixator were removed, and the clean femurs were rehydrated in PBS for 3 hours at room temperature. The load cell was applied directly onto the callus, preloaded to a minimum of 0.03 N with the assistance of specimen protection and re-zeroed. Load was applied at a rate of 1 mm/minute until failure, and force-extension profiles were recorded. The resulting data were analysed using the BlueHill 3 (Instron) software package and the maximum force prior to fracture (Figure 2.3) of the injured femur was compared to the contralateral uninjured femur.

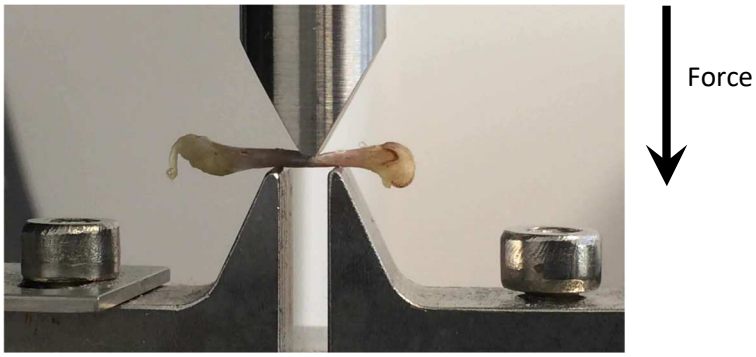

Figure 2.2 Setup of mechanical 3-point bend testing apparatus.

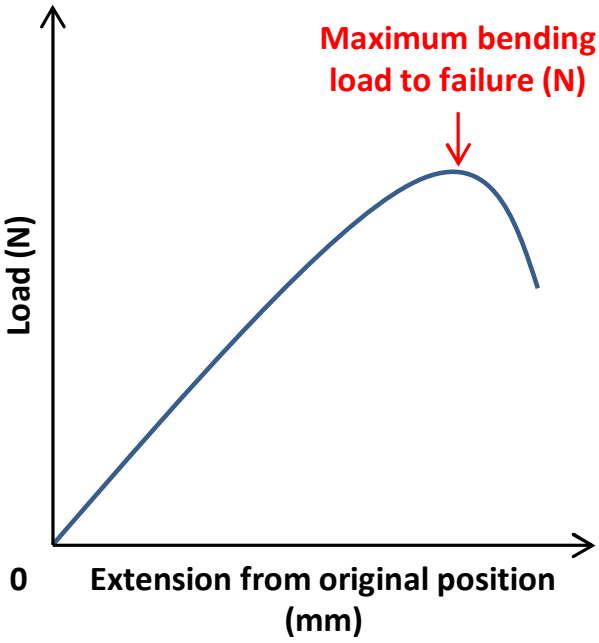

Figure 2.3 Graphical representation of load versus extension profiles as recorded with mechanical 3-point bend testing apparatus. The maximal load prior to fracture (red arrow) is shown. For healthy C57Bl/6J mice 28 days post-fracture this value is typically between 10-28 N, and occurs after 0.15-0.45 mm of extension.

2.8. Isolation of stem cells

BD LSRFortessa X-20 and BD FACSAria III were used for flow cytometry and fluorescence activated cell sorting (FACS), respectively. Subsequent data analyses were performed with the FlowJoV10 software (TreeStar). Murine skeletal, muscle, and haematopoietic stem cells were defined and

freshly isolated according to previously reported protocols[101,114,115]. Whole bone, muscle, and bone marrow cell suspensions were created by respectively crushing femurs and enzymatically digesting with collagenase 800 U/ml (Worthington-Biochem, CLS-2), or mincing thigh muscles and enzymatically digesting with collagenase 800 U/ml and dispase 1 U/ml (Gibco, 17105-041), or extracting bone marrow plugs by flushing femurs with FACS buffer (Miltenyi Biotec, 130-091-221) using a 25 gauge needle. Bone and bone marrow cell suspensions were also enriched by treatment for 5 minutes with red blood cell lysis buffer (Sigma, R7757). Thereafter all suspensions were strained through 70 µm and 40 µm filters (Greiner Bio-One, 542070, 542040) and stained with respective antibodies. Definitions were: mSSC, $CD45^{-}Ter119^{-}Tie2^{-}AlphaV^{+}Thy^{-}6C3^{-}CD105^{-}CD200^{+}$; mMuSC, $CD31^{-}CD45^{-}Sca\text{-}1^{-}VCAM1^{+}$; mHSC, $Lineage^{-}(CD2^{-}CD3^{-}CD4^{-}CD5^{-}CD8^{-}CD11a^{-}CD11b^{-}TER119^{-}B220^{-}Gr\text{-}1^{-})c\text{-}Kit^{+}Sca\text{-}1^{+}CD34^{-}CD48^{-}CD150^{+}$. Antibodies were: mSSC, CD45 (30-F11, BD, 563053), TER-119 (TER-119, BD, 563323), Tie2 [CD202b] (TEK4, Biolegend, 124010), AlphaV [CD51] (RMV-7, Biolegend, 104106), Thy1.1 [CD90.1] (OX-7, Biolegend, 202520), Thy1.2 [CD90.2] (30-H12, 105328), 6C3 [Ly-51] (6C3, Biolegend, 108314), CD105 (MJ7/18, Biolegend, 120416), CD200 (OX-90, BD, 565547); mMuSC, CD31 (MEC13.3, Biolegend, 102510), CD45 (30-F11, Biolegend, 103112), Sca-1 (D7, Biolegend,108120), VCAM [CD106] (429, Biolegend, 105720); HSC CD2 (RM2-5, Biolegend, 100112), CD3 (17A2, Biolegend, 100236), CD4 (RM4-5, Biolegend, 100516), CD5 (53-7.3, Biolegend, 100626), CD8 (53-6.7, Biolegend, 100712), CD11a (M17/4, Biolegend, 101120), CD11b (M1-70, Biolegend, 101212), B220 [CD45R] (RA3-6B2, Biolegend, 103212), Gr-1 (RB6-8C5, Biolegend, 108412), TER-119 (TER-119, Biolegend, 116212), c-Kit [CD117] (2B8, Biolegend, 105814), Sca-1 (D7, Biolegend, 108120), CD34 (HM34, Biolegend, 128608), CD48 (HM48-1, Biolegend, 103432), CD150 (TC15-12F12.2, Biolegend, 115904). Stem cells were also stained for the presence of surface CXCR4 (2B11, BD, 740926), and intracellular HMGB1 (3E8, Biolegend, 651403). Human $CD34^{+}$ haematopoietic stem and progenitor cells were isolated from human peripheral blood leucocyte cones (John Radcliffe Hospital, NHS Blood and Transplant) by magnetically activated cell sorting (MACS) using the CD34 MicroBead Kit (Miltenyi Biotech, 130-046)[116] and an autoMACS machine.

2.9. Cell migration

1000 freshly FACS isolated mSSCs[101] in 6 µl of DMEM were placed in the middle observation channel of collagen coated µ-Slide Chemotaxis slides (Ibidi, 80322). A chemotactic gradient was established across the observation channel by pipetting 70 µl DMEM 0% FBS into the left reservoir, and into the right reservoir either 0.15 ug/ml or 1.5 ug/ml CXCL12, or 0% or 20% FBS controls (Figure 2.4). The channels and reservoirs were plugged to prevent evaporation and cell migration was followed by time-lapse microscopy using an automated xyz motorized stage (Prior Scientific, Prior Proscan II), a climate chamber at 37°C, 5% CO_2, with humidity (Solent Scientific), a spinning disk Nikon Eclipse TE2000-U microscope with a 10x objective, and Volocity 6.3 (PerkinElmer) recording software. Cells were monitored over a period of 22 hours by capture of brightfield images every 5 minutes. Migration of 50 cells was analysed using the automatic tracking function within the Imaris 6.7 (Bitplane) software, and represented using the Chemotaxis and Migration Tool 2.0 (Ibidi). Cells were excluded if track length was less than 50 µm.

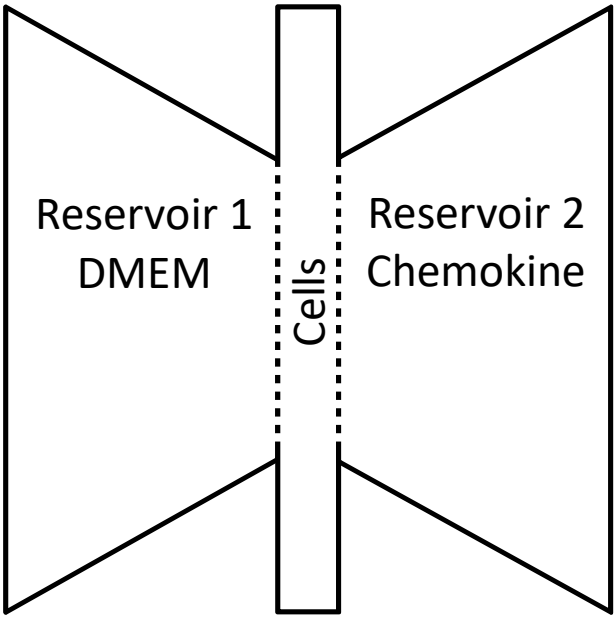

Figure 2.4 Schematic of chemotaxis assay setup

2.10. Cell cycle kinetics

To evaluate cell cycle propensity, which is defined as the proportion of cells which cycle in a given time period, pulse labelling with BrdU (Abcam, ab142567) was performed with animals injected with 10 mg of BrdU i.p. 10 hours[117] before cell isolation from whole femurs. Mice were treated locally at the time of fracture with 15 mg/kg FR-HMGB1, 15 mg/kg 3S-HMGB1, 15 mg/kg BMP2 (Peprotech, 120-02), or 50 µl of PBS vehicle control. To evaluate speed of entry to cell cycle, continuous labelling with BrdU was performed by administering 6.5 mg/ml in their drinking water with 5% sucrose for the indicated period. BrdU incorporation was quantified with the commercially available BrdU FlowKit (BD, 51-2354AK) as per manufacturer's instructions. Following cell isolation and staining, cells were fixed and permeabilized with Cytofix/Cytoperm (BD, 51-2090KE) for 15 minutes at room temperature, buffered with Permeabilization Buffer Plus (BD, 51-2356KC) for 10 minutes at 4°C, re-fixed with Cytofix/Cytoperm for 5 minutes at room temperature, then treated with 30 µg/ml DNase (BD, 51-2358KC) for 1 hour at 37°C to expose incorporated BrdU, and lastly stained with anti-BrdU (BD, 347583). Mice were treated systemically at the initiation of continuous BrdU administration with an i.v. injection of 15 mg/kg FR-HMGB1, 15 mg/kg 3S-HMGB1, or 100 µl of PBS vehicle control. The cells from these mice were compared to cells from the fractured side of injured mice that had also been administered continuous BrdU.

2.11. Mitochondrial DNA

DNA was extracted from 1000 freshly FACS isolated mSSCs[101], mMuSCs[114], and mHSCs[118], and from 10000 trypsinised hMSCs, and 10000 MACS isolated hHSPCs, using the QIAamp DNA Micro Kit (Qiagen, 56304) as per manufacturer's instructions. mtDNA was quantified by qRT–PCR using primers amplifying the Cytochrome B region on mtDNA (TaqMan, Mouse: Mm04225271_g1 CYTB; Human: Hs 02596867_s1 MT_CYB) relative to the β-globin region on gDNA (Taqman, Mouse: Mm 01611268_g1 Hbb-b1; Human: 00758889_s1 HBB). Mice were treated systemically with an i.v. injection of 0.75 mg/kg FR-HMGB1, 0.75 mg/kg 3S-HMGB1, or 100 µl of PBS vehicle control. The cells from these mice were compared to cells from the uninjured contralateral side of fractured animals.

hMSCs were treated for 16 hours with 10 μg/ml FR-HMGB1 in DMEM, 10 μg/ml 3S-HMGB1 in DMEM, DMEM vehicle control, or osteogenic media supplemented with 10 μg/ml BMP2. Whole human peripheral blood leucocyte cones were treated for 2 hours with 1.5 μg/ml FR-HMGB1, 1.5 μg/ml 3S-HMGB1, 10 ng/ml IFN-γ (Miltenyi Biotec, 130-096-482), or RPMI (Lonza, BE12-702F) vehicle control.

2.12. Cellular ATP

Cellular ATP levels of 1000 freshly FACS isolated mSSCs, mMuSCs, and mHSCs, and from 10000 trypsinised hMSCs, and 10000 MACS isolated hHSPCs, were quantified using the commercially available ATP Bioluminescence Assay Kit CLS II (Roche, 11699695001), and used as per manufacturer's instructions. Cells were pelleted, boiled in 100 mM Tris, 4 mM EDTA, pH 7.75 for 2 minutes, pelleted again, and luciferase reagent was added to the supernatant. This was then read on a FLUOstar Omega (BMG Labtech) spectrophotometer with the luminescence optic. Mice were treated systemically with an i.v. injection of 0.75 mg/kg FR-HMGB1, 0.75 mg/kg 3S-HMGB1, or 100 μl of PBS vehicle control. The cells from these mice were compared to cells from the uninjured contralateral side of fractured animals. hMSCs were treated for 16 hours with 10 μg/ml FR-HMGB1 in DMEM, 10 μg/ml 3S-HMGB1 in DMEM, DMEM vehicle control, or osteogenic media supplemented with 10 μg/ml BMP2. Whole human peripheral blood leucocyte cones were treated for 2 hours with 1.5 μg/ml FR-HMGB1, 1.5 μg/ml 3S-HMGB1, 10 ng/ml IFN-γ (Miltenyi Biotec, 130-096-482), or RPMI (Lonza, BE12-702F) vehicle control.

2.13. Cell size

Freshly FACS isolated mSSCs, mMuSCs, and mHSCs, trypsinised hMSCs, and MACS isolated hHSPCs, were placed onto a haemocytometer and stained with 0.4 % trypan blue solution (Sigma, T8154). Bright field images of the haemocytometer were acquired with an Olympus CKX41 microscope using a x40 objective lens. The analysis of cell diameter was manually performed using the Fiji distribution of ImageJ2 software (NIH)[119]. Mice were treated systemically with an i.v. injection of 0.75 mg/kg FR-

HMGB1, 0.75 mg/kg 3S-HMGB1, or 100 µl of PBS vehicle control. The cells from these mice were compared to cells from the uninjured contralateral side of fractured animals.

2.14. c-Met inhibition

Mice were treated i.p. twice a day for 5 consecutive days with 7.5mg/kg of the c-Met inhibitor PHA 665752 (Selleckchem, S1070), or 7.5 µl DMSO in 400 µl of PBS vehicle control, or they were treated i.p. once a day for 2 consecutive days with 0.5 mg/kg anti-cMet (R&D, AF527), or 0.5 mg/kg goat igG isotype control (R&D, AB-108) in 400 µl of PBS. Following the treatment period mice were sacrificed, mMuSCs isolated, and stained for CXCR4 surface expression.

2.15. Haematological injury model

Mice were warmed in a heating box, transferred to a restraining device, and a single i.v. injection of 150 mg/kg 5-fluorouracil[115,120,121] (Sigma, F6627) was administered via the tail vein. 40 µl of peripheral blood was collected at the times indicated from the tail vein with EDTA-containing Microvettes (Sarstedt). 10 µl of this sample was smeared onto slides, air-dried, stained with Giemsa (Sigma, GS500) and May Grunwald solutions (RA Lamb, 310-D), and neutrophils and leucocytes were counted with light microscopy using an Olympus BX51 microscope and a x40 objective lens to determine the differential neutrophil count. The remainder of the sample was treated for 5 minutes with red blood cell lysis buffer (Sigma, R7757), stained with 0.4 % trypan blue solution (Sigma, T8154), and leucocytes were counted with a haemocytometer to quantify total peripheral leucocytes. Together with the differential neutrophil count as above, the total neutrophil count was also determined. Mice were treated systemically at the time of injury or systemically 2 weeks prior to injury with an i.v. injection of 0.75 mg/kg FR-HMGB1, 0.75 mg/kg 3S-HMGB1, or 100 µl of PBS vehicle control.

2.16. Muscle injury model

The most commonly used murine muscle injury models are barium chloride ($BaCl_2$), cardiotoxin, notexin, and freeze injury[122]. As alarmins are key regulators of inflammation it was important to study muscle healing in a model which had a well-defined and relatively brief window of inflammation to permit practical studies, and the inflammatory cells return to baseline one-month post-injury only in the $BaCl_2$ and cardiotoxin models[122]. In addition the seminal paper which first described the G_{Alert} phase had utilised the $BaCl_2$ model[117], so to determine if our findings were consistent with theirs, it was essential to use the same model.

Mice were anesthetized by aerosolised 2 % isoflurane, given analgesia, transferred to a warming pad and the right lower hindlimb was shaved and skin prepared with povidine iodine. 80 µl of 1.2% $BaCl_2$ (Sigma, 217565) was injected into the tibialis anterior (TA) muscle along its length[117]. Immediately postoperatively mice were given s.c. 0.125 mg/kg buprenorphine for analgesia, allowed to mobilise freely, and given further postoperative s.c. 0.125 mg/kg buprenorphine analgesia daily for 2 days. Mice were euthanised and TA muscles extracted at the times indicated, fixed in paraformaldehyde (Santa Cruz Biotechnology, sc-281692) for 24 hours, embedded in paraffin, sectioned, stained with haematoxylin and eosin to identify centrally nucleated fibres, and imaged with an Olympus BX51 using a x40 objective lens. The cross-sectional area (CSA) of the fibres that were approximately midway along the proximal–distal axis of the TA muscle belly was manually measured using the Fiji distribution of ImageJ2 software (NIH)[119]. Mice were injected intramuscularly at the time of injury or intravenously 2 weeks prior to injury, with 0.75 mg/kg FR-HMGB1, 0.75 mg/kg 3S-HMGB1, or 50 µl or 100 µl of PBS vehicle control respectively.

2.17. Statistical analysis

Statistical analyses were performed using GraphPad Prism 7 (GraphPad Software). Unless stated otherwise, significance was calculated using two-tailed unpaired Student's t-tests. For microCT callus volumes, bone mineral density, and *in vivo* cycling to continuous BrdU administration, significance

was calculated using non-linear curve fitting and the F-test. All results are shown as mean ± SD, except for curve fitting results which are shown as mean ± 95% CI. Results were considered statistically significant when $p < 0.05$. Significant results were expressed using asterisks, where * $p < 0.05$, ** $p < 0.01$, *** $p < 0.001$, **** $p < 0.0001$. This convention was used throughout.

Chapter 3. Alarmins in human samples and their in vitro effects

3.1. Introduction

Following injury, there is a cascade of spatiotemporally regulated molecular and cellular cues which lead initially to inflammation and ultimately tissue regeneration and repair. Whilst inflammation is classically considered to be deleterious in the tissue healing process, previous studies by our group, and others, have shown that upregulation of inflammatory signals can promote tissue regeneration and repair[108,109]. For example, selected inflammatory cytokines have been shown to promote the osteogenic differentiation of a variety of progenitor cells and enhance fracture healing[108]. As alarmins are some of the most upstream mediators of the inflammatory cascade, it is possible that they may also be important in orchestrating the downstream events of fracture healing. A candidate approach, focussing on alarmins S100A8/A9 and HMGB1, was taken because both had been associated with regulating osteogenic differentiation[62,84].

Importantly extracellular HMGB1 exists in different redox states, with each redox form having contrasting effects on immune cells[86]. When fully reduced (FR) all-thiol HMGB1 is released from necrotic cells, it promotes chemotaxis of leucocytes[86]. Following oxidation to the disulfide (DS) form in the extracellular milieu, it instead induces proinflammatory cytokine production by local immune cells[86,123]. Both FR and DS-HMGB1 are terminally fully oxidised to an all-sulfonate form, which to current knowledge is functionally inert, promoting neither chemotaxis nor proinflammatory cytokine induction. Therefore, to assess the effects of HMGB1, both the FR and DS forms of HMGB1, were tested. An additional recombinant non-oxidisable all-serine form (3S) of HMGB1 was also tested to confirm the properties restricted to FR-HMGB1.

3.2. Hypothesis

Alarmins are elevated following fracture injury in both humans and mice, and have a direct effect on the osteogenic differentiation of hMSCs.

3.3. Results

3.3.1. Systemic levels of alarmins post-fracture in humans

It was important to first determine if there was a change in the systemic levels of alarmins following fractures in patients. To acquire early human plasma samples from patients who had sustained a fracture, and unfractured controls, I setup a collection network by engaging with staff at the John Radcliffe Hospital Clinical Biochemistry Laboratory (N. Mullee, T. James, and B. Shine), and the Kadoorie Centre for Critical Care Research and Education (P. Sangeetha, K. Lewis, E. Tutton, M. Costa, and K. Willett). The human plasma samples were from the patient's first in-hospital blood sampling, typically within 4 hours post-fracture. I also completed the research ethics forms and attained approval from all the necessary regulatory bodies (CTRG, REC, HRA, and OUH). After this six month long setup process, patient samples were collected over two months. The levels of the alarmins S100A8/A9 and HMGB1 were found to be significantly elevated in samples from patients who had sustained a fracture, as measured by ELISA (Figure 3.1 a). Healthy control unfractured samples were sourced from the John Radcliffe Hospital Blood and Transplant Department.

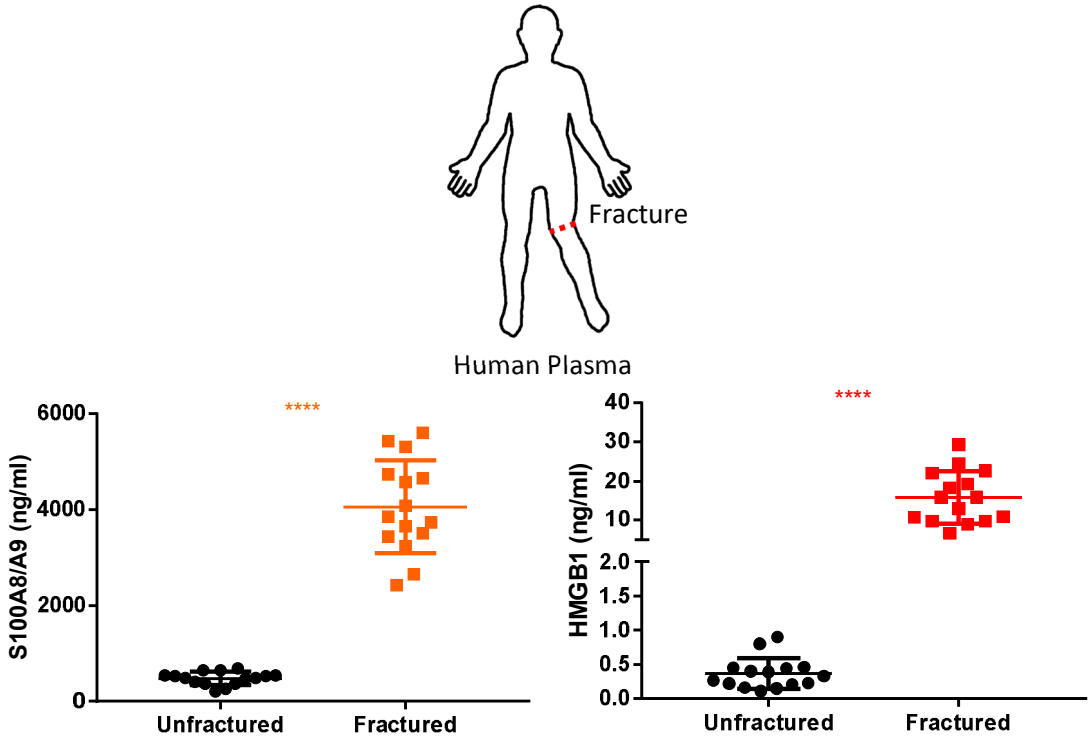

Figure 3.1 Systemic levels of alarmins post-fracture in humans. Plasma levels of S100A8/A9 and HMGB1 are elevated post-femoral fracture in patients, as measured by ELISA (n = 15 human fractured and unfractured donors). As the samples were de-identified, there was no information on the sex or age of the samples, only that patients had sustained a femoral fracture.

3.3.2. Direct effect of alarmins on human monocytes and human MSCs

The proinflammatory actions of S100A8/A9 and HMGB1 were validated by measuring the release of proinflammatory cytokines from monocytes on exposure to these reagents. A well-described technique for isolating primary human monocytes is by magnetic separation from human peripheral blood leucocyte cones[124,125]. Therefore, I engaged with staff at the John Radcliffe Hospital Blood and Transplant Department, and the Dustin Group (E. Kurtz), to gain access to human peripheral blood leucocyte cones. I also liaised with staff at the Centre for Clinical Vaccinology and Tropical Medicine (E. Clutterbuck, and A.J. Pollard) and at Miltenyi Biotec (C. Marchant) to gain access to a fully automated magnetically-activated cell separation machine (autoMACS Pro Separator, Miltenyi Biotec). This resulted in a reliable and local source of human peripheral blood mononuclear cells, and a consistent and efficient method for isolating primary human monocytes. For high quality alarmin proteins, the group already had a ready supply of high-quality S100A8/A9 proteins through a collaboration with T. Vogl (University of Münster, Germany). I initiated and co-ordinated a working understanding between our group, the Bianchi Group (San Raffaele University, Italy) and HMGBiotech (A. Preti), for an economically sustainable supply of HMGB1 proteins (50% off RRP), and validated the reagents with functional assays (Figure 3.2 a).

Exposure of freshly isolated human monocytes to S100A8, S100A9, or DS-HMGB1 but not FR or 3S-HMGB1, led to an increase of TNF in the media as measured by ELISA (Figure 3.2 a), which validated the function of these reagents. LPS, a PAMP, was used as a positive control. Subsequently the alarmins were tested for their direct effects on the osteogenic differentiation of hMSCs. In the presence of osteogenic media, hMSCs were treated with alarmins and ALP activity was measured as a marker of osteogenic differentiation at day 7[53,126]. None of the alarmins tested was found to have a direct effect on the osteogenic differentiation of hMSCs (Figure 3.2 b).

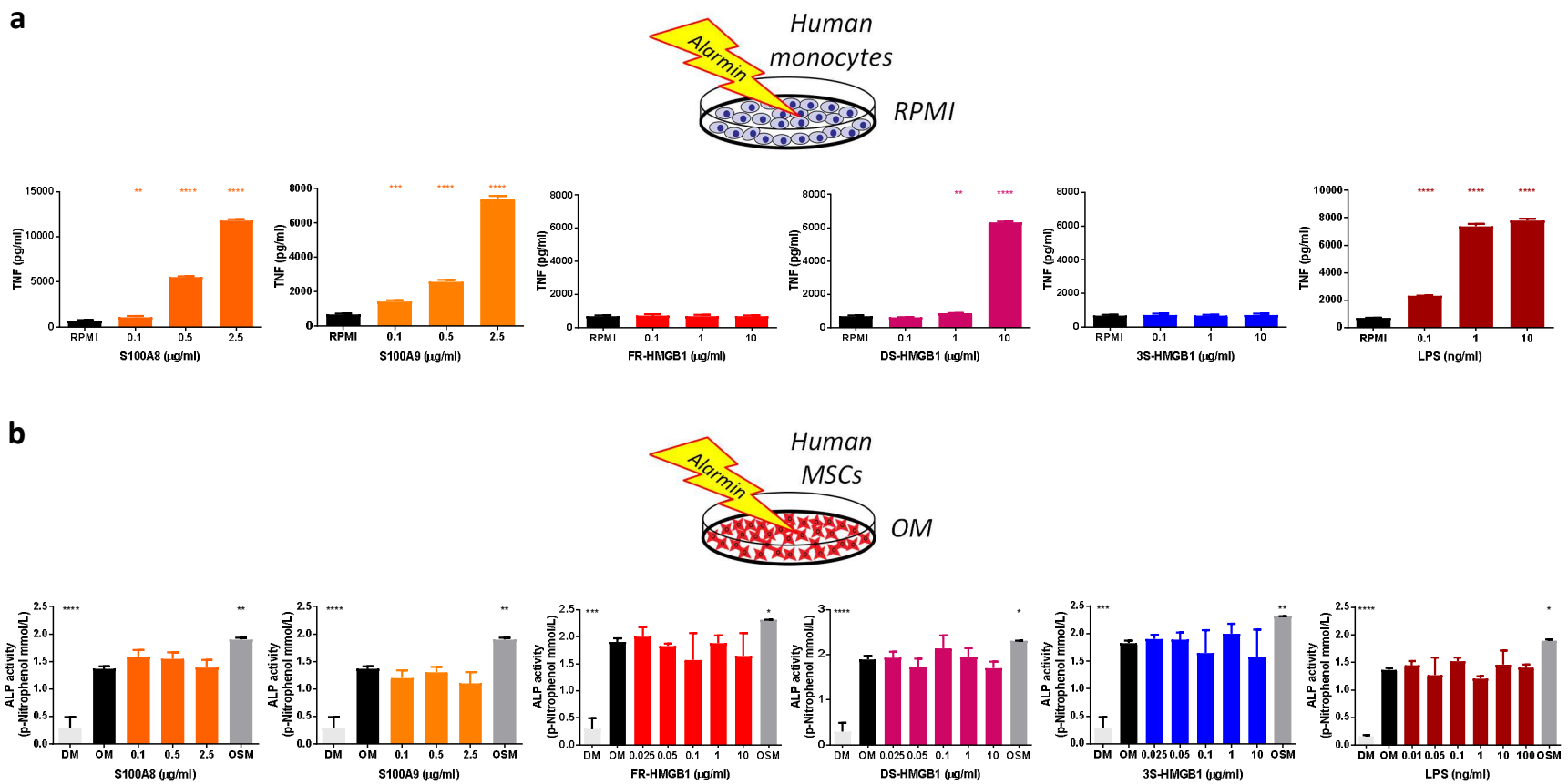

Figure 3.2 Direct effect of alarmins on human monocytes and human MSCs. (a) S100A8, S100A9, DS-HMGB1, or LPS induced the release of TNF from monocytes as measured by ELISA. (b) None of the alarmins tested had a direct effect on the osteogenic differentiation of hMSCs as measured by ALP activity. Representative graphs with similar results in 3 independent experiments; n = 3 monocyte and 3 hMSC donors; significance is versus RPMI or OM control. DM = maintenance media, OM = osteogenic media, OSM = oncostatin M (positive control).

3.3.3. Human monocyte mediated effects of alarmins on human MSCs

Our group had previously shown that immune cells play key roles in the fracture healing process[109]. In particular, it had been demonstrated that monocytes promoted the osteogenic differentiation of hMSCs by releasing the osteogenic factor oncostatin M (OSM)[53]. Therefore, it was possible that while the alarmins in question did not promote osteogenic differentiation directly, they could do so indirectly via activation of monocytes. To test this, human monocytes were first treated with alarmins. The resultant supernatant was subsequently transferred onto hMSCs and ALP activity quantified. S100A8, S100A9, DS-HMGB1 and LPS treated monocyte supernatants inhibited the osteogenic differentiation of hMSCs (Figure 3.3 a). As the release of OSM from monocytes is dependent on monocytes being in direct contact with hMSCs[53], it was possible that alarmins may have promoted osteogenic differentiation indirectly by a monocyte-contact dependant mechanism. To test this, monocytes were co-cultured with hMSCs and treated with alarmins. Treatment with S100A8, S100A9, DS-HMGB1 or LPS also inhibited the osteogenic differentiation of hMSCs (Figure 3.3 b).

hMSCs are known to have a long population doubling time, and in our hands it took a substantial amount of time to achieve confluency (8-10 days for 175cm^2 flask). In addition, large scale tissue culture was required to achieve the cell numbers necessary to perform these experiments which involved testing thirty experimental conditions, in technical and biological triplicate. Therefore to perform these experiments efficiently and because these combination monocyte-hMSC experiments required the simultaneous sample preparation of multiple peripheral blood leucocyte cones and hMSCs flasks followed by magnetic sorting of human monocytes from different donors, they were performed in conjunction with the post-doctoral scholar in our group, A.I. Espirito Santo.

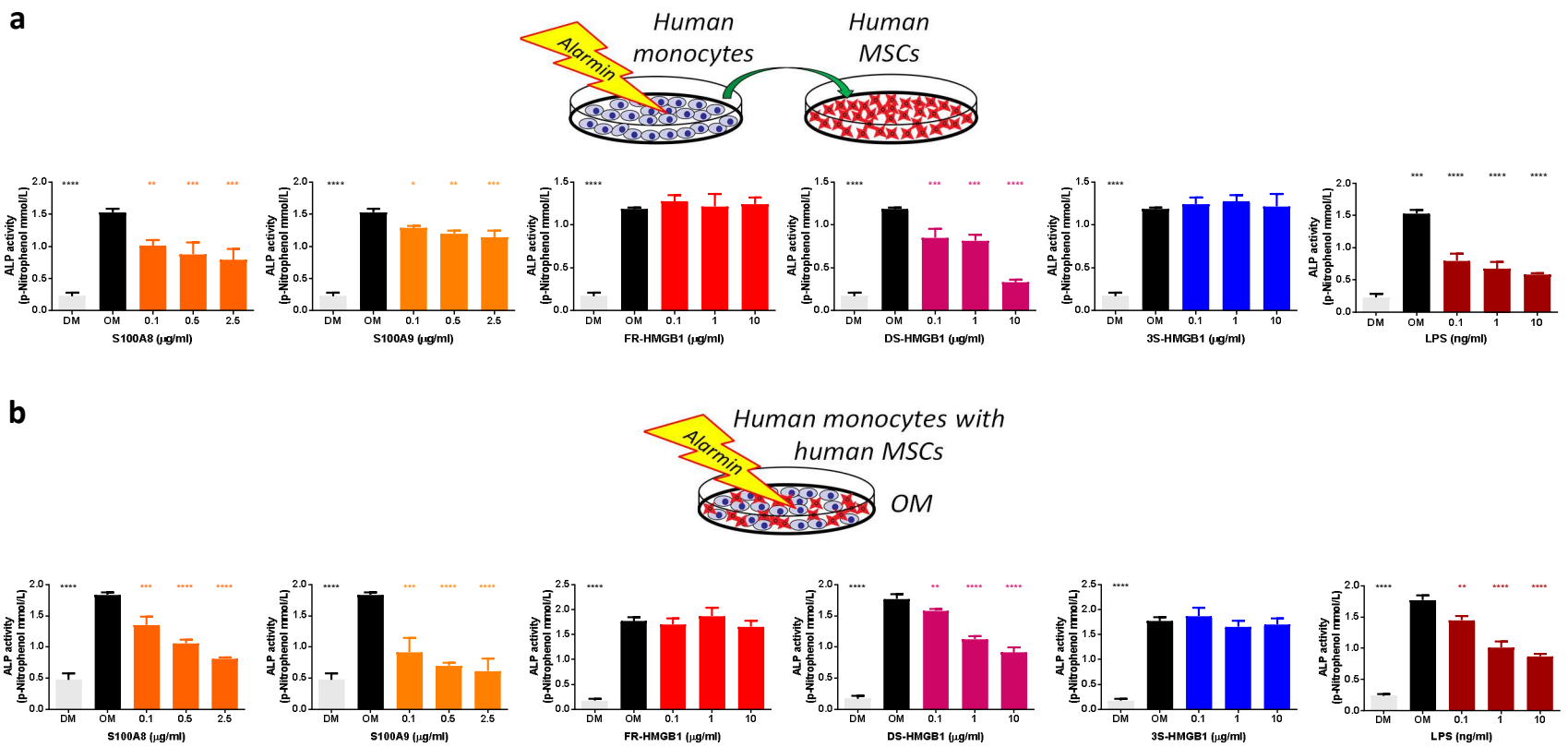

Figure 3.3 Human monocyte mediated effects of alarmins on hMSCs. (a) S100A8, S100A9, DS-HMGB1, or LPS treated monocyte supernatants inhibited the osteogenic differentiation of hMSCs, as measured by ALP activity. (b) Treatment of monocyte-hMSC co-cultures with S100A8, S100A9, DS-HMGB1 or LPS inhibited the osteogenic differentiation of hMSCs, as measured by ALP activity. Representative graphs with similar results in 3 independent experiments; n = 3 monocyte and 3 hMSC donors; significance is versus OM control. DM = maintenance media, OM = osteogenic media.

3.3.4. Pre-treatment effects of alarmins on human MSCs

As alarmins are amongst the earliest mediators released upon cell damage and death, I reasoned that soon following fracture, resident progenitor cells may be exposed to alarmins prior to osteogenic signals, which are upregulated gradually after injury[45,127]. Therefore I modelled this temporal sequence *in vitro* by pre-treating hMSCs with alarmins for 16 hours and subsequently incubating them with osteogenic media. Only pre-treatment with FR, or 3S-HMGB1 increased the osteogenic differentiation of hMSCs (Figure 3.4 a). A summary of the assays and results performed in this chapter are displayed in heatmap form (Figure 3.4 b).

a

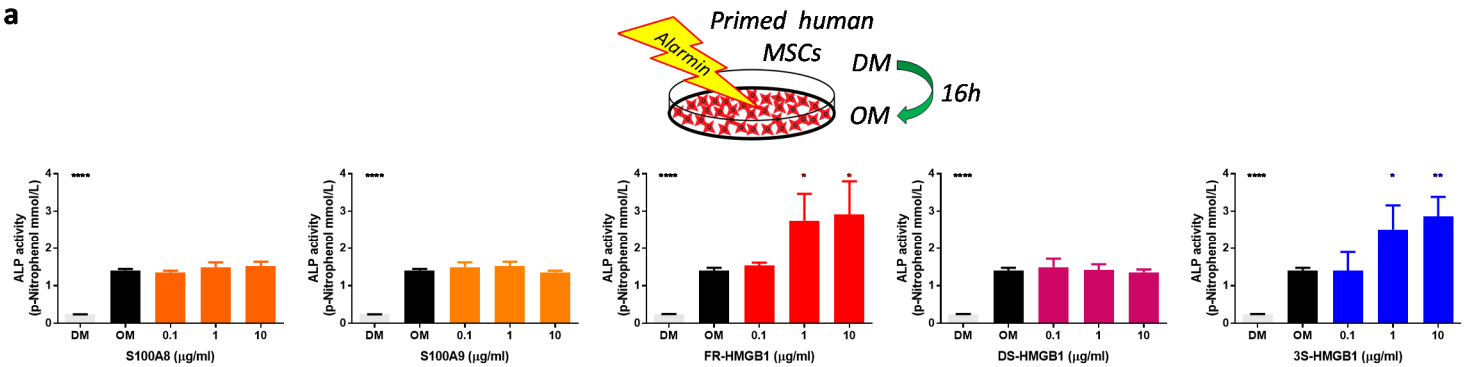

b

Early immune triggers		Elevated post-fracture in humans and mice	Inflammatory cytokine (TNF) release	Direct MSC	Monocyte supernatant	MSC-monocyte co-culture	Primed MSC
Alarmins/ DAMPs	S100A8						
	S100A9						
	FR-HMGB1						
	DS-HMGB1						
	3S-HMGB1						
PAMPs	LPS						

Figure 3.4 Priming effects of alarmins on human MSCs, and heatmap representation of total results. (a) Pre-treating hMSCs with FR or 3S-HMGB1 promoted osteogenic differentiation as quantified by ALP activity. Representative graphs with similar results in 3 independent experiments; n = 3 monocyte and 3 hMSC donors; significance is versus OM control. DM = maintenance media, OM = osteogenic media. (b) Heatmap representation of the assays performed to study the effect of alarmins on the osteogenic differentiation of hMSCs. Green = fold change >1, red = fold change <1, black = no fold change; colour brightness indicates dose trend.

3.4. Discussion

The local and systemic release of a variety of alarmins following a range of injuries in humans is well established[128]. However, it has not been shown previously that the alarmins S100A8/A9 and HMGB1 are released systemically following human fracture injury. As alarmins are released immediately after injury, I acquired the first in-hospital collection of human blood samples from patients who had sustained a femoral fracture. These samples showed a marked elevation in S100A8/A9 and HMGB1 proteins (4059 ± 971.6 ng/ml; 15.82 ± 6.68 ng/ml; mean ± SD) compared to unfractured controls (479.3 ± 136.2 ng/ml, 0.37 ± 0.23 ng/ml; mean ± SD). This systemic level HMGB1 post-fracture was significantly less than previously recorded levels following massive trauma (~550 ng/ml)[128], which indicated that that the systemic levels of HMGB1 post-injury were dependent on the severity of injury. This would be consistent with HMGB1 being released from injured cells, and more HMGB1 being released if there were more injured cells. In addition, the systemic levels of HMGB1 post-fracture were lower than the levels previously reported in local fracture haematoma post-injury (~30 ng/ml)[129], which indicated that the source of HMGB1 was the injury site. This was consistent with HMGB1 being released from injured cells, and the site of injury containing the injured cells. However it is possible that some HMGB1 may also have been released systemically from activated circulating immune cells[64].

To validate the alarmin reagents, they were functionally compared to LPS, because it is a known PAMP, which are the exogenous counterparts to DAMPS/alarmins, and potently induces the release of pro-inflammatory cytokines from human monocytes. S100A8, S100A9, DS-HMGB1, and LPS, but not FR or 3S-HMGB1, led to the release of TNF by monocytes. These findings are consistent with the known pro-inflammatory effects of S100A8, S100A9, DS-HMGB1, and LPS, and the lack of inflammatory effects of FR and 3S-HMGB1[86,128].

Following a fracture, a variety of progenitor cells, including MSCs[130,131], can contribute to the formation of new bone by undergoing osteogenic differentiation to become osteoblasts. ALP activity

is a reliable marker of osteogenic differentiation, and its *in vitro* induction is predictive of *in vivo* bone forming capacity[126]. To test whether alarmins could induce osteogenic differentiation, a series of experiments designed to study any direct or indirect osteogenic effects on human MSCs was carried out. Direct addition of S100A8, S100A9, FR, DS or 3S-HMGB1 did not affect the osteogenic differentiation of hMSCs. These results are at odds with a previous report that HMGB1 directly promoted the osteogenic differentiation of hMSCs[84]. However, explanations for these apparently conflicting results include the authors of the previous publication using a HMGB1 preparation which had an unknown redox state, a different and non-commercially validated source of hMSCs, and an ALP staining assay that required manual quantification, as opposed to the highly sensitive colorimetric ALP activity assay I used.

Previous work by this group showed that monocytes promoted the osteogenic differentiation of hMSCs by releasing the osteogenic factor oncostatin M (OSM) when they were in direct contact with hMSCs[53]. Since it is well-know that alarmins are able to affect the function of monocytes[128], it was possible that alarmins affected the osteogenic differentiation of hMSCs acted via their interactions with monocytes. To model this system *in vitro*, human monocytes were treated with alarmins and that supernatant was subsequently transferred onto hMSCs. In addition, co-cultures of monocytes and hMSCs were treated with alarmins. S100A8, S100A9, or DS-HMGB1 treated monocyte supernatants inhibited the osteogenic differentiation of hMSCs. Similarly, monocyte-hMSC co-cultures treated with S100A8, S100A9, or DS-HMGB1 exhibited inhibited osteogenic differentiation. A possible explanation for the inhibition of osteogenic differentiation is that S100A8, S100A9, and DS-HMGB1 induce the release of multiple mediators from monocytes, including inhibitors of osteogenic differentiation. In particular, I confirmed that S100A8, S100A9, and DS-HMGB1 induce the release of TNF from monocytes, and it has been previously shown that high levels of TNF inhibit the osteogenic differentiation of hMSCs *in vitro*[132].

The classic *in vitro* model for determining whether a molecule has an effect on osteogenic differentiation involves directly treating cells in the presence of a medium which contains osteogenic signals. However, this assay does not reflect the *in vivo* temporal sequence of molecular events following a fracture, especially as it relates to alarmins. Elevated levels of alarmins were present in samples collected within hours after fracture injury. In comparison, osteogenic signals are only gradually upregulated days after fracture injury[127]. Therefore I reasoned that *in vivo*, MSCs would be exposed to alarmins prior to osteogenic signals. I modelled this molecular temporal sequence *in vitro* by pre-treating hMSCs with alarmins prior to exposing them to osteogenic media. Under these conditions, only pre-treatment with FR or 3S-HMGB1 increased the osteogenic differentiation of hMSCs. The relevance of this *in vitro* finding at the tissue-level *in vivo* will be presented in the following chapter.

In summary, the work described in this chapter shows that the alarmins S100A8/A9 and HMGB1 are elevated in the systemic circulation soon after fracture injury in humans, and only pre-treatment with FR or 3S-HMGB1, which do not induce pro-inflammatory cytokine production, promoted osteogenic differentiation. These findings show that HMGB1 in its fully reduced form may be an important early mediator for fracture healing, and FR and 3S-HMGB1 may represent potential therapeutic targets for the acceleration of fracture healing (Figure 3.5).

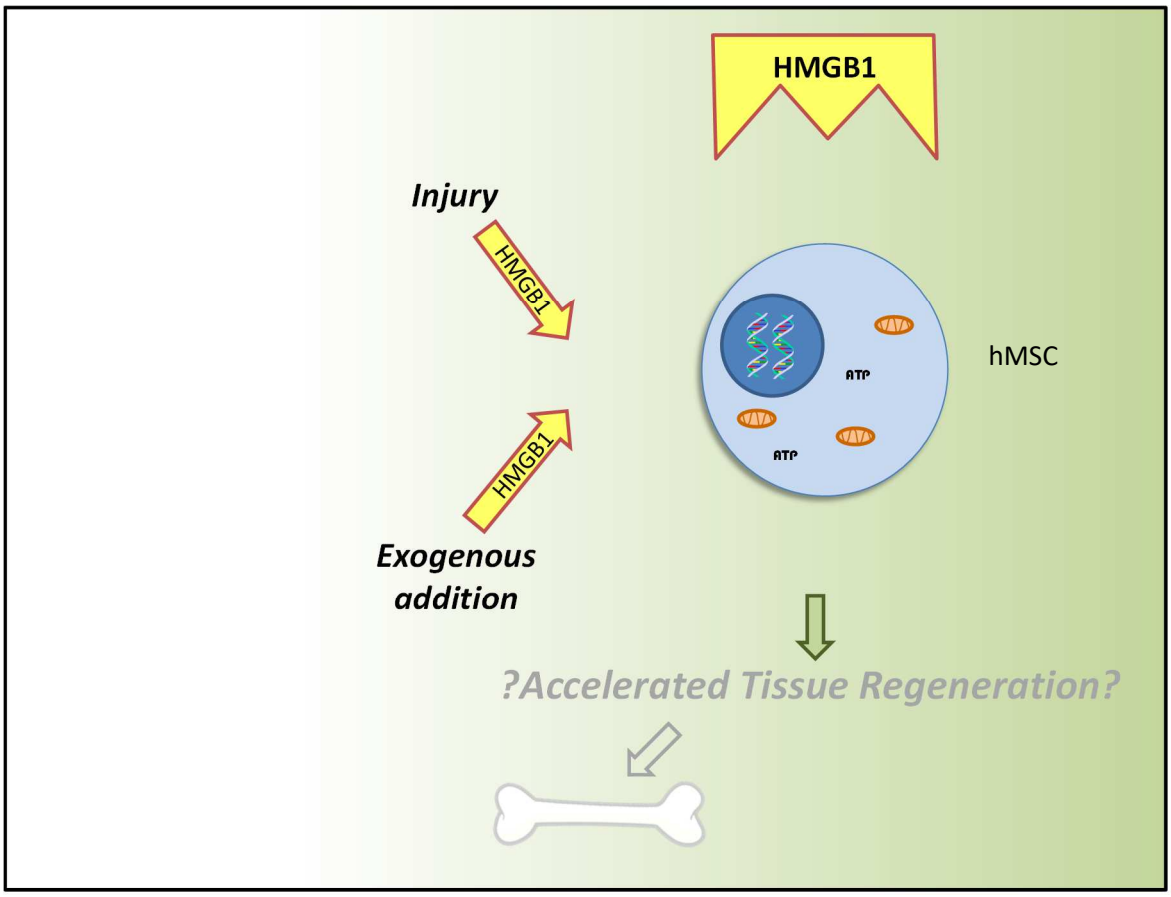

Figure 3.5 Schematic of findings from this chapter. Human clinical samples and primary human cells identified HMGB1 as a candidate molecule to accelerate fracture healing. Its *in vivo* effects and significance will be discussed in the following chapter.

Chapter 4. Alarmins in murine samples and their in vivo effects

4.1. Introduction

Based on the findings that pre-treatment with FR or 3S-HMGB1 increased the osteogenic differentiation of hMSCs *in vitro*, I sought to assess if this was relevant at the tissue-level *in vivo*. With the publication of consensus guidelines calling for a global update to fracture models[133], and the limitations of the existing fracture model within the group, it was clear that my studies needed a more versatile fracture model. In particular, I needed an animal model and analytical methodology that would allow me to longitudinally follow and quantify the course of fracture healing *in vivo*, and also permit functional mechanical strength testing at the final time point.

In routine orthopaedic practice, and in clinical trials, longitudinal radiographic investigations are the most widely used tool for assessing the progression of fracture healing. Therefore, similar assessment of murine models of fracture healing would have increased translational relevance. Radiographic assessments of bone tissue are also well-known to correlate well with histological findings[134,135], and have the important added advantage of being non-destructive, thereby allowing longitudinal assessment of each animal. Following the optimisation of the model and analyses methods, it would be important to confirm that there was a systemic increase in alarmins post-fracture in this animal model to ensure relevance to the human condition. Subsequently, the effect of modulating the alarmins pathway by gain of function and loss of function experiments, as informed by the *in vitro* data in the previous chapter, could be assessed *in vivo*.

4.2. Hypothesis

The development of a murine femoral fracture model stabilised with an external fixator would permit *in vivo* longitudinal assessment of fracture healing over a time course, and terminal mechanical strength testing. Post-fracture release of HMGB1 and S100A8/9 in humans would be reflected in this animal model and modulation of alarmin pathways would affect the healing of fractures in this model.

4.3. Results

4.3.1. Optimisation of murine fracture model

To assess if fracture healing was accelerated the ideal animal model would allow serial *in vivo* measurements over a time course. This would be possible using *in vivo* microCT assessments. However, metal across the fracture site, for example with intramedullary fixation, leads to radiographic scatter and interference, and the consequent artefact would preclude accurate analysis. Therefore, a model utilising an external fixator was required. Furthermore, such an approach would provide a consistent level of fracture stability compared to simple intramedullary pin fixation, which lacks rotational and axial stability, and thereby reduces the number of animals required to attain statistical power. A critical functional assessment of fracture healing is mechanical strength testing, and the femur is far better suited to bend testing with its cylindrical cross-section and uniform profile as compared to the triangular cross-section and tapered profile of the tibia (Figure 4.1 a, b). Furthermore, when the animal begins to weight bear through the hindlimb, tibial fracture models occasionally have the unintended consequence of also incurring a fibula fracture. This fibula fracture causes a second callus, which tends to merge with the tibial callus and makes its analyses impossible (Figure 4.1 a). Analysis of the fracture callus would also be facilitated by a uniform osteotomy configuration. Therefore, I decided to use a Gigli wire saw to create a uniform osteotomy, instead of bone clippers which caused irregular and comminuted fractures (Figure 4.1 a). A femoral fracture model would also provide a pocket following dissection of the soft tissue where soluble exogenous materials can be injected (Figure 4.1 c). Finally, it was important that the external fixator body was small and light so as not to encumber movement of the animal (Figure 4.1 d).

Having decided upon a femoral fracture model that would be stabilised with an external fixator, I experimented with a variety of designs and materials for the fixator body and mounting pins (Table 4.1). I eventually settled on a commercially available jig (RISystem) (Figure 4.1 b), where the fixator body was made from radiolucent polyether ether ketone (PEEK), and the pins from high-speed

stainless steel. The combined weight of the fixator body and mounting pins was 0.2 g, which only represented 1% of an average 12 week old female C57BL/6J mouse. To learn the operative technique and animal care procedures, I engaged with S. Zwingenberger (Technische Universität Dresden, Germany) who had extensive experience with the use of this external fixator model, and organised for him to come to our institute to teach me his model and technique. Thereafter, I wrote a new animal license protocol, and went through the nine-month long animal license amendment process which involved multiple meetings with the institutional vets, the institutional ethics committee, and the Home Office inspector. I repeated this process when the entire animal license was due to be renewed, and again when institutional vets decided the technical wording of the protocol could be further refined.

The 12-14 week old female C57BL/6J mice that were planned for experiments due to their ready availability and common use in the fracture healing field[108,109] were significantly smaller (20 g) than the 40 g mice previously used by S. Zwingenberger for this procedure[111]. Therefore, I spent substantial additional time practising and refining my operative skills. Even with the larger 40 g mice, this model necessitates a surgical assistant for dynamic positioning of the leg and fixator. I was assisted in this capacity by A.I. Espirito Santo. At the time of writing, we have performed 511 operations, with a 0% mortality rate, 0% infection rate, 0% early cull rate, and have taught it to the Chenu Group from the Royal Veterinary College (Figure 4.1 e).

S. Zwingenberger had optimised a large osteotomy gap size to create a lack of physical tissue scaffold to consistently attain non-unions[111]. Physical tissue scaffold is a necessary component of the normal fracture healing process[136], so such a substantial defect may have overshadowed and confounded my ability to assess if targeting alarmins could accelerate the normal fracture healing process. Therefore, a fracture model, with a less dramatic physical tissue scaffold defect, which consistently attained union was more suitable. After experimenting with a variety of osteotomy gap sizes (Table 4.2), I settled on the gap size of 0.5 mm because it was a reproducible gap size in my

hands, and it was also the largest gap size tested where 100% of mice still achieved union by day 28. This provided a consistent baseline of controls, whilst still being sufficiently long enough for an improvement or delay in the healing process to be detectable.

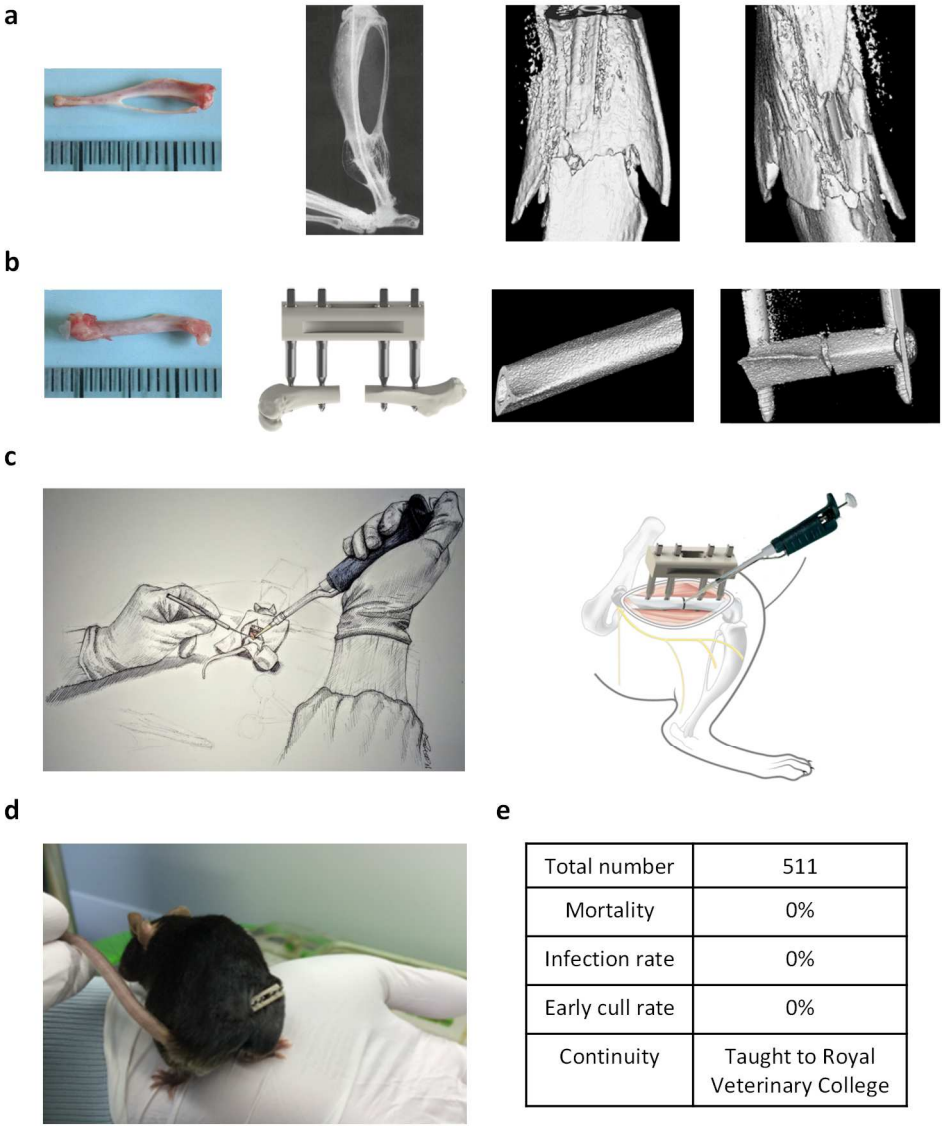

Total number	511
Mortality	0%
Infection rate	0%
Early cull rate	0%
Continuity	Taught to Royal Veterinary College

Figure 4.1 Optimisation of murine fracture model. (a) Photo of murine tibia[133], radiograph[133] and 3D micro-CT reconstruction of the murine tibial fracture with simple intramedullary pin fixation. (b) Photo of murine femur[133], illustration of external fixator assembly[111] and 3D microCT reconstructions of murine femoral fracture with external fixator. (c) Illustration of the administration of local treatments[111], courtesy of F. Corra. (d) Photograph of external fixator *in situ*. (e) Table of animal welfare outcomes of the femoral fracture model.

Table 4.1 External fixator components and material optimisation.

External fixator components	External fixator materials	Acceptability
Fixator body	3D printed PLA (Radcliffe Science Library, University of Oxford) 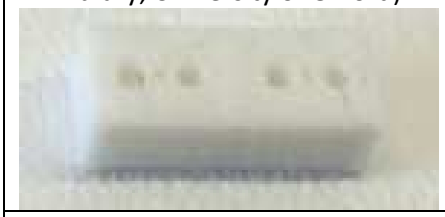	Not malleable enough to insert mounting pins
	3D printed acrylic (Shapeways) 	Eaten away *in situ* by mice
	Casted PEEK (RISystem) 	Acceptable
Mounting pins	High carbon steel (Physics Department, University of Oxford) 	Too brittle
	Partially titanium coated high speed steel (Proops Brothers) 	Corrodes after autoclaving
	High-speed stainless steel (RISystem) 	Acceptable

Table 4.2 Osteotomy gap size optimisation. n = 10 for each group.

Osteotomy gap size (mm)	Rate of union at 28 days	Acceptability
0.3	100%	Acceptable 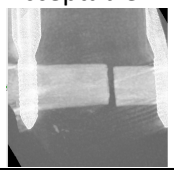
0.5	100%	Acceptable 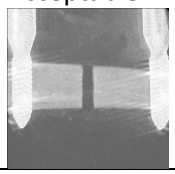
0.7	90%	1. High rate of inconsistent osteotomy gap size (90%) 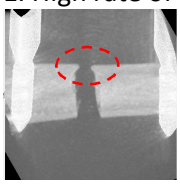 2. High rate of metal Gigli saw pieces left *in situ* (40%) 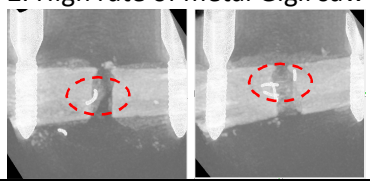
1.5	20%	1. High rate of inconsistent osteotomy gap size and shape (100%) 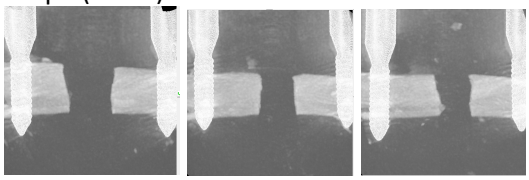 2. High non-union rate (80%) D0 D28 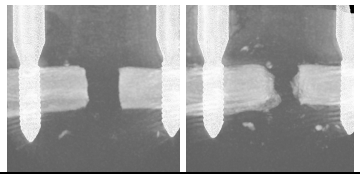

4.3.2. Systemic levels of alarmins post-fracture in mice

Following the optimisation of the murine fracture model, I sought to validate it with respect to human fractures, specifically regarding systemic alarmin levels post-fracture. Systemic blood samples were collected from mice 3 hours post-fracture and there was a marked elevation in the plasma levels of S100A8/A9 and HMGB1, as measured by ELISA (Figure 4.2). This showed that the murine femoral fracture model reflects the level of trauma and tissue injury experienced by human patients suffering femoral fractures, as assessed by elevated circulating levels of alarmins. The elevated systemic levels of HMGB1 post-fracture that I measured was also concordant with a previous study[137], that also used a murine femoral fracture model, and found elevated levels of HMGB1 at 1h, 4h and 6h post-fracture.

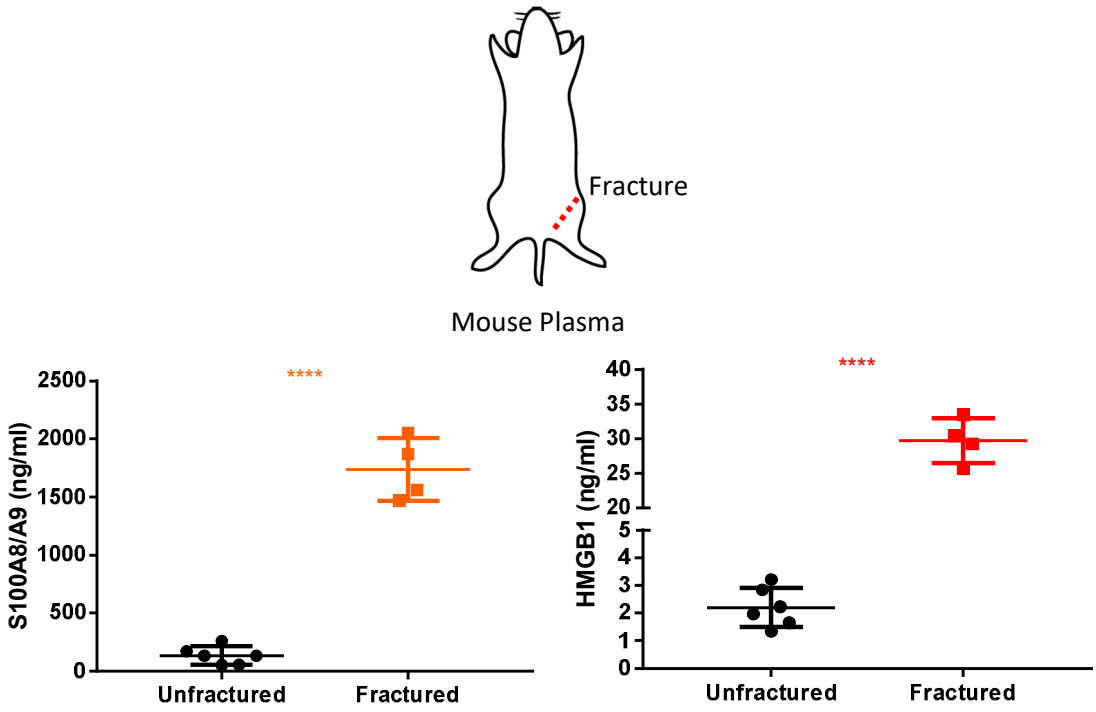

Figure 4.2 Systemic levels of alarmins post-fracture in mice. Plasma levels of S100A8/A9 and HMGB1 are elevated post-femoral fracture in mice, as measured by ELISA (n = 6 mouse unfractured and 4 fractured donors).

4.3.3. Optimisation of in vivo microCT analyses

Fluoroscopy images generated by the screening process of *in vivo* microCT clearly showed the classical healing pattern of fracture healing, progressing from a visible gap to a fusiform callus through to a 'flatter' callus during the remodelling phase (Figure 4.3) (ref). The 3D voxel co-registration function in the microCT analyses software permitted alignment of samples scanned at different time points so that new tissue formed was clearly visualised and analysed (Figure 4.4). Therefore, despite it being a lengthy process, with a simple two condition experiment requiring the analyses of 160 data points (1 experimental and 1 control group, 10 mice per group, and 8 imaging time points), I was confident that the methodology would accurately quantify and compare the microCT parameters of samples at each time point.

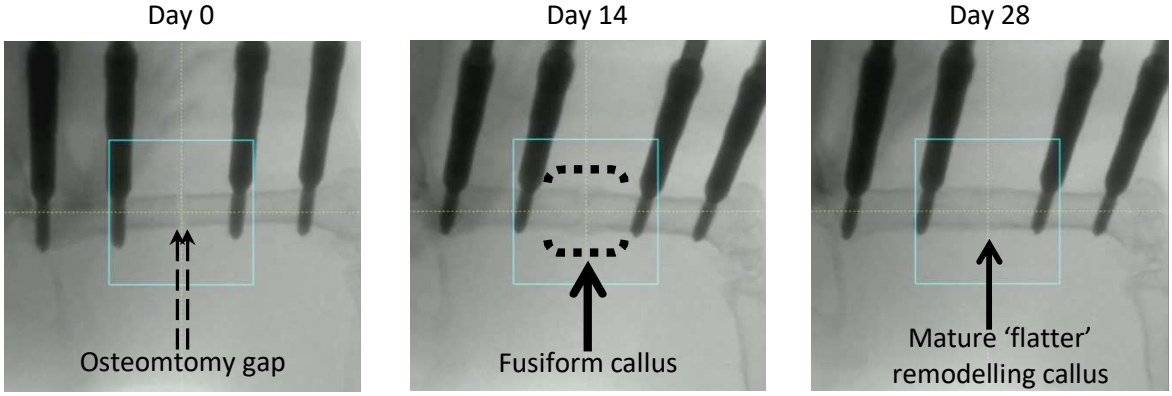

Figure 4.3 *In vivo* fluoroscopy scans of a single mouse over a time course. Representative scan at day 0 clearly shows the osteotomy gap, at day 14 there is the classical fusiform early callus, and at day 28 the callus is 'flatter' during the remodelling phase.

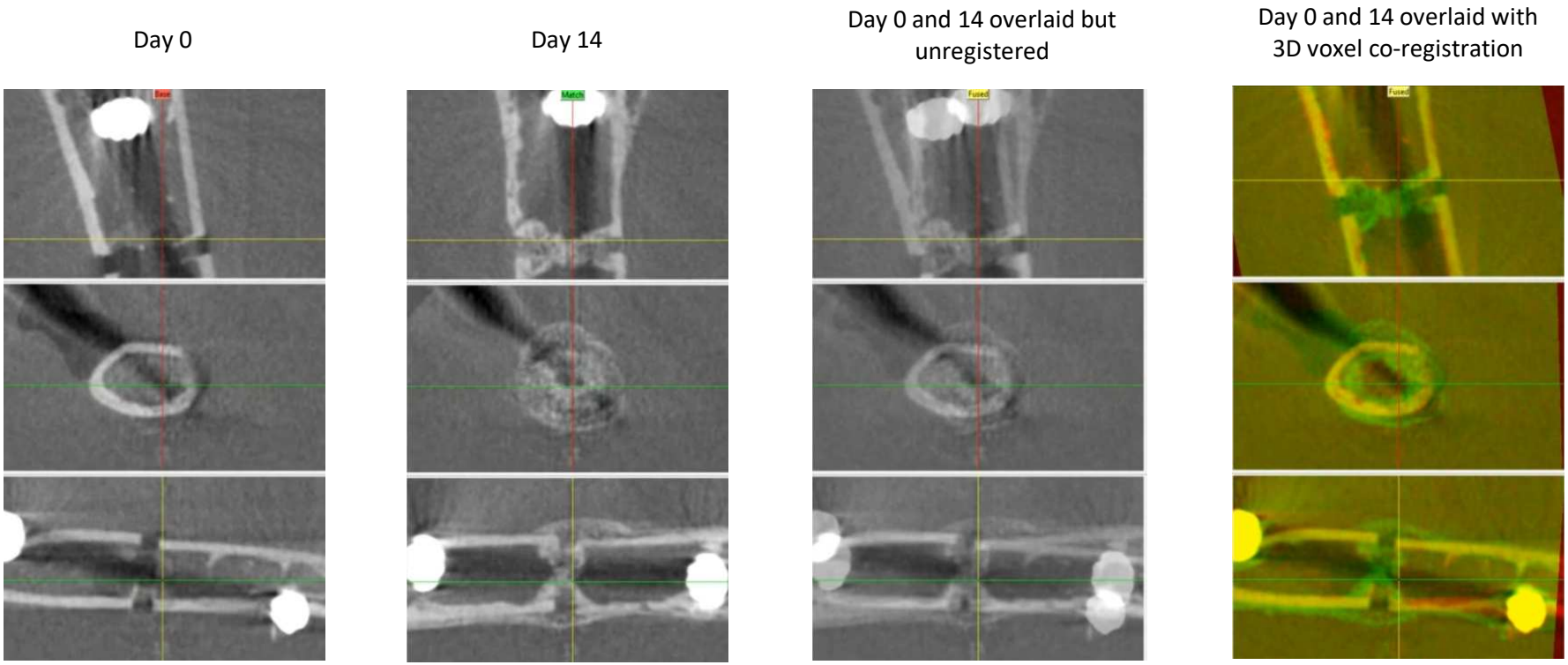

Figure 4.4 Co-registration of *in vivo* microCT images. Overlaying images captured at different time points with 3D voxel co-registration permits accurate visualisation and measuring of new skeletal tissue (green).

To quantify the amount of accelerated healing, I sought to compare the entire callus volume data sets (Figure 4.5 a). The F-test facilitated the statistical comparison of curves, and together with the mathematical biologists O. Dushek (Sir William Dunn School of Pathology), C. Peele (The Kennedy Institute of Rheumatology) and K. Cai (University of New South Wales, Australia), we generated suitable mathematical models with a high fidelity of fit for our data points. The three equations we generated and tested were:

$$f_1(t) = at^n . e^{\frac{-t^m}{b}}$$

$$f_2(t) = \frac{a}{1 + e^{-k(t-c)}} + \frac{b . e^{-k(t-c)}}{[1 + e^{-k(t-c)}]^2}$$

$$f_3(t) = \frac{a . t^2}{(t-c)^2 + b}$$

$t = time, ie. x\ axis$

$f(t) = a\ function\ of\ time, ie. y\ axis$

$a, b, c, k, m, n = programmable\ constants$

The best goodness of fit (R^2) was consistently achieved with $f_3(t)$ (Figure 4.5 b), so this was used for all future callus volume curve fittings.

a

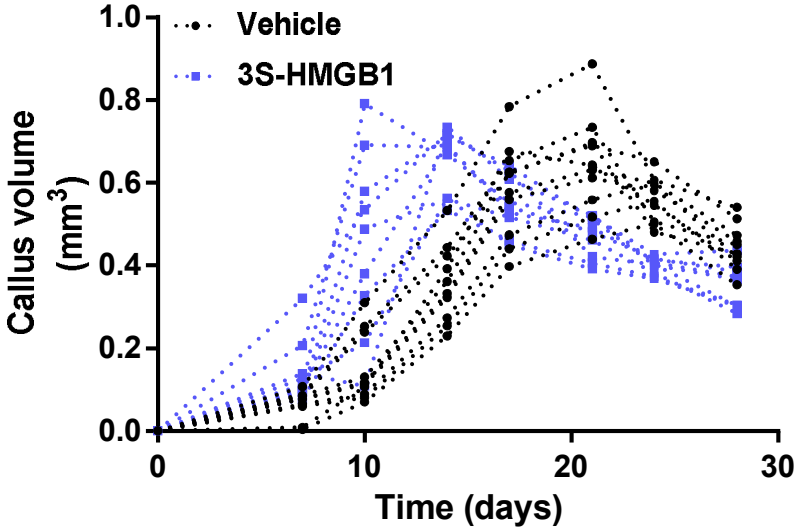

b

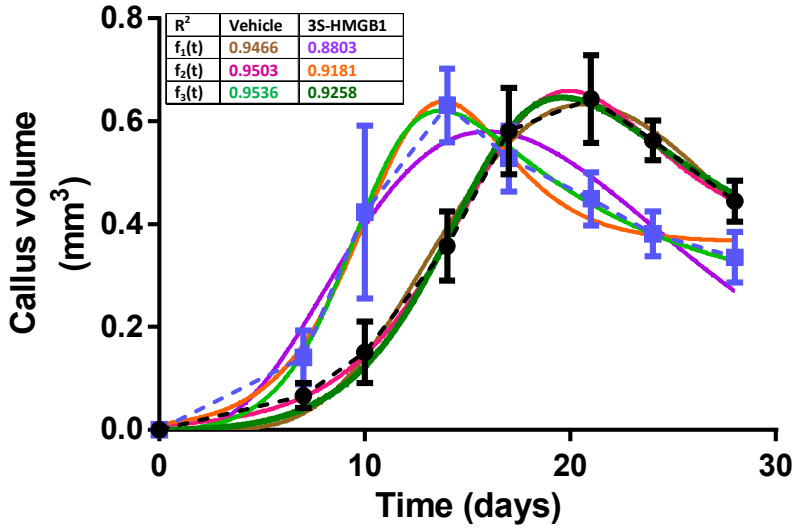

Figure 4.5 Mathematical modelling and curve fitting of microCT callus volume data. (a) Callus volume shown for each individual animal in the experiment (n =10 for each group). (b) Callus volume data fitted to various mathematical models and displaying their goodness of fit (R^2) (n =10 for each group).

4.3.4. Effect of exogenous HMGB1 on fracture healing

With the fracture model and microCT analyses optimised, the effect of exogenous HMGB1 on fracture healing was tested. The *in vitro* assays in the previous chapter revealed that only FR and 3S-HMGB1 improved osteogenic differentiation, therefore to adhere to the reduction and refinement principles of the 3R guidelines I focussed on the *in vivo* effects of FR and 3S-HMGB1. Both these redox forms of HMGB1 accelerated healing, which was apparent on visual inspection of *in vivo* microCT radiographs (Figure 4.6 a) and evidenced by left shifts of the callus volume and the callus bone mineral density curves. The acceleration of healing was quantified as 21.4% and 29.8% respectively (Figure 4.6 b). This accelerated healing was confirmed with functional testing of the femurs at day 28, which showed that fractured femurs treated locally with FR or 3S-HMGB1 had significantly higher mechanical strength compared to vehicle controls (Figure 4.6 c). In addition, a range of doses of 3S-HMGB1 was administered and bend testing showed a dose dependant increase in mechanical strength (Figure 4.7). The range of doses was chosen based on previous literature which had shown improved healing with 20 mg/kg and 10mg/kg in skin and heart injury models[128], respectively, albeit using a HMGB1 preparation which had an unknown redox state, and the Bianchi Group (E. Venereau, San Raffaele University, Italy), kindly informing us they had unpublished data of efficacy at 0.75 mg/kg and 7.5 mg/kg in a cardiotoxin model of injury, using the highly purified proteins from HMGBiotech, which we were also using.

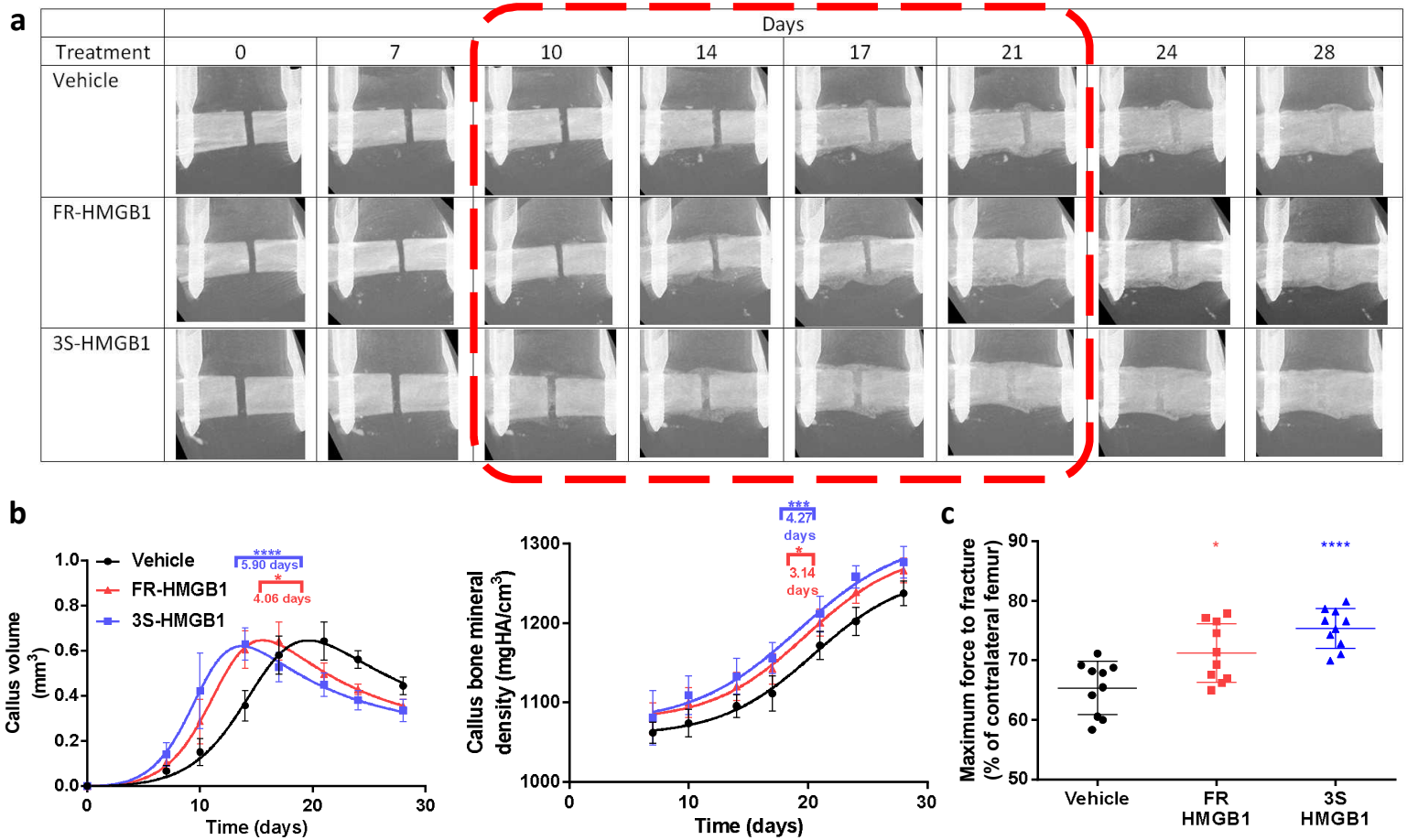

Figure 4.6 Effect of exogenous HMGB1 on fracture healing. (a) Representative *in vivo* microCT radiographs, (b) callus volumes, callus bone mineral densities, and (c) mechanical strength of FR and 3S-HMGB1 treated fractures showing accelerated fracture healing compared to vehicle controls (n = 10 for each group).

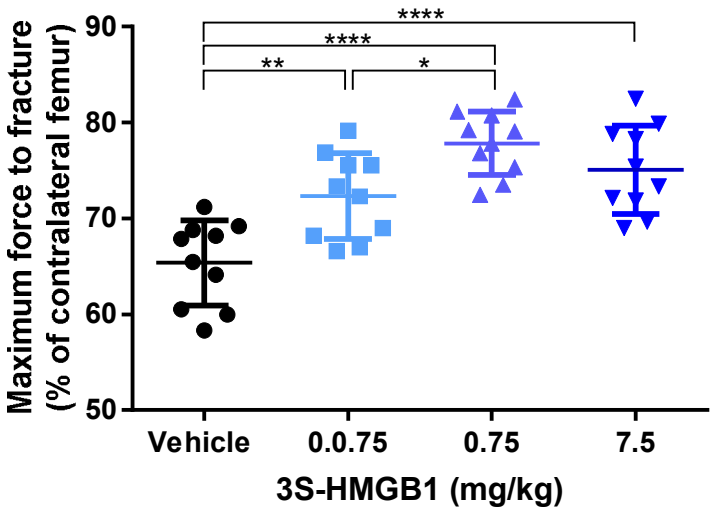

Figure 4.7 Effect of exogenous 3S-HMGB1 on fracture healing. Dose dependant increase in mechanical strength following exogenous 3S-HMGB1 treatment (n = 10 for each group).

4.3.5. Generation and validation of inducible Hmgb1$^{-/-}$ mice

The increase in resistance to bending force seen with exogenous administration of FR or 3S-HMGB1, led me to next examine the effects of genetic loss of function of HMGB1, to determine the significance of endogenous HMGB1 to the fracture healing process. As HMGB1 is ubiquitous and its release in the fracture environment would originate from multiple cell types that have been injured, and constitutional gene deletion of HMGB1 was perinatally lethal[138], I sought to generate inducible whole body *Hmgb1*$^{-/-}$ mice. To do this I engaged with T. Taniguchi, H. Yanai, and J. Nishio (University of Tokyo, Japan) to source *Hmgb1*$^{fl/fl}$ mice, and the Vincent Group (P. Sacitharan, J. Zarebska, and T. Vincent) to source *Rosa Cre-ER*$^{T2+/+}$ [139] mice. I wrote the institutional approval and transfer forms, and after the 11-month process to transfer and receive the *Hmgb1*$^{fl/fl}$ mice, they were crossed with *Rosa Cre-ER*$^{T2+/+}$ mice. After five months a colony of *Hmgb1*$^{fl/fl}$ *Rosa Cre-ER*$^{T2+/+}$ mice, otherwise known as inducible whole body *Hmgb1*$^{-/-}$ mice, was established. I did not observe any untoward animal mortality. Following tamoxifen administration, the loss of intracellular HMGB1 in skeletal, bone marrow, and muscle cells was validated by intracellularly staining and flow cytometry (Figure 4.8 a). There was a reduction of intracellular HMGB1 protein of 92%, 94% and 86% respectively (Figure 4.8 b). I also validated the loss of extracellular HMGB1 by collecting systemic blood samples from *Hmgb1*$^{-/-}$ mice 3 hours post-fracture (Figure 4.8 c) and measured the levels of HMGB1 by ELISA. *Hmgb1*$^{-/-}$ mice had substantially less extracellular HMGB1 than fractured *Hmgb1*$^{fl/fl}$ mice and these levels were equivalent to those seen in the plasma of unfractured *Hmgb1*$^{-/-}$ mice (Figure 4.8 d).

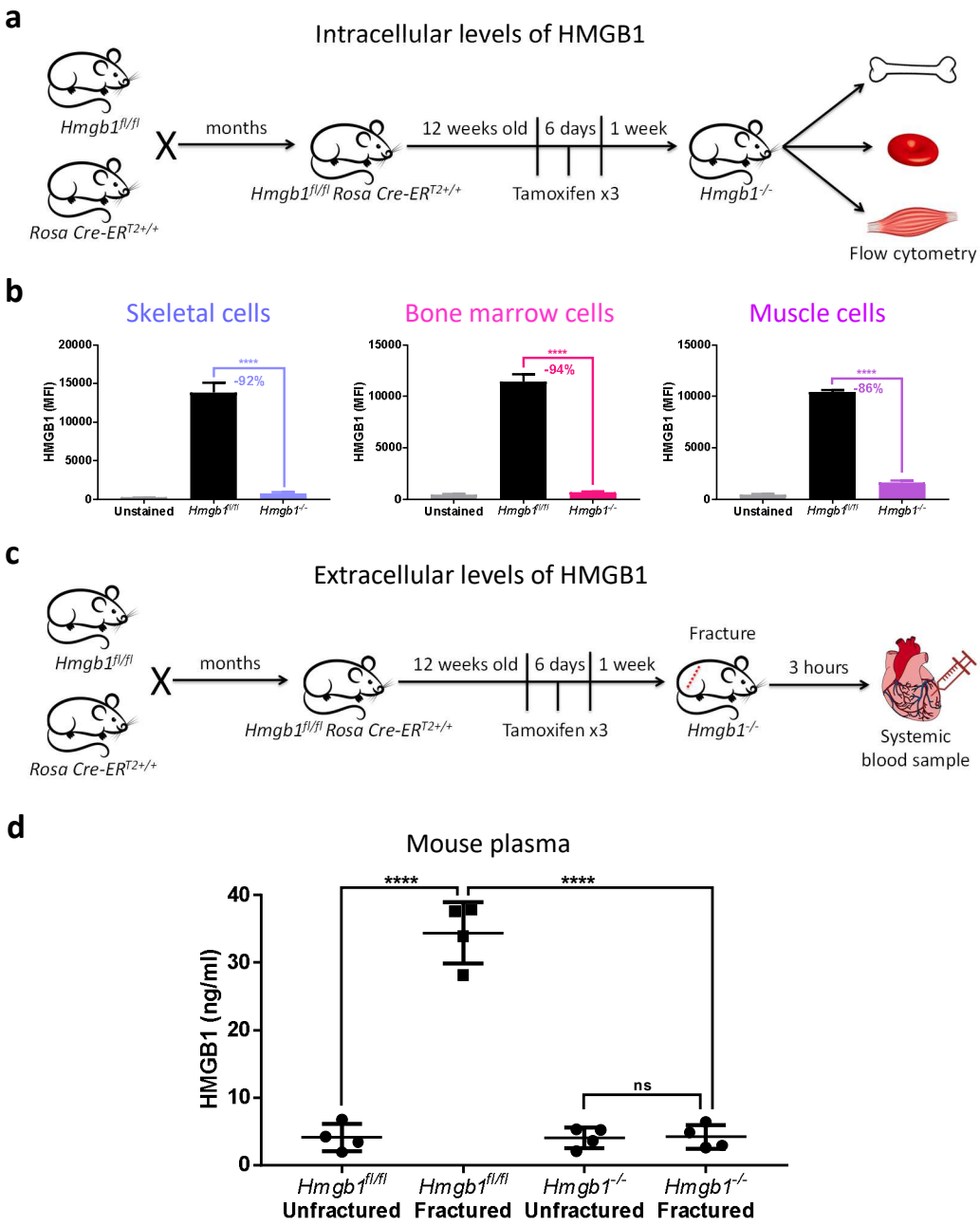

Figure 4.8 Generation and validation of inducible *Hmgb1*$^{-/-}$ mice. (a) Schematic for determining intracellular HMGB1 in *Hmgb1*$^{-/-}$ mice. (b) Skeletal, bone marrow, and muscle cells from *Hgmb1*$^{-/-}$ mice showed markedly reduced intracellular HMGB1 compared to *Hmgb1*$^{fl/fl}$ controls, as measured by intracellular staining and flow cytometry (n = 4 for each group). (c) Schematic for determining extracellular levels of HMGB1 post-fracture in *Hmgb1*$^{-/-}$ mice. (d) Plasma levels of extracellular HMGB1 were markedly lower in *Hmgb1*$^{-/-}$ fractured mice compared to *Hmgb1*$^{fl/fl}$ fractured mice, and equivalent to *Hmgb1*$^{-/-}$ unfractured mice, as measured by ELISA (n = 4 for each group).

4.3.6. Effect of genetic deletion of HMGB1 on fracture healing

With the successful generation and validation of inducible whole body *Hmgb1*$^{-/-}$ mice, we challenged them with the fracture model and assessed any effect on the fracture healing process. *Hmgb1*$^{-/-}$ mice displayed markedly delayed and impaired fracture healing (Figure 4.9 a), with a smaller and slower formed callus volume and lower callus bone mineral density at all time points (Figure 4.9 b). The bridging callus was also significantly weaker on functional testing compared to *Hmgb1*$^{fl/fl}$ controls (Figure 4.9 c). The healing curves and mechanical strength of fractured femurs from *Hmgb1*$^{fl/fl}$ controls were similar to those from wild type C57BL/6J.

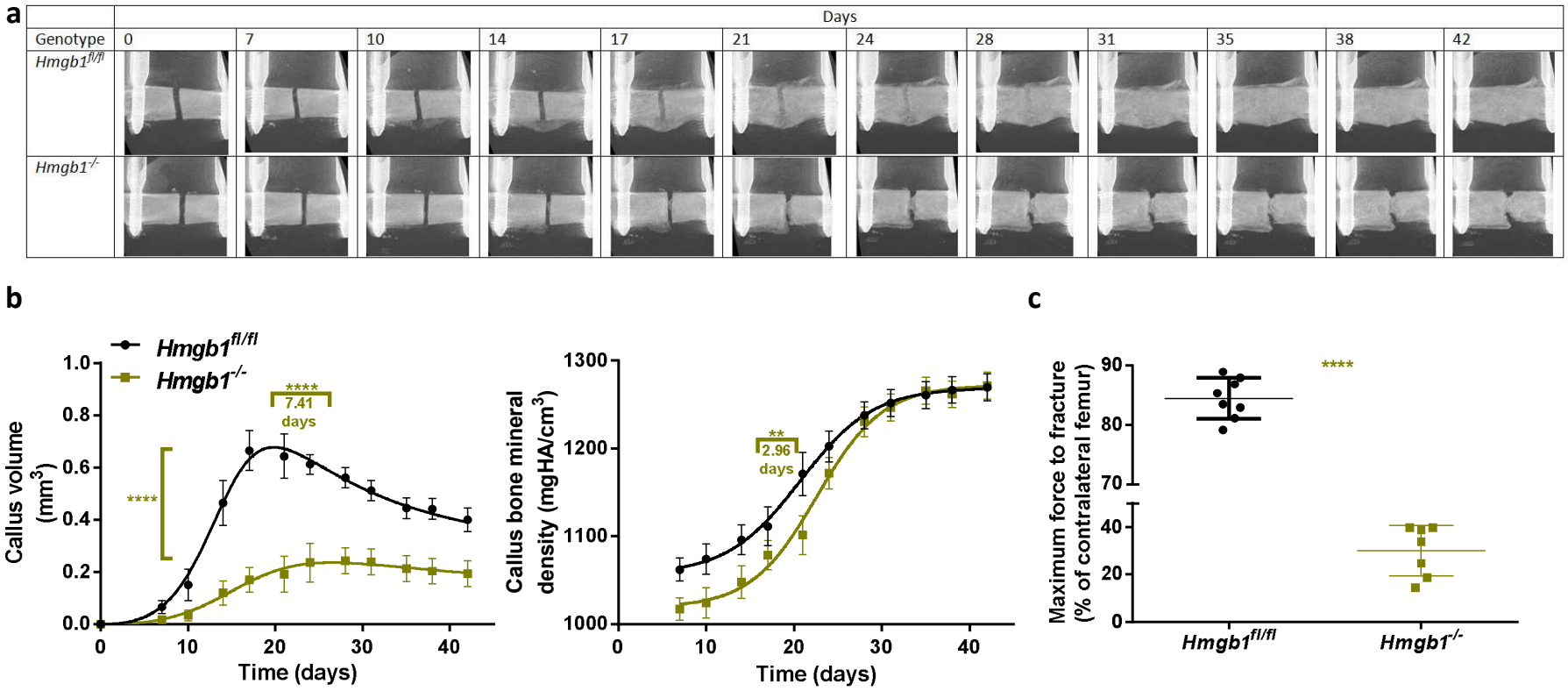

Figure 4.9 Effect of genetic deletion of HMGB1 on fracture healing. (a) Representative *in vivo* microCT radiographs, (b) callus volumes, callus bone mineral densities, and (c) mechanical strength of *Hmgb1*$^{-/-}$ fracture callus showing a markedly delayed and impaired fracture healing process compared to *Hmgb1*$^{fl/fl}$ controls (n = 7 *Hmgb1*$^{-/-}$, and 8 *Hmgb1*$^{fl/fl}$ *mice*).

4.4. Discussion

The role of HMGB1 in fracture healing is unknown. Based on the *in vitro* result that pre-treatment with FR or 3S-HMGB1 promoted osteogenic differentiation, I sought to assess if exogenous administration of HMGB1 could accelerate fracture healing *in vivo*. With a consensus paper in the fracture healing field strongly supporting mechanical strength testing as a critical healing parameter, and urging for an update from the current practice of using tibial fracture models with simple intramedullary pin fixation, there was a clear need to seek out a new model[133]. In order to study the acceleration of healing, we would need a model that permitted serial *in vivo* measurements over a time course in the same animal. Therefore, after a thorough review of the existing models, I determined that a femoral fracture model stabilised with an external fixator and healing assessed using *in vivo* microCT and terminal mechanical strength testing would be most suitable for our purposes.

Subsequently I extensively optimised and refined the materials and methodology of the protocol. I then demonstrated that there was a rise in systemic levels of S100A8/A9 and HMGB1 levels post-fracture in mice, which mirrored the circulating levels of alarmins in humans post-fracture. This confirmed that the fracture model accurately reflected the human fracture condition with regards to elevated levels of alarmins post-fracture. It was also concordant with HMGB1 being a highly evolutionarily conserved molecule. Thereafter I optimised the analyses of the *in vivo* microCT data using suitable mathematical models to curve fit the data. This allowed the comparison of entire healing curve data sets to definitively quantify the acceleration of healing.

Following optimisation of the methodology, exogenous FR or 3S-HMGB1 was administered at the fracture site and *in vivo* microCT showed a clear acceleration in healing of approximately 20% and 30%, respectively. This improvement in healing was functionally confirmed with FR or 3S-HMGB1 treated fractures displaying greater mechanical strength at day 28 compared to vehicle controls. The trend of slightly faster healing of 3S compared to FR-HMGB1 is concordant with the notion that the

bioavailability of exogenous non-oxidisable 3S-HMGB1 would be higher than exogenous FR-HMGB1 because the oxidative inflammatory environment would oxidise FR-HMGB1 to the other redox forms and lose its FR-HMGB1 effects, whereas 3S-HMGB1 would remain in its existing redox form.

To further determine the role of HMGB1 in fracture healing I assessed the role of endogenous HMGB1 by performing genetic loss of function experiments. Inducible whole body *Hmgb1*$^{-/-}$ mice were generated and challenged with the fracture model. These mice displayed significantly delayed and impaired fracture healing compared to *Hmgb1*$^{fl/fl}$ as measured by *in vivo* microCT and mechanical strength parameters. These findings show that endogenous HMGB1 plays a key role in the rate and quality of fracture healing *in vivo*. This is concordant with the impaired healing of muscle tissue that was observed in mice where HMGB1 was partially deleted (*Hmgb1*$^{+/-}$)[140]. The contribution of endogenous extracellular HMGB1 is discussed further in the following chapter.

In summary, the work described in this chapter shows the development and validation of a robust murine fracture model and associated analytical techniques, and the generation and validation of inducible whole body *Hmgb1*$^{-/-}$ mice. This work allowed the effects of modulating the alarmin pathways in fracture healing to be tested and quantified *in vivo*. Collectively the data demonstrate that endogenous HMGB1 is critical to fracture healing and exogenous addition can accelerate this process.

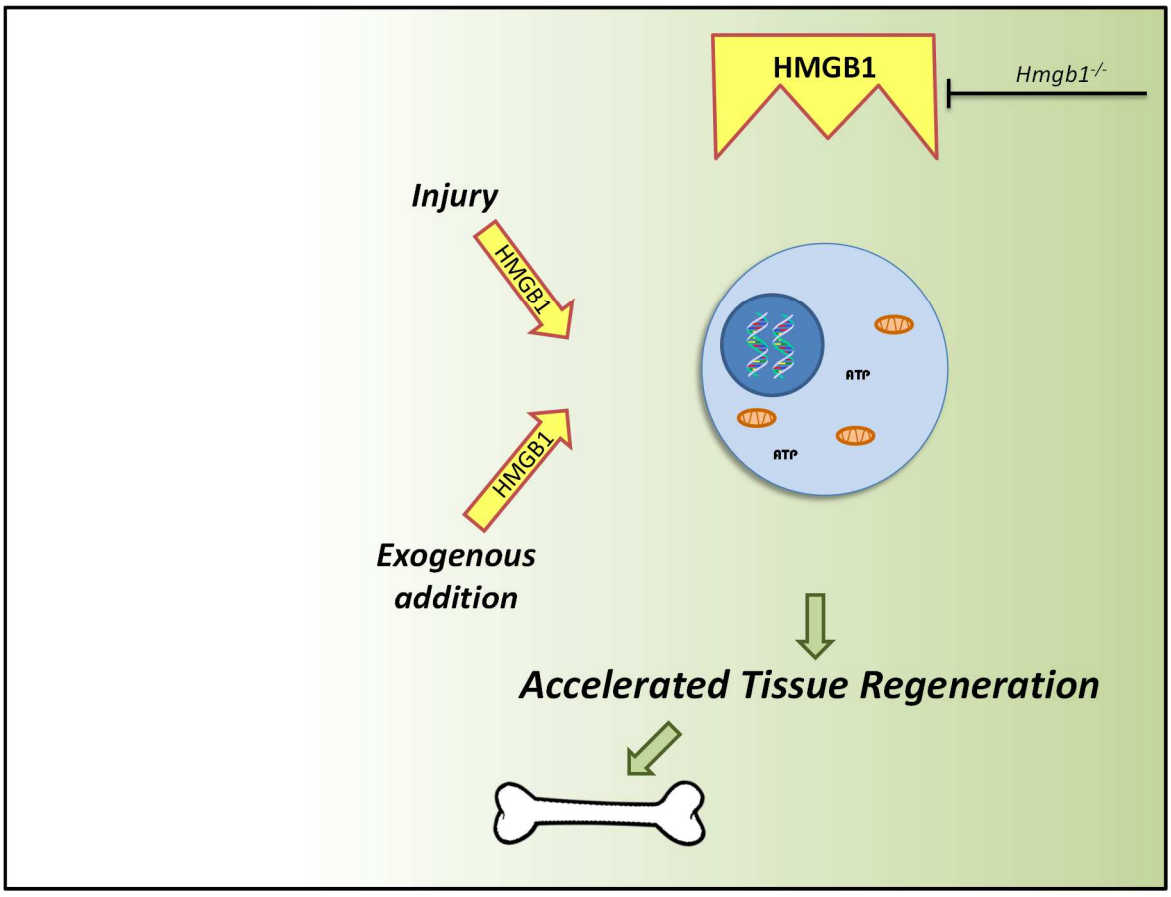

Figure 4.10 Schematic of findings from this chapter. Novel in vivo model and analyses, and *Hmgb1*$^{-/-}$ mice showed that exogenous and endogenous HMGB1 modulated the rate of fracture repair. The molecular pathway by which HMGB1 accelerated fracture healing will be discussed in the following chapter.

Chapter 5. Molecular pathway of HMGB1

5.1. Introduction

Based on the finding that HMGB1 modulates the rate of fracture healing I sought to understand the molecular pathway through which it acted. In the field of immunology, it has previously been shown that FR-HMGB1 is capable of forming a heterocomplex with free CXCL12, a chemokine, which in turn binds to the receptor, CXCR4[88]. The resultant conformational change in CXCR4 enhances the chemotaxis of CXCR4 expressing leucocytes compared to CXCL12 alone. FR-HMGB1 can also interact with the RAGE receptor leading to the secretion of CXCL12, which can in turn be bound by free FR-HMGB1[88]. Therefore, I sought to test if HMGB1-CXCL12 heterocomplex levels were detectable and elevated post-fracture in patients, and mice. If they were, then it would be possible that HMGB1 accelerated fracture healing by interacting with CXCL12 and CXCR4 which enhanced the migration of CXCR4 expressing cells to the fracture site. I planned to test this using small molecule inhibitors of the HMGB1-CXCL12 and CXCL12-CXCR4 interactions, and confirm it with the testing of exogenous CXCL12 alone.

5.2. Hypothesis

HMGB1 modulates the rate of fracture healing by forming a heterocomplex with CXCL12, which in turn binds to the receptor CXCR4.

5.3. Results

5.3.1. Systemic levels of HMGB1-CXCL12 heterocomplex post-fracture

If HMGB1 accelerates fracture healing by forming a heterocomplex with CXCL12, then systemic levels of the HMGB1-CXCL12 heterocomplex should be elevated post-fracture in patients and mice. For advice and expertise on detecting and quantifying levels of the HMGB1-CXCL12 heterocomplex, I engaged with M. Uguccioni (Institute for Research in Biomedicine, Switzerland), whose group first developed a hybrid ELISA to detect the HMGB1-CXCL12 heterocomplex. Utilising their hybrid ELISA protocol, elevated levels of HMGB1-CXCL12 heterocomplex were detected in samples from both patients (Figure 5.1 a) and mice (Figure 5.1 b) that sustained femoral fractures. The level of HMGB1-CXCL12 was less than the level of total HMGB1 (Figure 4.2) which suggests that some of the HMGB1 may have already oxidised into the DS and TOX forms. The known HMGB1-CXCL12 heterocomplex inhibitory effects of glycyrrhizin were also validated in this fracture model, with fractured mice that were treated locally with glycyrrhizin displaying markedly less HMGB1-CXCL12 compared to fractured controls, and equivalent to unfractured controls (Figure 5.1 b).

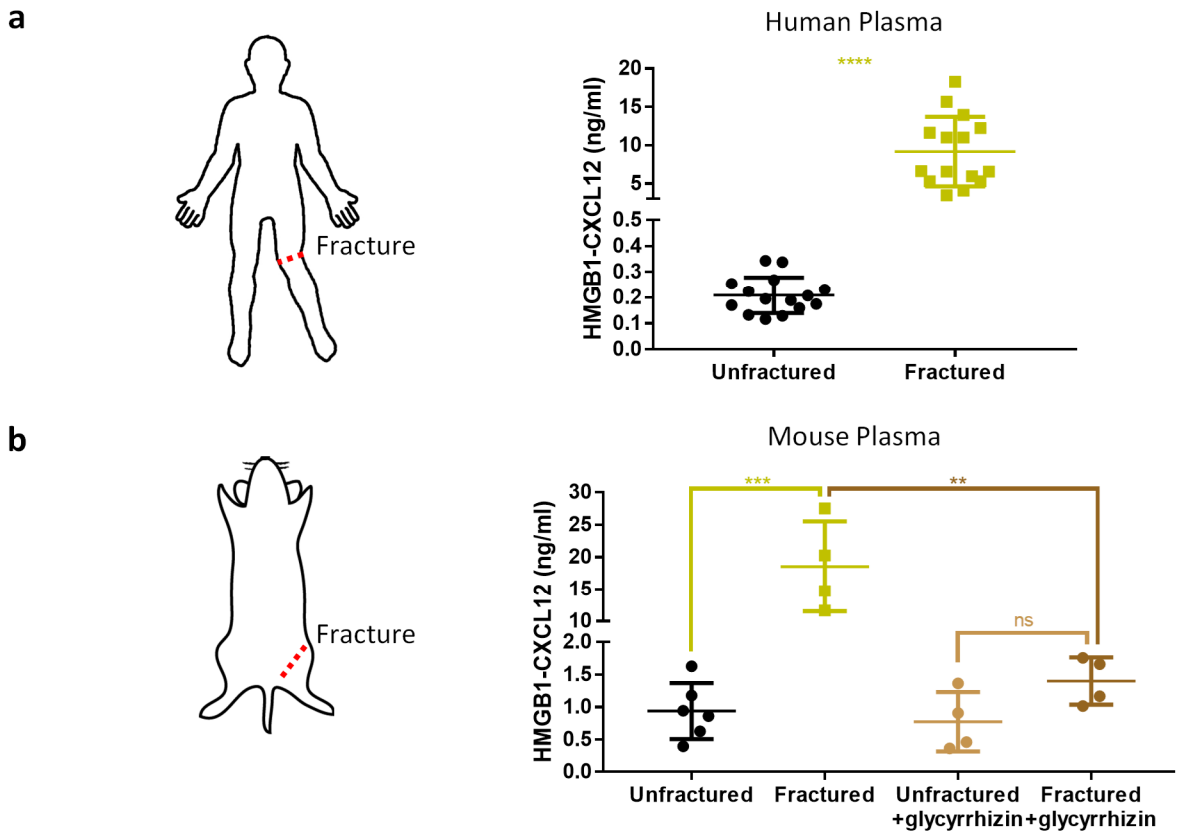

Figure 5.1 Systemic levels of the HMGB1-CXCL12 heterocomplex post-fracture. (a) Plasma levels of HMGB1-CXCL12 are elevated post-fracture in humans, as measured by ELISA (n = 15 human fractured and unfractured samples). (b) Plasma levels of HMGB1-CXCL12 are elevated post-fracture in mice, and glycyrrhizin inhibits formation of the HMGB1-CXCL12 heterocomplex, as measured by ELISA (n = 6 murine unfractured, 4 fractured, 4 glycyrrhizin-treated unfractured and fractured donors).

5.3.2. Effect of inhibiting HMGB1-CXCL12 interaction on fracture healing

Glycyrrhizin is the only molecule has been shown to inhibit the effects of extracellular HMGB1 *in vitro* and *in vivo*, by specifically inhibiting the formation of the HMGB1-CXCL12 heterocomplex[88,141]. Structural nuclear magnetic resonance and surface plasmon resonance assays showed that it blocks CXCL12 from binding to HMGB1 by interacting with the binding site for CXCL12 on the BoxB region of HMGB1[88]. It does not interact with the RAGE binding region of HMGB1[141]. Therefore, to assess if the accelerated healing effects of HMGB1 were due to it forming a complex with CXCL12, fractured mice were treated with glycyrrhizin and their healing was monitored. Local administration of glycyrrhizin initially delayed fracture healing with a slower formed callus volume, and less callus bone mineral density (Figure 5.1 a, b). However, by day 28 the glycyrrhizin treated healing curves had merged with the vehicle treated curves (Figure 5.1 b), and mechanical strength was not significantly different (Figure 5.1 c). This showed that extracellular HMGB1 modulated the rate of fracture healing, but did not dictate the completion of fracture healing.

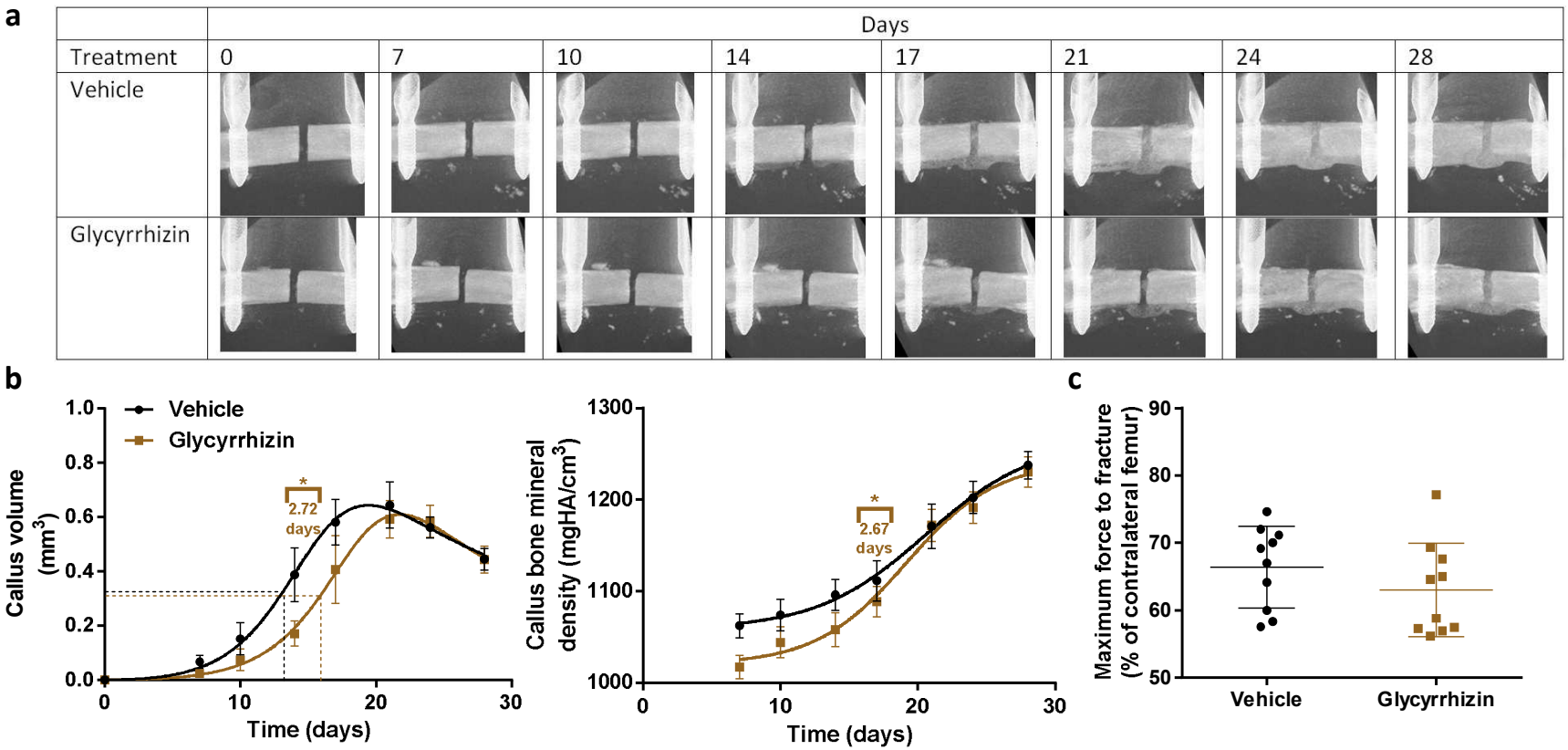

Figure 5.2 Effect of inhibiting HMGB1-CXCL12 interaction on fracture healing. (a) Representative *in vivo* microCT radiographs, (b) callus volumes, callus bone mineral densities, and (c) mechanical strength of glycyrrhizin treated mice showing a markedly delayed fracture healing process compared to vehicle controls (n = 10 for each group).

5.3.3. Effect of inhibiting CXCL12-CXCR4 interaction on fracture healing

AMD3100 is a specific and clinically approved small molecule inhibitor of the CXCL12-CXCR4 interaction[142]. Therefore to assess if the accelerated healing effects of HMGB1 were due to it forming a complex with CXCL12, which would in turn bind to CXCR4, fractured mice were treated with AMD3100 and their healing was monitored. Local administration of AMD3100 led to impaired fracture healing with a smaller callus volume (Figure 5.3 a, b). It also completely abolished the accelerated healing effects of FR and 3S-HMGB1, with fractured femurs having healing curves (Figure 5.3 a, b) and mechanical strength that were similar to vehicle treated controls at day 28 (Figure 5.3 c). This showed that the HMGB1-CXCL12 heterocomplex was accelerating healing by interacting with CXCR4.

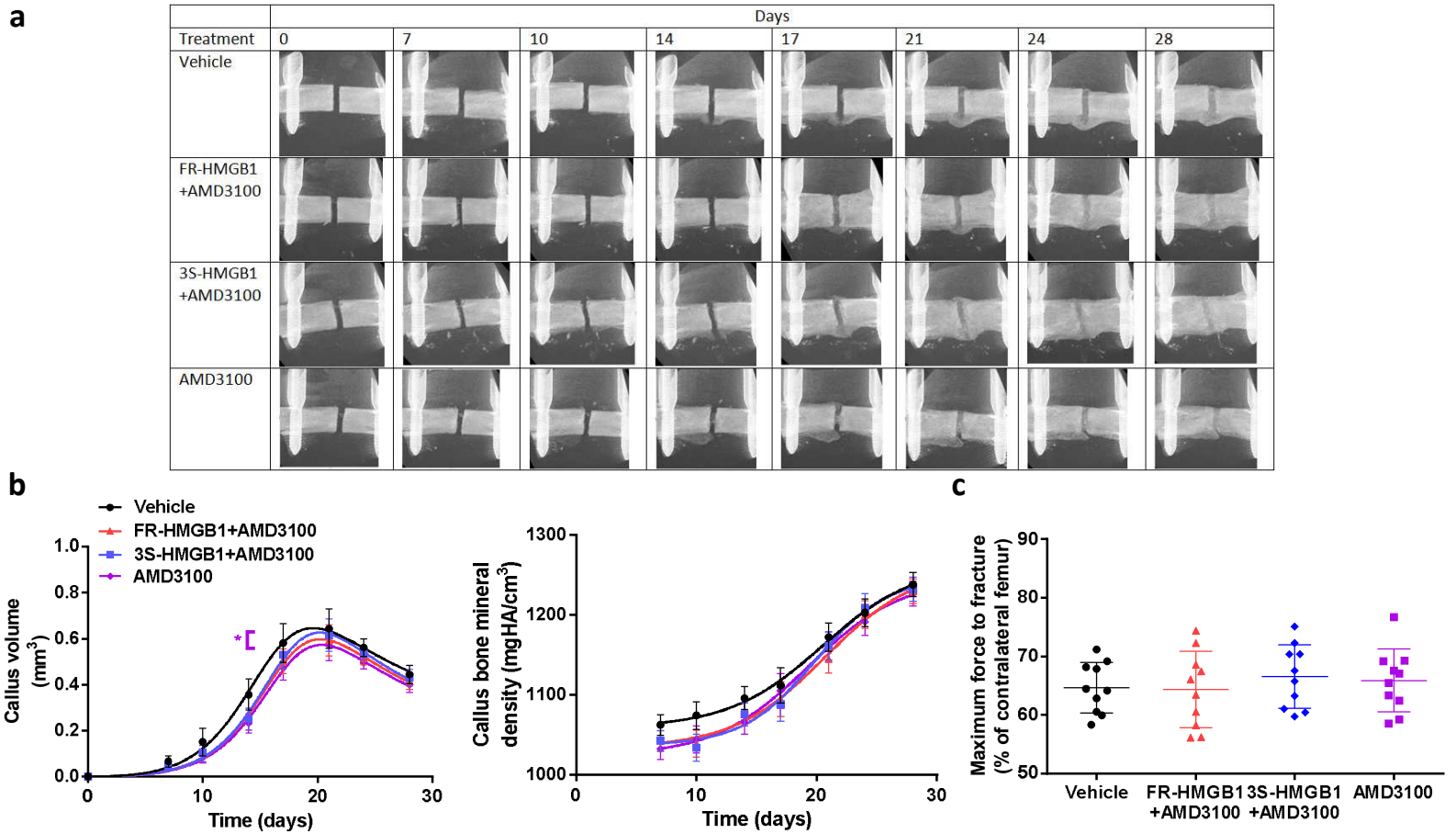

Figure 5.3 Effect of inhibiting CXCL12-CXCR4 interaction on fracture healing. (a) Representative *in vivo* microCT radiographs, (b) callus volumes, callus bone mineral densities, and (c) mechanical strength of AMD3100 treated mice showing that AMD3100 obliterates the accelerated healing effects of FR and 3S-HMGB1 treatment, and AMD3100 treatment alone reduces callus volume compared to vehicle controls (n = 10 for each group).

5.3.4. mSSCs expression of functional CXCR4

With the recent identification and specification of the murine skeletal stem cell (mSSC), and it being proven that this cell contributes to fracture repair[101], I choose to assess if the HMGB1-CXCL12-CXCR4 interaction could affect this cell. Therefore, I engaged with C. Chan (Stanford University, USA) for his expertise on mSSC biology and their protocol for isolating mSSCs. Subsequently CXCR4 staining and flow cytometry determined that mSSCs express surface CXCR4 (Figure 5.4 a). Going further, I wanted to determine if the surface CXCR4 expressed was functional. To do this, I planned to test if mSSCs migrated to a gradient of CXCL12, which is a known chemokine and binding partner of CXCR4. Modern and more accurate methods of assessing cellular migration *in vitro*, involve time-lapse microscopy and computerised cell tracking analyses. Therefore, I engaged with the Dustin Group (E. Abu Shah) for their time-lapse microscopy expertise and resources. Subsequently mSSC trajectory plots showed that they did migrate to a CXCL12 gradient (Figure 5.4 b), and quantification of the mSSCs' Euclidean distance from their starting point showed there was a dose-response to CXCL12 (Figure 5.4 c). Collectively this proved that mSSCs express functional CXCR4.

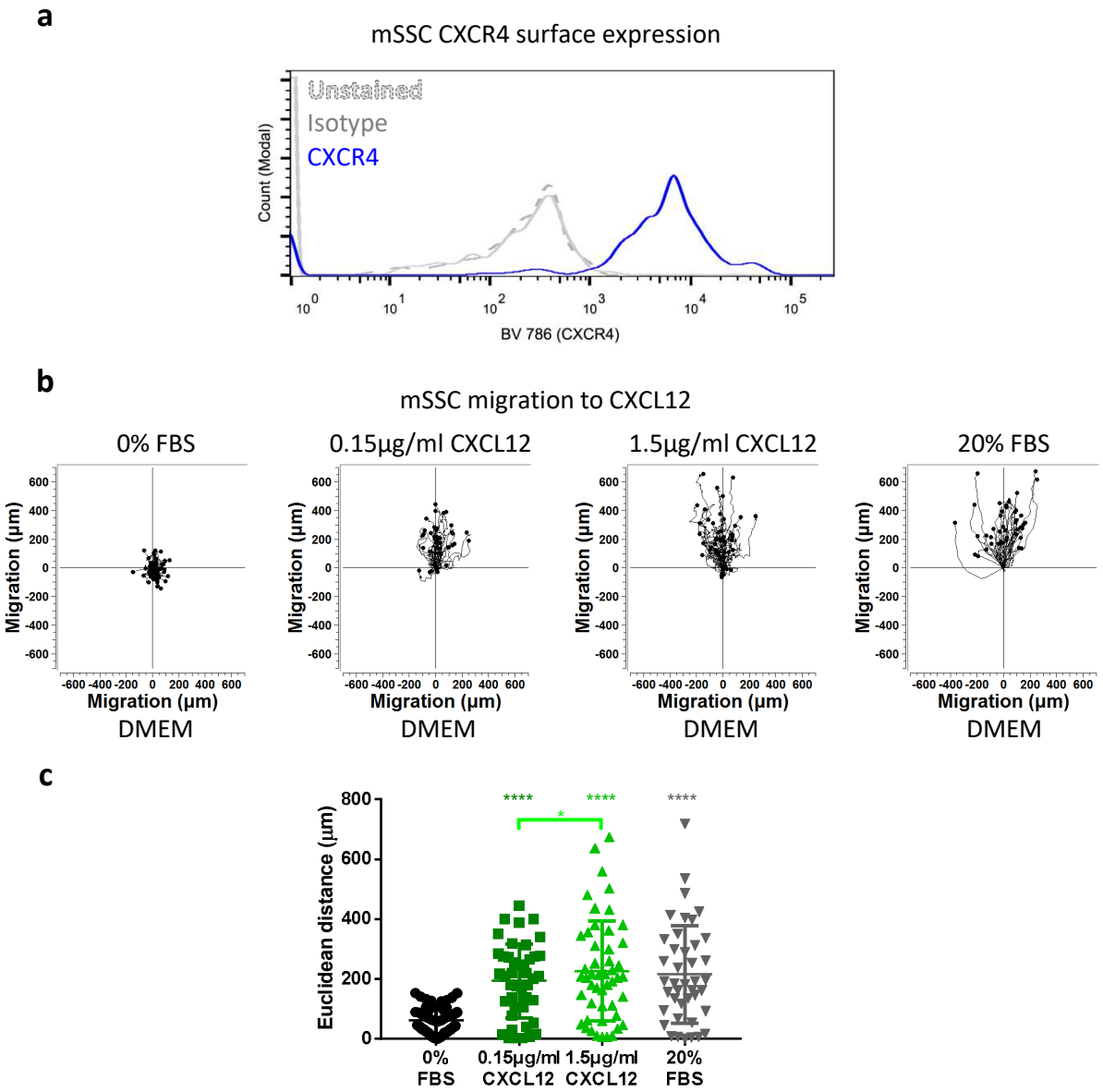

Figure 5.4 mSSCs expression of functional CXCR4. (a) Representative histogram plot of CXCR4 surface expression on mSSCs, as determined by flow cytometry (similar results observed in 3 independent experiments). (b) Representative time-lapse microscopy trajectory plots of mSSCs migrating to CXCL12, or 0% or 20% FBS control (50 cells measured for each condition, with similar results observed in 3 independent experiments). (c) mSSCs migrate to CXCL12, with a dose response, as determined by time lapse microscopy and measured by Euclidean distance (50 cells measured for each condition, similar results observed in 3 independent experiments). DMEM = Dulbecco's Modified Eagle Medium.

5.3.5. Effect of exogenous CXCL12 on fracture healing

The only previously defined function of the HMGB1-CXCL12 heterocomplex was the enhancement of leucocyte chemotaxis, compared to CXCL12 alone[88]. As mSSCs are capable for migrating towards CXC12 alone, it was possible that the accelerated fracture healing effects of the HMGB1-CXCL12 heterocomplex, were due to enhanced CXCL12 mediated migration of mSSCs to the fracture site. To determine if only elevated CXCL12 mediated migration was necessary to accelerate fracture healing, mice were treated locally with exogenous CXCL12. This resulted in aberrant regeneration with a larger fracture callus volume (Figure 5.5 a, b) and no increase in callus bone mineral density (Figure 5.5 b) or mechanical strength (Figure 5.5 c). This showed that exogenous CXCL12 alone is insufficient to accelerate fracture healing, and that the HMGB1-CXCL12 heterocomplex is accelerating fracture healing via a different mechanism.

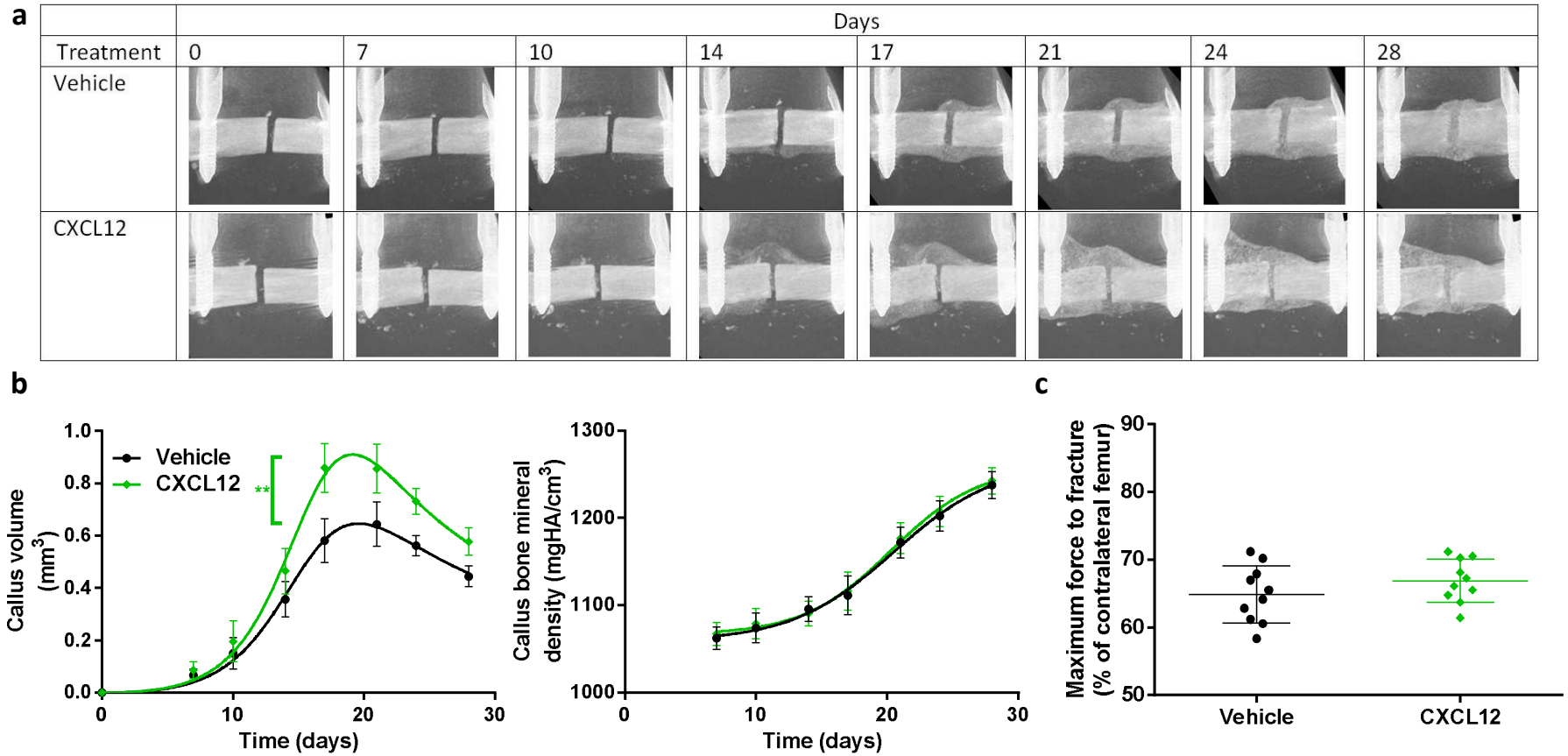

Figure 5.5 Effect of exogenous CXCL12 on fracture healing. (a) Representative *in vivo* microCT radiographs, (b) callus volumes, callus bone mineral densities, and (c) mechanical strength of CXCL12 treated mice showing aberrant healing with a larger callus volume and no increase in bone mineral density, or mechanical strength (n = 10 for each group).

5.4. Discussion

The molecular pathway by which HMGB1 modulates fracture healing is unknown. Immunological studies had shown that HMGB1 can interact with a variety of molecules and receptors, with the FR redox form of HMGB1 being able to interact with CXCL12 to form a heterocomplex[88]. This in turn binds to CXCR4, which enhances leucocyte migration compared to CXCL12 alone. Therefore I hypothesised that HMGB1 might act via this molecular pathway, with the cellular effect of enhancing the migration of callus-contributing cells to the fracture site, and thereby accelerate fracture healing. To test this, it was first verified if there was an elevated systemic level of the HMGB1-CXCL12 heterocomplex in post-fracture human and mice plasma samples, by using a hybrid ELISA. The positive result suggested that HMGB1 may be accelerating fracture healing forming a heterocomplex with CXCL12, and was in concordance with both HMGB1 and CXCL12 being highly evolutionarily conserved molecules.

To test the role of the HMGB1-CXCL12 interaction, fractured mice were treated with a small molecule HMGB1-CXCL12 inhibitor, glycyrrhizin[88,141]. Local administration of glycyrrhizin at the fracture site inhibited formation of the HMGB1-CXCL12 heterocomplex and resulted in initially delayed fracture healing. However, at the terminal time point had similar mechanical strength as vehicle controls. This suggested that endogenous extracellular HMGB1, and the heterocomplex it formed with CXCL12, were critical modulators of the rate of fracture healing, but not essential for the ultimate completion of fracture healing.

The importance of the CXCL12-CXCR4 interaction for the HMGB1-CXCL12 heterocomplex to mediate its effects on fracture healing was assessed by treating fractured mice with a small molecule CXCL12-CXCR4 inhibitor. AMD3100 treated mice had smaller callus volumes which is concordant with the previous finding that genetic or pharmacological inhibition of the CXCL12-CXCR4 impairs fracture healing, by reducing migration of $CXCR4^{+}$ callus-contributing cells to the fracture site[143]. Most importantly AMD3100 completely abolished the accelerated healing effects of FR and 3S-HMGB1.

This indicated that the CXCL12-CXCR4 interaction was critical for the HMGB1-CXCL12 heterocomplex to accelerate fracture healing.

Despite many cells being reported to contribute to the fracture healing process very few have been conclusively proven with genetic lineage tracing or immunophenotypic cell isolation. I decided to investigate the murine skeletal stem cell because it had been clearly immunophenotypically defined and characterised, and proven to contribute to the fracture callus[101]. Also its very recent discovery meant a limited amount had been published about it, and there would be fertile space for interesting and novel findings. Flow cytometry and cell migration assays showed that the mSSC expressed functional CXCR4, which suggested that the HMGB1-CXCL12-CXCR4 pathway may directly act upon the mSSC. These cellular effects are discussed in the following chapter.

As it had been described that compared to the CXCL12-CXCR4 interaction, the HMGB1-CXCL12-CXCR4 interaction simply enhanced cell chemotaxis, it may have been possible that supraphysiologically upregulating the CXCL12-CXCR4 axis and subsequently enhancing cell chemotaxis may have sufficed to accelerate fracture healing. However exogenous administration of CXCL12 resulted only in aberrant healing with no acceleration of healing. This result was recently corroborated by others who with *ex vivo* microCT found that exogenous administration of CXCL12 leads to a larger fracture callus, and showed no improvement in callus bone mineral density or mechanical strength[143]. This shows that exogenous CXCL12 alone is not enough to accelerate fracture healing and suggests that HMGB1 is acting via another mechanism.

In summary, the work described in this chapter establishes HMGB1-CXCL12-CXCR4 as a molecular axis by which HMGB1 accelerates fracture healing. It also suggests that this axis has another effect beyond enhanced CXCL12 mediated cell migration, and this other mechanism is crucial to the accelerated fracture healing effects of HMGB1.

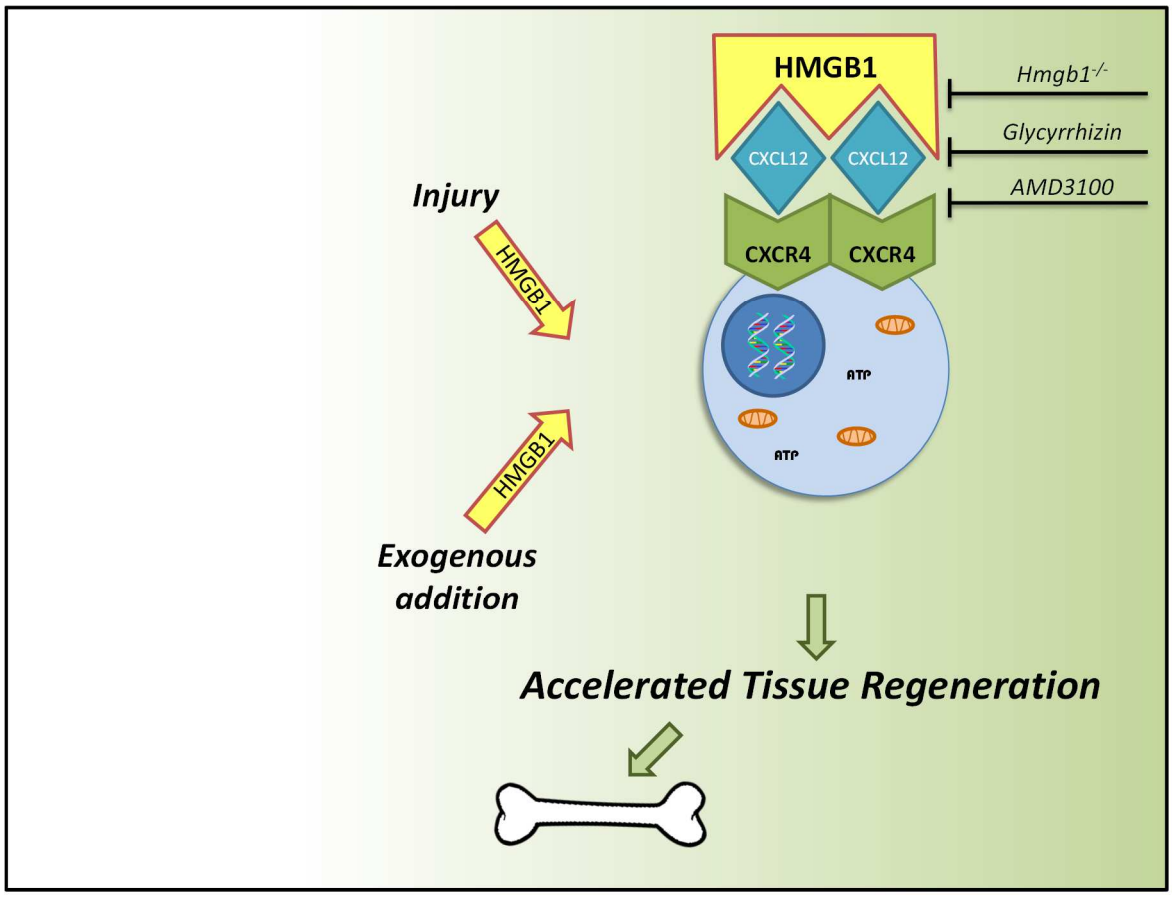

Figure 5.6 Schematic of findings from this chapter. Human and murine samples, and *in vivo* small molecule inhibition studies show that HMGB1 accelerates fracture healing by forming a heterocomplex with CXCL12, and this in turn interacts with CXCR4. It is possible that this axis acts directly on mSSCs since mSSCs express functional CXCR4, and this will be discussed further in the following chapter.

Chapter 6. Cellular effects of HMGB1

6.1. *Introduction*

Based on the findings that HMGB1 modulated the rate of fracture healing via a HMGB1-CXCL12-CXCR4 molecular axis and that mSSCs expressed functional CXCR4, I hypothesised that this axis may exert a direct effect on mSSCs to accelerate fracture healing. I reasoned that this effect may pertain to the cycling of mSSCs, because the necessary process of differentiation that occurs during tissue regeneration, which during fracture healing is specifically osteogenic differentiation, is encapsulated within the fundamental stem cell process of asymmetric cell division[144,145] (Figure 6.1). During asymmetric cell division, the stem cell will cycle and divide to generate one daughter cell with a stem cell fate (self-renewal), and another daughter cell which is programmed to differentiate[145]. It is important to note that stem cells also undergo symmetric cell division, where two identical daughter cells are produced that are either both identical to the original stem cell (symmetric self-renewal) or both programmed to differentiate (symmetric differentiation). Symmetric stem cell division is particularly evident when an expansion in stem cell numbers is noted, such as during development[146], or following injury[147]. And for some stem cell populations, such as skin epidermal stem cells, there is clear evidence that a combination of asymmetric cell division, symmetric self-renewal and symmetric differentiation can all occur[148–151] within a single pool of stem cells to maintain appropriate numbers of stem cells, and cells that will differentiate.

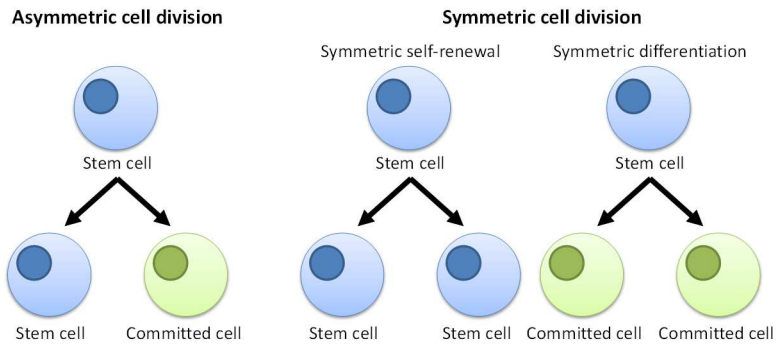

Figure 6.1 Schematic of asymmetric stem cell division compared to symmetric cell division. Stem cells can maintain homeostasis by undergoing division into two daughter cells, one that is identical to the original stem cell (self-renewal), and another that is committed to a mature cell fate.

A review of the literature also indicated that in addition to mediating chemotaxis, the CXCL12-CXCR4 axis was also a well-established stem cell cycle regulator, specifically it enforces the quiescence of haematopoietic stem cells[152–157] (Figure 6.2). Therefore, I hypothesised that the HMGB1-CXCL12-CXCR4 axis, which involves a different conformational change in CXCR4 compared to CXCL12 alone, alternatively affected the cell cycle of mSSC in a manner that would ultimately lead to accelerated fracture healing (Figure 6.2).

6.2. Hypothesis

HMGB1 accelerates fracture healing by increasing the cycling of mSSCs.

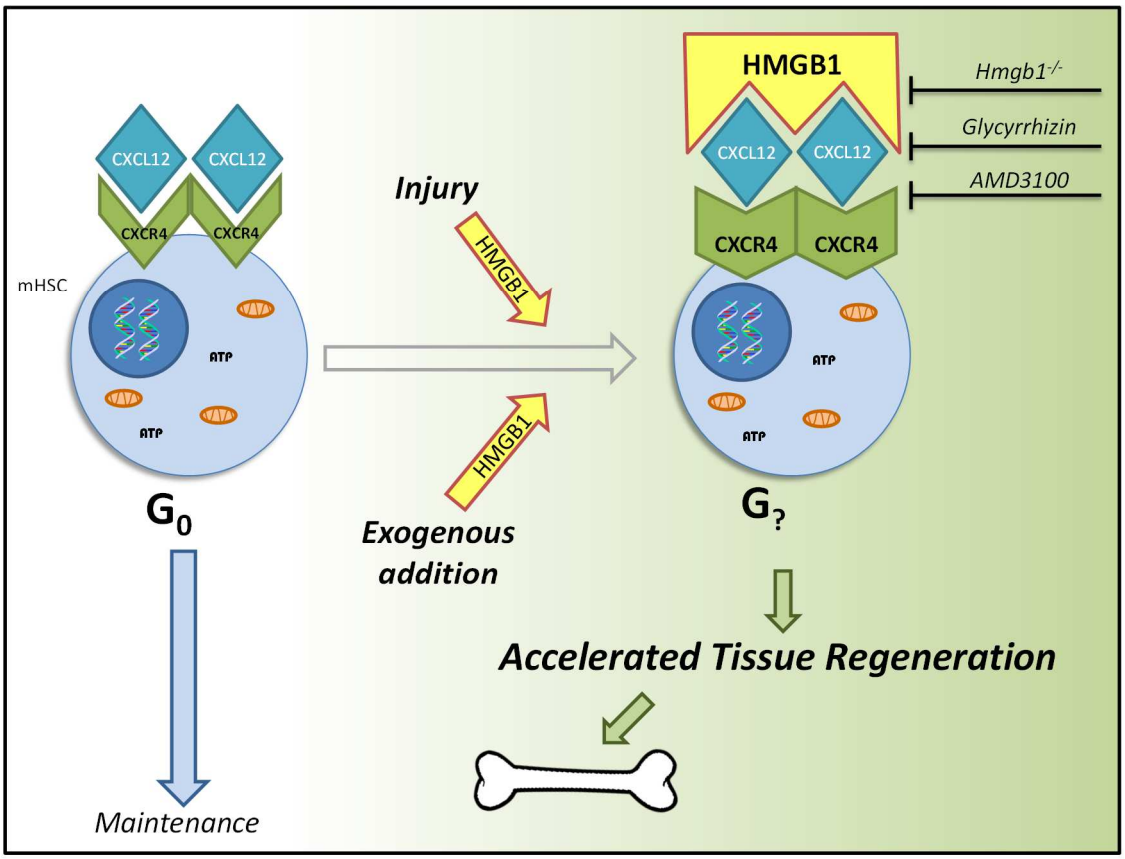

Figure 6.2 Schematic of hypothesis of this chapter. With CXCL12-CXCR4 being a well-established axis of haematopoietic stem cell quiescence, and the HMGB1-CXCL12-CXCR4 interaction causing a different conformational change in CXCR4 compared to CXCL12 alone, I hypothesised that the HMGB1-CXCL12-CXCR4 axis may affect the cell cycle of stem cells to accelerate healing.

6.3. Results

6.3.1. In vivo propensity to cycle of mSSCs post-fracture

A well-established method of ascertaining cell cycle behaviour is the use of bromodeoxyuridine assays. BrdU is a synthetic analogue of thymidine and is incorporated into the DNA of cycling cells. It can subsequently be detected by flow cytometry techniques. However, following injury there is such a rapid degree of cycling that continuous administration BrdU assays, which measure cumulative cell cycling, are unlikely to detect changes[158]. Instead pulse labelling for a shorter time period over multiple time points, which measures the propensity to cycle, is more likely to detect changes. Therefore, I pulse labelled fractured animals to compare the propensity to cycle of mSSCs from animals treated with vehicle, FR or 3S-HMGB1, at various time points. BMP2, a recognised mSSC activator[101], was used as a positive control. mSSCs from vehicle treated animals had an increased propensity to cycle over time, which correlated with the known rising levels of osteogenic signals post-fracture[45,127] (Figure 6.3). In comparison, mSSCs from animals treated locally with exogenous HMGB1 or BMP2, both showed an initial increased propensity to cycle. However, mSSCs from BMP2-treated mice returned to levels equivalent to vehicle controls by day 5 (Figure 6.3). These data are consistent with the requirement of activation signals to be continuously present for ongoing cell cycling and the necessity for sustained release preparations of BMP2 to accelerate fracture healing clinically[14]. In contrast, mSSCs from HMGB1-treated mice had a sustained and increased propensity to cycle, indicating a lasting cellular effect had occurred that allowed the cells to respond beyond the initial stimulus (Figure 6.3). Collectively these data showed that in the context of fracture healing, FR and 3S-HMGB1 treatment increased the propensity to cycle of mSSCs for a sustained period, and that this effect was markedly different compared to a known mSSC activator.

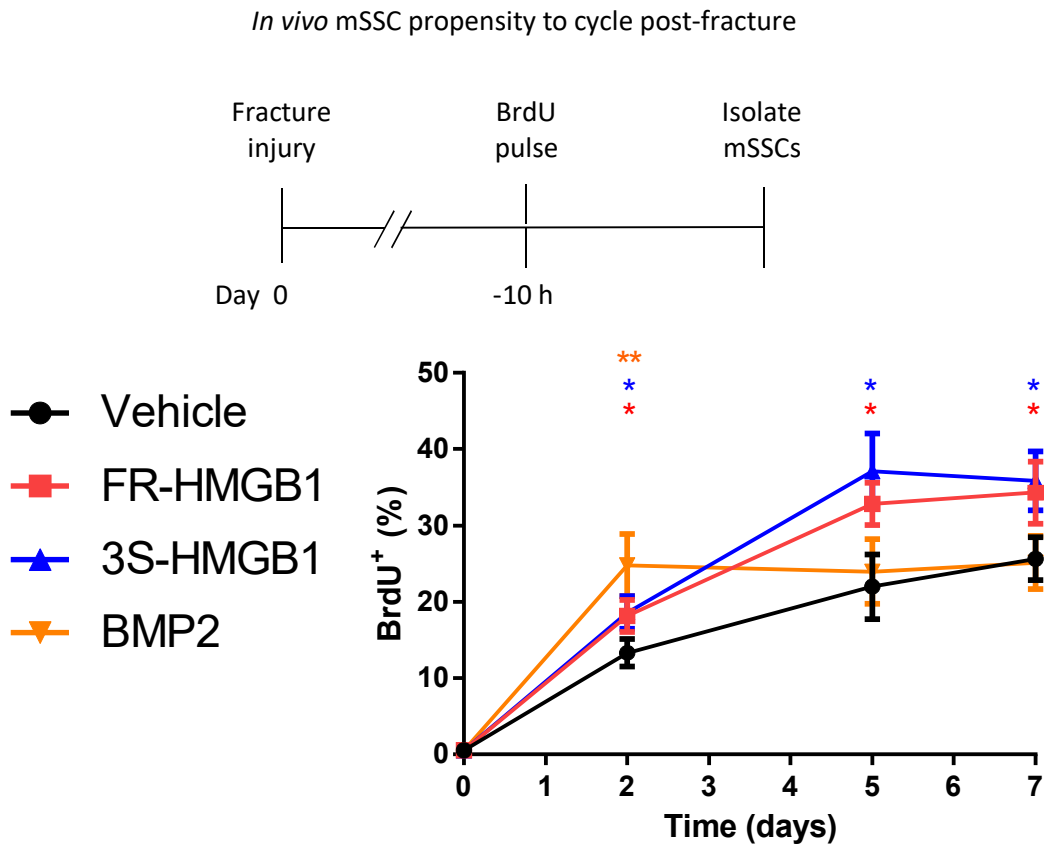

Figure 6.3 *In vivo* propensity to cycle of mSSCs post-fracture. Only mSSCs from animals treated locally with exogenous FR or 3S-HMGB1 dynamically adapted to the known physiologically rising levels of growth factors with a sustained increased propensity to cycle (n = 4 for each condition and time point).

6.3.2. CXCR4 expression of mHSC and mMuSCs, and HMGB1-G_{Alert} hypothesis

It has been known for over 40 years that a priming injury results in accelerated tissue regeneration of a second distant injury in the same animal[159,160]. However, this phenomenon was only recently explained by an elegant series of experiments which demonstrated that an unknown systemic mediator transitioned murine muscle (mMuSCs) and haematopoietic stem cells (mHSCs) distant to the site of initial injury to a state of the cell cycle, intermediate between G_0 and G_1, termed G_{Alert}[117]. In contrast to deeply quiescent G_0 stem cells, G_{Alert} cells are more metabolically active, as evidenced through findings such as increased cellular levels of ATP, and are poised to efficiently enter the cell cycle upon receiving an activation signal.

Based on the findings of elevated systemic levels of HMGB1 post injury, increased osteogenic differentiation of HMGB1-primed hMSCs, accelerated fracture healing with exogenous HMGB1 treatment, and higher propensity to cycle of mSSCs from HMGB1 treated mice, and that mSSCs expressed functional CXCR4 akin to mHSCs[152–157] and mMuSCs[161], I hypothesised that HMGB1 may accelerate fracture healing by transitioning mSSCs to the G_{Alert} state. In addition, I hypothesised that this effect may extend to other stem and progenitor cells which are known to express CXCR4, including mHSCs, mMuSCs, hHSPCs, and hMSCs. I engaged with the A. Grover, and C. Nerlov (Weatherall Institute of Molecular Medicine) for their expertise in HSC biology and isolation and confirmed that mHSCs (Figure 6.4 a) and mMuSCs (Figure 6.4 b) did indeed express surface CXCR4.

a

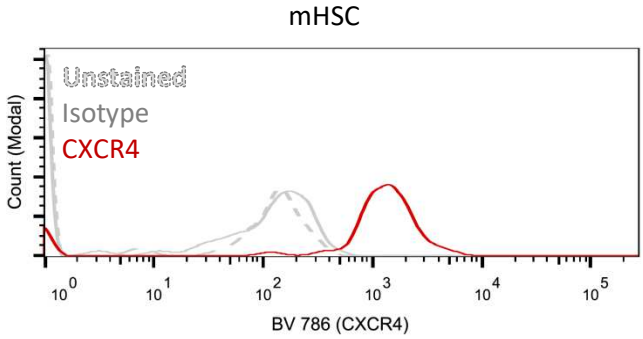

b

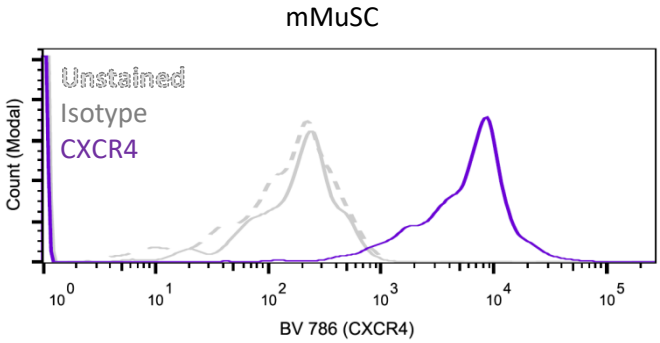

Figure 6.4 CXCR4 surface expression. (a) mHSCs, and (b) mMuSC express surface CXCR4 as shown by CXCR4 staining and flow cytometry (representative histogram plots, similar results observed in 3 independent experiments).

6.3.3. In vivo mTORC1 dependency

A feature of the transition from G_0 to G_{Alert}, and the subsequent enhanced healing is that it is mTORC1 dependent[117]. I engaged with L. Chantranupong (Massachusetts Institute of Technology, USA) for her expertise in mTORC1 biology and *in vivo* mTORC1 inhibition protocols. Based on these I assessed the *in vivo* mTORC1 dependency of the effects of exogenous HMGB1 on fracture healing using a specific and clinically approved small molecule inhibitor of mTORC1, rapamycin. Local administration of rapamycin completely abolished the effects of exogenous FR and 3S-HMGB1 of accelerating fracture healing, as assessed by *in vivo* microCT and mechanical strength testing (Figure 6.5). This indicated the accelerated fracture healing effects of exogenous HMGB1 are mTORC1 dependent. My acute inhibition of mTORC1 did not grossly affect the normal fracture healing process, and this is concordant with others previously showing that even chronic mTORC1 inhibition only delays the initial phase of fracture healing[162].

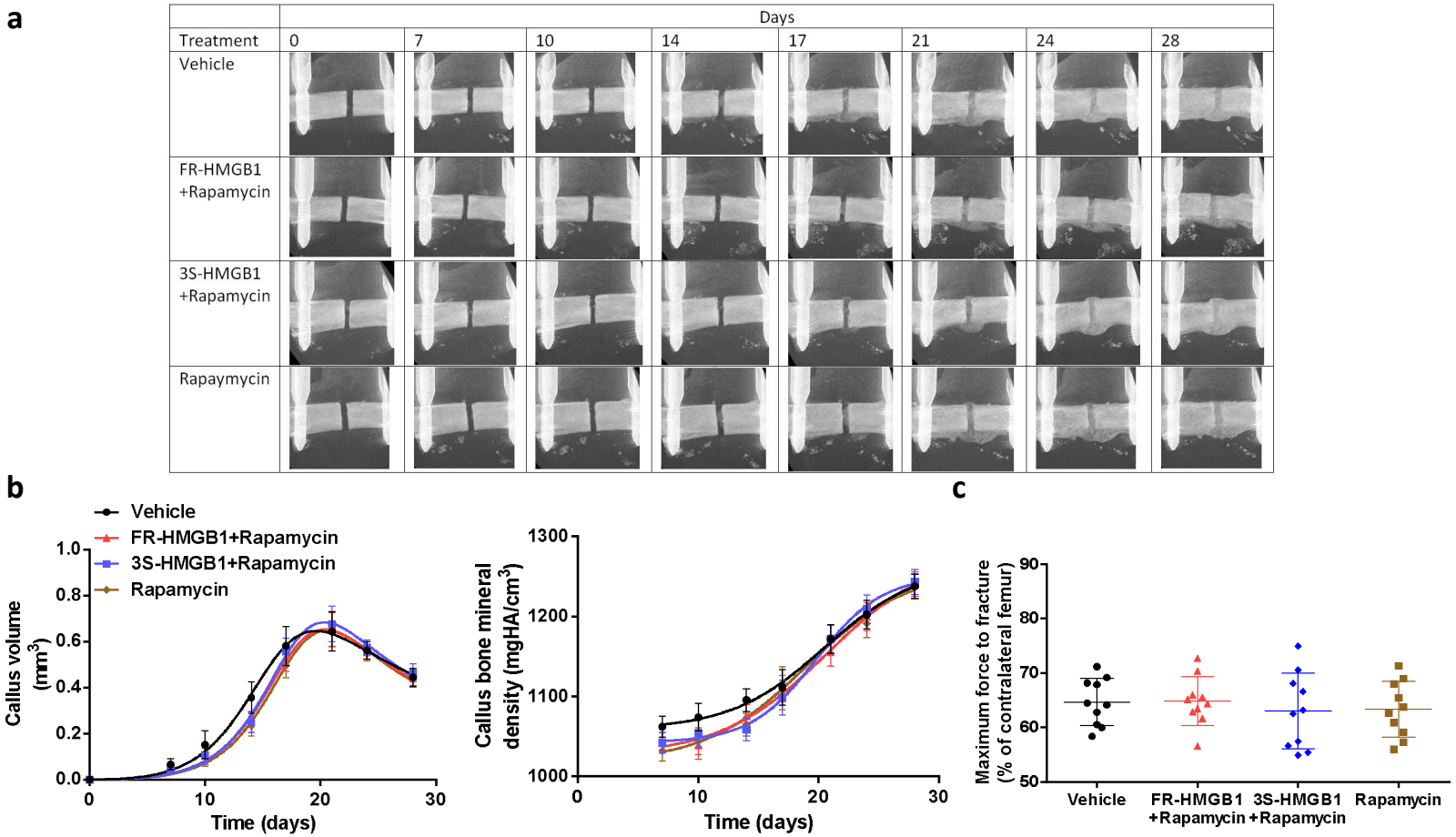

Figure 6.5 Effects of HMGB1 are mTORC1 dependent *in vivo*. (a) Representative *in vivo* microCT radiographs, (b) callus volumes, callus bone mineral densities and (c) mechanical strength of rapamycin treated mice, showing rapamycin completely abolished the accelerated fracture healing effects of FR and 3S-HMGB1 (n = 10 for each group).

6.3.4. Cellular ATP

G_0 stem cells mainly rely on glycolytic pathways, whereas G_{Alert} cells are characterised by increased levels of cellular ATP[117]. Therefore, changes to cellular ATP levels in mSSC, mHSC, and mMuSC from mice that had been systemically administered FR or 3S-HMGB1 were compared to vehicle treated controls, and cells that were contralateral to a fracture injury (#alerted). mSSCs, mHSCs, and mMuSCs from mice treated with HMGB1 showed increased levels of cellular ATP compared to vehicle treated controls, and equivalent to fracture alerted stem cells (Figure 6.6). In contrast, stem cells from fractured *Hmgb1*$^{-/-}$ mice did not transition to G_{Alert} (Figure 6.7).

Changes to the levels of cellular ATP in $CD34^+$ hHSPCs, and hMSCs that had been treated with FR or 3S-HMGB1 were compared to vehicle (quiescent) controls, or IFN-γ activated and BMP2 activated controls, respectively. $CD34^+$ hHSPCs, and hMSCs treated with HMGB1 displayed increased levels of cellular ATP compared to vehicle controls, but substantially less than IFN-γ activated and BMP2 activated cells, respectively (Figure 6.6).

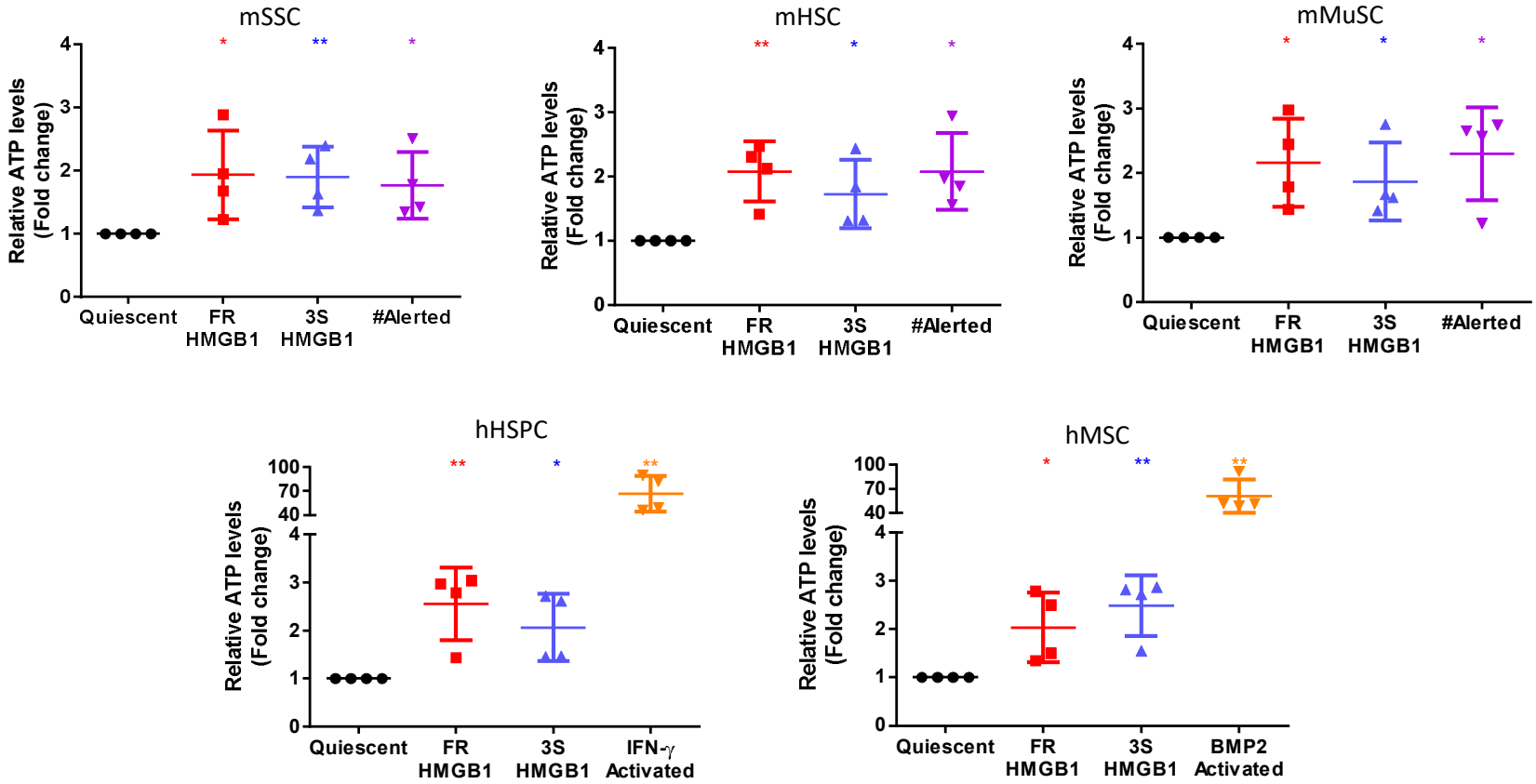

Figure 6.6 *In vivo* cellular ATP of stem cells from HMGB1 treated mice. mSSCs, mHSCs, and mMuSCs from mice treated systemically with FR or 3S-HMGB1 displayed increased cellular ATP compared to vehicle controls, and equivalent to cells from the limb contralateral to the fracture (#alerted) (n = 4 for each condition). hHSPC, and hMSCs treated *ex vivo* and *in vitro* respectively with FR or 3S-HMGB1 show elevated cellular ATP compared to vehicle controls (quiescent) but much lower than IFN-γ or BMP2 activated cells, respectively (n = 4 HSPC donors, 4 hMSC donors).

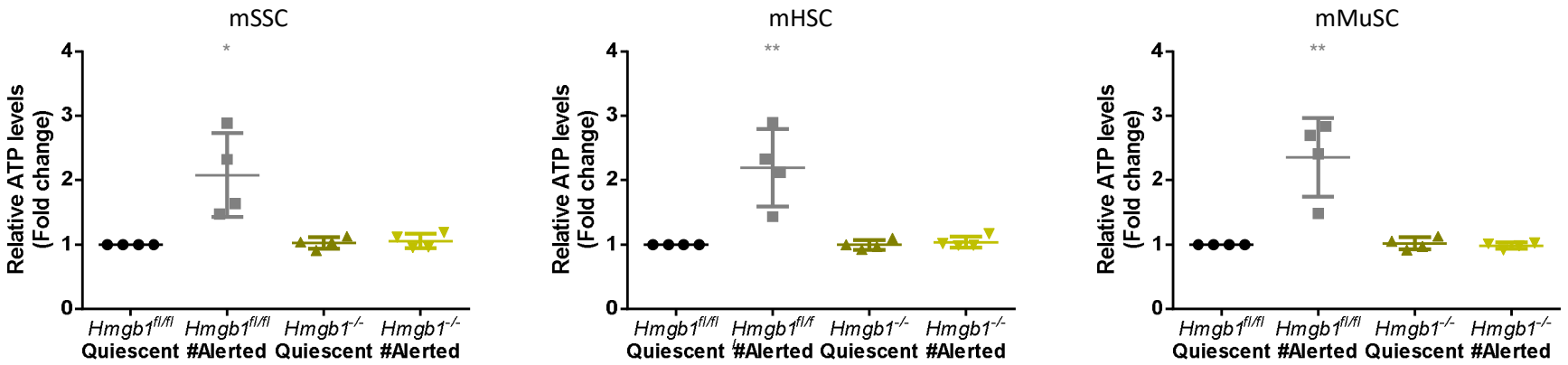

Figure 6.7 *In vivo* cellular ATP of stem cells from *Hmgb1*$^{fl/fl}$ and *Hmgb1*$^{-/-}$ mice. mSSCs, mHSCs, and mMuSCs from the limb contralateral to the fracture of *Hmgb1*$^{fl/fl}$ mice (*Hmgb1*$^{fl/fl}$ #alerted) display elevated ATP levels compared to quiescent cells from unfractured mice (*Hmgb1*$^{fl/fl}$ quiescent). However, stem cells from the limb contralateral to the fracture of *Hmgb1*$^{-/-}$ mice (*Hmgb1*$^{-/-}$ #alerted) do not (n = 4 for each condition).

6.3.5. Cell size

The primary cellular feature which led others to investigate the G_{Alert} state was the observation that stem cells in the limb contralateral to an injury had a small but significant increase in cell size[117]. Only substantial injuries, such as fractures, can transition stem cells to G_{Alert}, whereas simple venepuncture is insufficient[117]. Therefore, changes to the cell size of mSSCs, mHSCs, and mMuSCs from mice that had been systemically administered FR or 3S-HMGB1 was compared to vehicle treated controls. Fracture injury had also been shown to transition cells to G_{Alert}, so cells that were contralateral to a fracture injury (#alerted) were the positive 'alerted' control. mSSCs, mHSCs, and mMuSCs from mice treated with i.v. HMGB1 showed increased cell size compared to vehicle treated controls, and equivalent to fracture alerted stem cells (Figure 6.8). Quantification of cell diameters was performed in conjunction with A.I. Espirito Santo for more accurate measurements.

When performing this experiment and others that involved the isolation of multiple different types of stem cells, the reduction principles of the 3R's guidelines were adhered to by isolating all the different stem cell types from the same animal whenever possible to minimise the number of animals used and economise on reagents. However, the isolation of just one mSSC, mHSC, or mMuSC, sample involved dissection of hind limbs, mechanical and enzymatic digestion, antibody staining, and FACS, all of which required a minimum 6 h, 4 h, and 7 h for each stem cell type respectively. If these stem cells were isolated sequentially, the delay between samples would result in cell death and confounding *ex vivo* cell alterations. To avoid these aberrations, the stem cells had to be isolated efficiently, which required the simultaneous dissection of hind limbs, mechanical and enyzymatic digestion, and antibody staining of multiple samples and the operation of multiple FACS machines in tandem. Therefore, the isolating of multiple different types of stem cells was performed in conjunction with A.I. Espirito Santo.

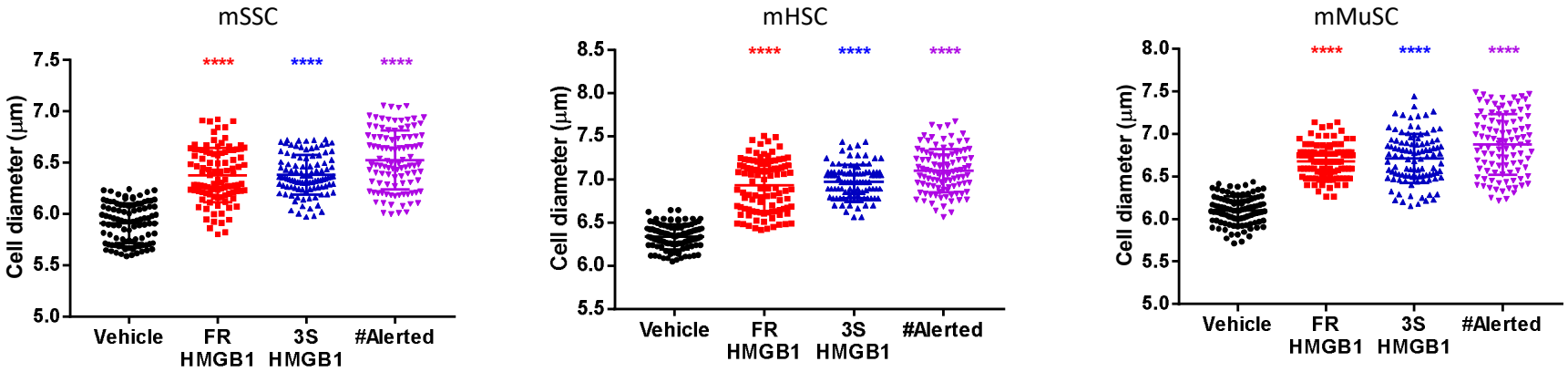

Figure 6.8 *In vivo* size of stem cells from HMGB1 treated mice. mSSCs, mHSCs, and mMuSCs from mice treated systemically with FR or 3S-HMGB1 displayed increased cell size compared to vehicle controls, and equivalent to cells from the limb contralateral to the fracture (#alerted) (100 cells measured for each condition, similar results observed in 3 independent experiments).

6.3.6. Mitochondrial DNA

G_0 stem cells are relatively inactive metabolically, whereas G_{Alert} cells are characterised by increased expression of mitochondrial DNA[117]. Therefore, changes in the expression of mtDNA in mSSC, mHSC, and mMuSC from mice that had been systemically administered FR or 3S-HMGB1 were compared to vehicle treated controls, and cells that were contralateral to a fracture injury (#alerted). mSSCs, mHSCs, and mMuSCs from mice treated with HMGB1 showed increased mtDNA compared to vehicle treated controls, and equivalent to fracture alerted stem cells (Figure 6.9).

It was also important to know if these experimental findings also pertained to human cells. As $CD34^+$ hHSPCs and hMSCs also express CXCR4, it was possible HMGB1 may also transition them to G_{Alert}. Changes to the expression of mtDNA in $CD34^+$ hHSPCs, and hMSCs that had been treated with FR or 3S-HMGB1 were compared to vehicle (quiescent) controls, or IFN-γ activated and BMP2 activated controls, respectively. $CD34^+$ hHSPCs, and hMSCs treated with HMGB1 displayed increased mtDNA compared to vehicle controls, but substantially less than IFN-γ activated or BMP2 activated cells, respectively.

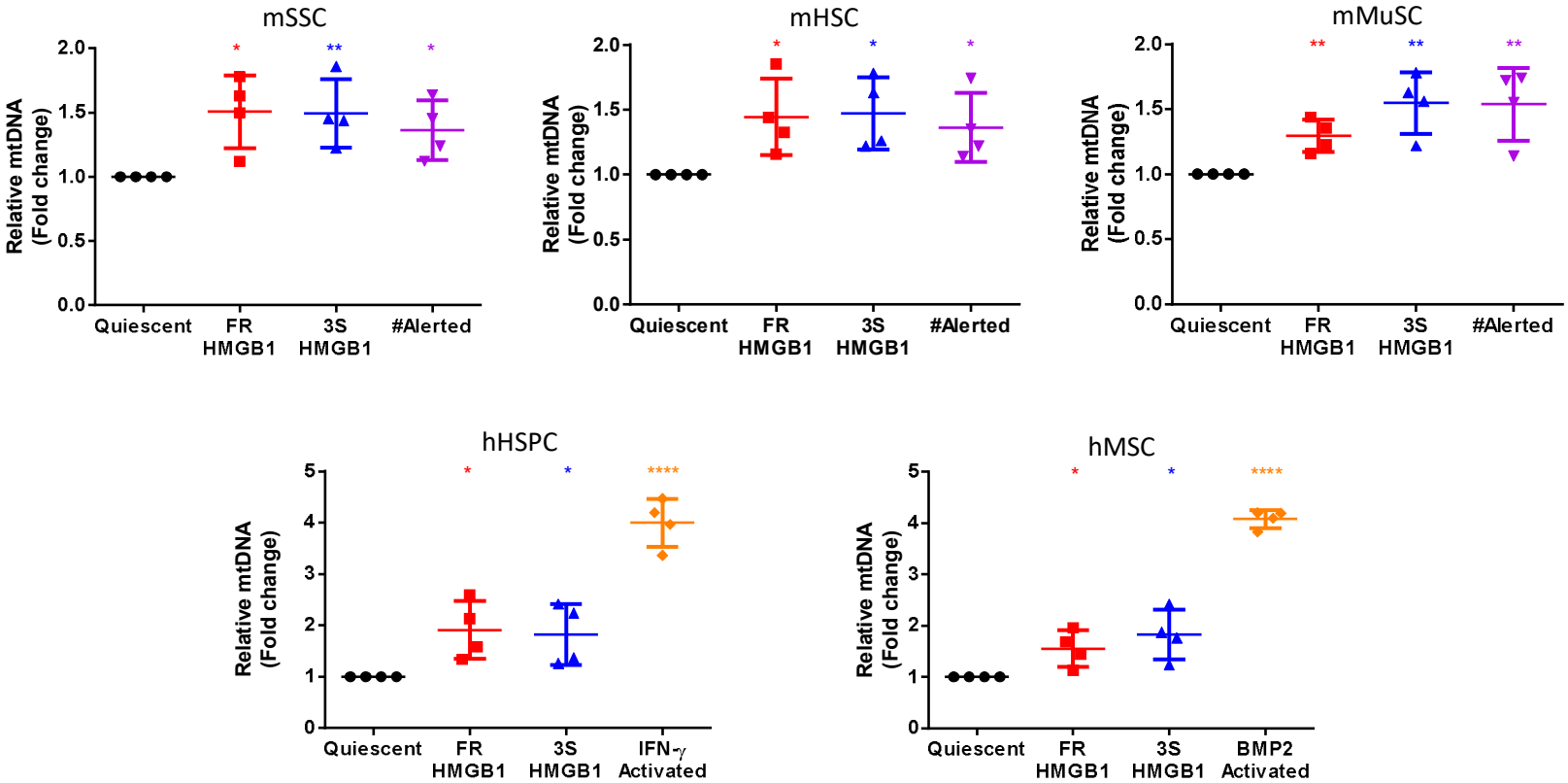

Figure 6.9 *In vivo* mitochondrial DNA of stem cells from HMGB1 treated mice. mSSCs, mHSCs, and mMuSCs from mice treated systemically with FR or 3S-HMGB1 displayed increased mitochondrial DNA compared to vehicle controls, and equivalent to cells from the limb contralateral to the fracture (#alerted) (n = 4 for each condition). hHSPC, and hMSCs treated *ex vivo* and *in vitro* respectively with FR or 3S-HMGB1 show elevated mitochondrial DNA compared to vehicle controls (quiescent) but much lower than IFN-γ or BMP2 activated cells, respectively (n = 4 HSPC donors, 4 hMSC donors).

6.3.7. In vivo speed of entry to cell cycle

G_{Alert} stem cells were previously shown to cycle faster than G_0 cells, but slower than injury activated stem cells[117]. However this was only determined by *in vitro* cell culture and the *in vivo* relevance of this finding remains controversial. Therefore I sought to assess the speed of entry to cell cycle *in vivo* by continuously administered high-dose BrdU. This assay utilised the dual properties of BrdU, to label cells that cycle whilst also acting as an injury signal at high doses that activates quiescent stem cells and recruits them into the cell cycle[115]. The mSSCs, mHSCs and mMuSCs in HMGB1-treated mice entered the cell cycle faster in response to continuous high dose BrdU compared to vehicle controls, but much slower than activated stem cells from the injured proximal hind limb of fractured animals (#activated) (Figure 6.10).

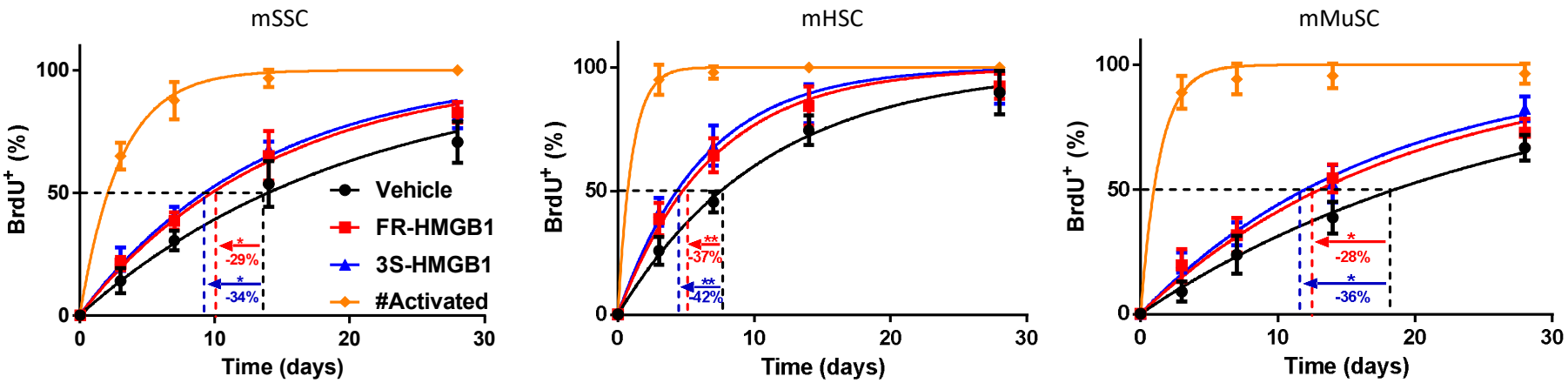

Figure 6.10 ***In vivo*** **cycling response of stem cells to high-dose continuous BrdU. mSSCs, mHSCs, and mMuSCs from mice treated systemically with FR or 3S-HMGB1 display faster entry to cell cycle** ***in vivo*****, but slower than cells from the ipsilateral limb to the fracture (#activated) (n = 4 for each condition and time point).**

6.3.8. c-Met and CXCR4 interaction

It has previously been shown that c-Met signalling is required for mMuSCs to transition to G_{Alert}[117]. In particular, the authors showed that mMuSCs within animals where c-Met had been specifically ablated from these cells (*Pax7 Cre*) failed to transition to G_{Alert} upon injury. I reviewed the literature and there were indications in the fields of developmental, cancer, and haematopoietic stem cell biology that the expression of c-Met and CXCR4 could affect each other[163–167]. Therefore, I assessed if inhibition of c-Met signalling affected the surface expression of CXCR4. As it was not possible to access mMuSC specific c-Met transgenic mice, I instead pharmacologically inhibited c-Met signalling using a small molecule inhibitor, PHA 665752, and a c-Met antibody. CXCR4 staining and flow cytometry revealed that this pharmacological inhibition of c-Met signalling dramatically reduced the expression of surface CXCR4 by approximately 50% (Figure 6.11 a, b). This loss of surface CXCR4 would have significantly impeded the HMGB1-CXCL12-CXCR4-G_{Alert} pathway and may at least in part explain why the Rando group observed that the mMuSCs from animals where c-Met had been specifically ablated from these cells failed to transition to G_{Alert}. Therefore, the HMGB1-CXCL12-CXCR4-G_{Alert} pathway is in keeping with the published findings regarding the requirement for intact c-Met signalling for the transition to G_{Alert} to occur.

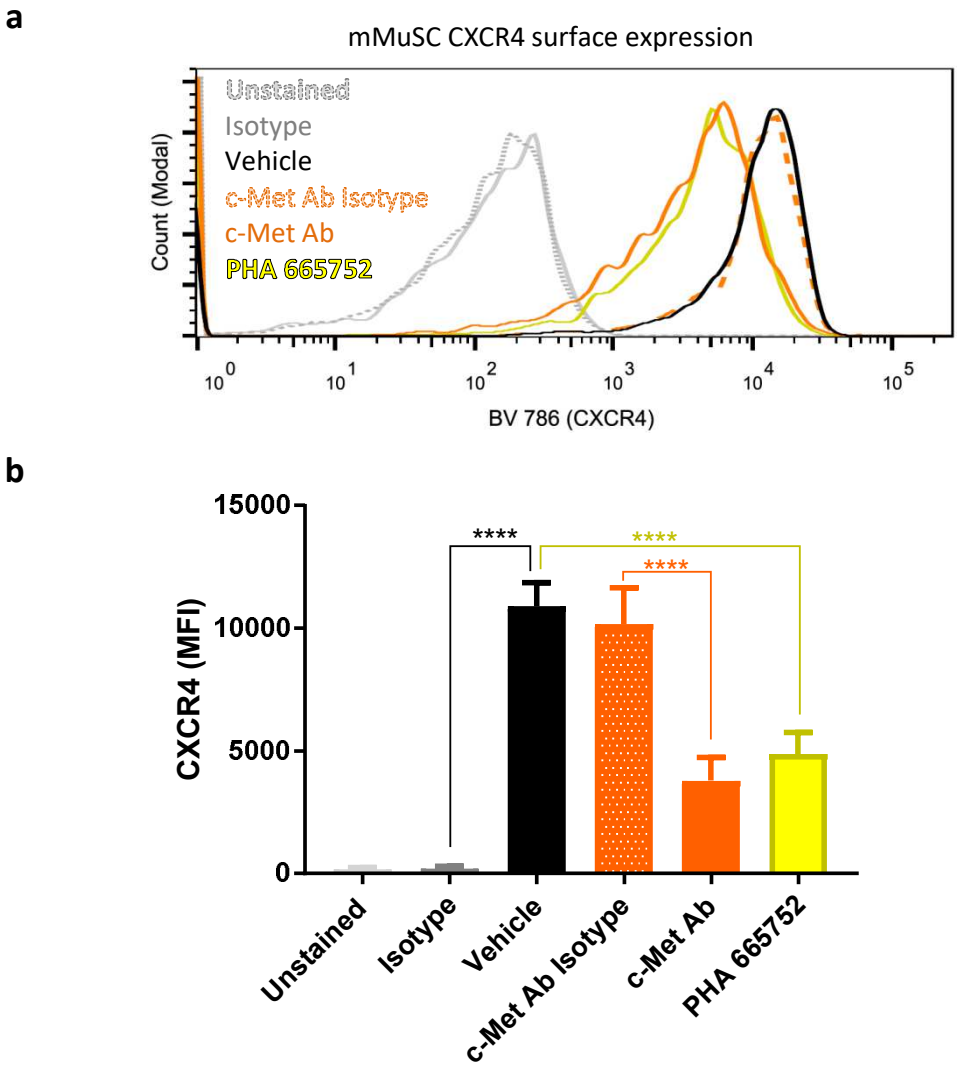

Figure 6.11 c-Met and CXCR4 interaction. (a) Representative histogram plot (similar results observed in 3 independent experiments), and (b) quantification of CXCR4 median fluorescence intensity (MFI), showing mMuSCs from mice treated with a c-Met inhibitor, PHA 665752, or anti-cMet, express substantially less surface CXCR4 compared to controls, as shown by CXCR4 staining and flow cytometry (n = 4 for each condition).

6.4. Discussion

The cellular mechanism by which HMGB1 modulates fracture healing is unknown. The work in the previous chapter showed that HMGB1 acts via CXCL12-CXCR4 to accelerate healing and previously the HMGB1-CXCL12 heterocomplex has been shown to enhance migration of leucocytes compared to CXCL12 alone. It is also known that the HMGB1-CXCL12 heterocomplex causes a different conformational change in CXCR4 compared to CXCL12 alone[88], and therefore could potentially initiate a different intracellular signalling cascade, resulting in a different cellular effect. As exogenous CXCL12 alone was insufficient to accelerate fracture healing, it was probable that the cellular effect through which HMGB1 accelerated fracture healing involved another mechanism, asides from enhanced cell migration.

Through extensive reading of quality literature, it became clear that the CXCL12-CXCR4 axis mediated many more cellular processes apart from chemotaxis. In particular, in the field of stem cell biology, the CXCL12-CXCR4 axis was a well-described cell cycle regulator, where it enforces the quiescence of mHSCs[152–157]. I reasoned that the cycling of stem cells was relevant to the fracture healing process because the well-known processes of cellular differentiation, which is essential for tissue regeneration, occurs during asymmetric stem cell division. Consequently, I hypothesised that the HMGB1-CXCL12-CXCR4 axis may affect the cell cycle of stem cells to accelerate healing.

BrdU assays are well established for studying cell cycle kinetics *in vivo*, and the most common method involves continuously administering low-dose BrdU, which measures cumulative cell cycling. However, it is has been recorded in other systems that the cumulative cycling of stem cells soon after injury can already be 100% by day 5 post-injury[158]. Therefore, it was not a suitable assay to test if HMGB1 increased the cycling of mSSCs in the context of fracture injury. I instead pursued BrdU pulse labelling experiments, which measure the propensity to cycle. These experiments revealed that exogenous FR and 3S-HMGB1 treatment increased the propensity to cycle of mSSCs for a sustained period, which was different to the short term increase caused by a recognised mSSC

activator. In addition, the mSSCs of FR and 3S treated mice, displayed an increasing propensity to cycle over time, and this mirrored the well-known rising upregulation of endogenous osteogenic signals that occurs post-fracture[45,127]. These data show that HMGB1 has a sustained and dynamic effect on the cycling of mSSCs, which is different to the short term and static effect of a recognised mSSC activator.

During the planning of the further investigation and characterisation of this dynamic effect on cell cycling, I continued to review the literature and a set of interesting studies appeared to have relevance from a molecular, cellular, and tissue-level perspective. A notable phenomenon was observed in rabbits in 1970, that an initial 'priming' injury resulted in accelerated tissue regeneration of a second distant injury in the same animal[159]. The nature of this phenomenon affecting tissues distant from the primary injury, suggested that it was due to a systemic mediator. This would be consistent with the findings that levels of HMGB1 were elevated systemically post-fracture. Furthermore, the tissue-level priming phenomenon seemed to be related to the cellular priming effect we had observed with HMGB1 pre-treatment of hMSCs *in vitro*, and accelerated fracture healing effects of exogenous HMGB1 *in vivo*.

Surprisingly this 'priming' phenomenon was not investigated further, seemingly forgotten by the scientific community for 35 years, until it was corroborated by a group from the military Naval Research Institute (USA) in 2005[160]. They showed that this effect also occurred in mice and did not require the participation of monocytes. This was consistent with the highly evolutionarily conserved structure of HMGB1, and the findings that the cellular priming effect I had observed with HMGB1 pre-treatment of hMSCs did not require monocyte conditioned supernatant or co-culture with monocytes.

Then in 2014 a landmark publication explained through an elegant series of experiments that this priming phenomenon was due to an unknown systemic mediator transitioning stem cells distal to the site of initial injury to a state of the cell cycle, intermediate between G_0 and G_1, that they termed

G_{Alert}[117]. When cells are in the more metabolically active G_{Alert} state, instead of the deeply metabolically quiescent G_0 state, they are better poised to enter the cell cycle. Therefore, G_{Alert} cells cycle more rapidly in response to activation signals, which in turn leads to accelerated tissue regeneration. Their finding of an injury signal affecting stem cells in a manner different to classical activators was consistent with the findings from the BrdU pulse labelling experiments that HMGB1 treatment affected mSSCs in a dynamic fashion.

The authors also confirmed that the systemic mediator was in peripheral blood, and this was consistent with our findings of elevated HMGB1 in plasma post-fracture. Furthermore, they demonstrated that mMuSCs and mHSCs could transition to G_{Alert}, and as both mMuSCs and mHSCs express functional CXCR4, it was possible that HMGB1 may have acted upon them via the HMGB1-CXCL12-CXCR4 axis to effect the transition to G_{Alert}. In addition, with the many parallels between developmental biology and adult stem cell biology, I noted that mSSCs, mMuSCs, and mHSCs all arose from the same embryonic germ layer, the mesoderm. Therefore, it was possible that all these cells may act in a similar fashion to a highly conserved injury signal, such as HMGB1. Consequently, with all this correlative evidence, I hypothesised that HMGB1 may accelerate fracture healing by transitioning mSSCs to the G_{Alert} state, and that this effect would extend to other stem cells that are known to express CXCR4, including mHSCs and mMuSCs.

The essential criteria describing the G_{Alert} state are mTORC1 dependency, increased cellular ATP, mitochondrial DNA and cell size, and faster entry to cell cycle[117]. Through *in vivo*, *ex vivo,* and *in vitro* assays it was shown that HMGB1 treatment transitioned mSSCs, mHSCs, mMuSCs, hHSPCs, and hMSCs to G_{Alert}, whereas stem cells from *Hmgb1*$^{-/-}$ mice did not transition to G_{Alert}. In addition it was shown that the HMGB1-CXCL12-CXCR4-G_{Alert} pathway was consistent with the previous finding that c-Met signalling needed to be intact for the G_{Alert} transition to occur[117], due to disrupted c-Met signalling severely downregulating expression of surface CXCR4.

In summary, the work described in this chapter establishes HMGB1 as a systemic factor that is capable of transitioning multiple CXCR4$^+$ murine and human stem and progenitor cells to G_{Alert} (Figure 6.10). For the skeletal system, the tissue-level effect of the cellular transition of mSSCs to G_{Alert}, was the acceleration of fracture healing. The tissue-level effect of the cellular transition of other stem and progenitor cells to G_{Alert} will be discussed in the following chapter.

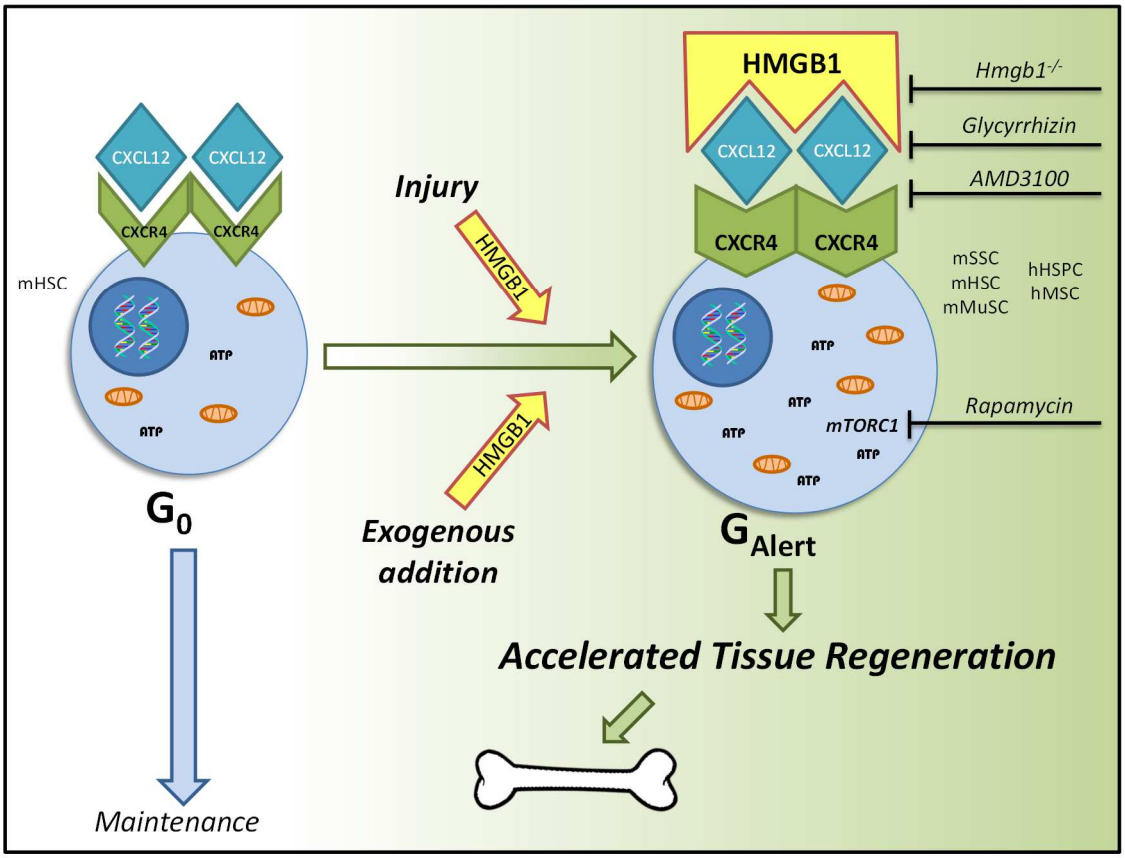

Figure 6.12. Schematic of findings from this chapter. HMGB1 transitions multiple human and murine stem and progenitor cells to G_{Alert}. The relevance of these cellular findings to multiple tissues will be discussed in the following chapter.

Chapter 7. Multiple tissue regenerative effects of HMGB1

7.1. Introduction

Based on the published findings that the injury-G_{Alert} pathway leads to accelerated muscle regeneration, and my data that the HMGB1-G_{Alert} pathway led to accelerated skeletal regeneration, and HMGB1 transitioned mSSCs, mHSCs, and mMuSCs to G_{Alert}, I investigated whether the HMGB1-G_{Alert} pathway would also accelerate haematopoietic and muscle regeneration. Studying the regeneration of these tissues would have important translational implications for patients who have suffered severe fractures and multi-trauma where substantial muscle injury and blood loss typically accompanies the skeletal injury. Furthermore, these studies would have substantial translational implications in the fields of oncology and chronic illness management, respectively.

Chemotherapy induced leucopoenia and neutropaenia results in an increased risk of infection with febrile neutropaenia being a medical emergency because it can lead to bacteraemia, sepsis, and death[168]. Accelerated haematopoietic regeneration would reduce the length of time (nadir) of clinical neutropaenia, thereby reducing the risk of infection and the treatment associated morbidity and mortality associated with chemotherapy[169]. Cachexia is a wasting syndrome defined by a relentless loss of skeletal muscle mass that is not amenable to treatment with a simply increased caloric intake[170,171]. It is seen in the late stages of almost every major chronic illness, such as up to 80%, 42%, 30%, and 60% of cancer, heart, lung and kidney disease patients respectively[170], and up to 25% of all cancer deaths are due to cachexia rather than directly from the tumour burden[171,172]. This is due to cachexia resulting in severe weakness which devastates the quality of life of patients by making routine activities difficult or impossible, increasing the risk of complications such as infections, and it is extremely distressing for family members to witness. The current understanding is that the underlying pathogenesis is due metabolic and immune dysfunction affecting the myofibre, with most research focused on how this affects the terminally differentiated myocyte within the myofibre[171]. Yet, despite significant academic and pharmaceutical investment into developing drugs that target these pathways, there are still no treatments available[170]. Accelerated

muscle regeneration would dramatically improve the quality of life of these patients and help them maintain their dignity at this stage of their lives.

The previous publication reported extended cell cycle kinetic studies that revealed that stem cells in the contralateral limb remained in G_{Alert} for 3-4 weeks[117]. This was consistent with the finding that HMGB1 resulted in mSSCs having a sustained and dynamic increased propensity to cycle and with the previous reports that injury-priming an animal as long as 2-4 weeks prior to the subsequent injury, still accelerated healing[159,160]. Therefore, I investigated whether animals pre-treated with HMGB1 two weeks prior to bone, haematopoietic or muscle injury, would still display accelerated healing. These HMGB1-priming studies would significantly widen the translational applicability of HMGB1, with it potentially being administered prior to situations of expected or planned injury, such as combat, sport, emergency or elective surgery. The latter are traditionally thought of as treatment modalities, but are themselves a form of injury, for which there are few approved treatments to accelerate healing despite people in the USA on average undergoing 9.2 surgical procedures in their lifetime[173].

7.2. Hypothesis

HMGB1 accelerates bone, haematopoietic and muscle tissue regeneration, even if administered two weeks prior to injury.

7.3. Results

7.3.1. Effect of exogenous HMGB1 on haematopoietic regeneration

5-Fluouracil (5-FU) is a clinically approved chemotherapeutic agent that is commonly used to treat a variety of cancers. Systemic administration reliably results in myeloablation. Therefore, it is a well-established model of haematopoietic injury that is used to study haematopoietic regeneration[120,121]. Importantly, the large amount of cell death that accompanies this model is programmed apoptotic cell death due to 5-FU creating a scarcity of thymidine[174], which is required for DNA replication. As apoptotic cell death only releases bound and functionally inert HMGB1, a large release of FR-HMGB1, which would overwhelm any exogenous administration, would not be expected. Therefore, I assessed whether HMGB1 administered systemically to mice would lead to accelerated recovery from 5-FU injury (Figure 7.1 a). I wrote the animal license protocol and again went through the lengthy animal license amendment approval process. Serial peripheral blood microsampling and cell counting revealed that FR and 3S-HMGB1 treated mice had a shorter duration of leucopaenia (Figure 7.1 b) and neutropaenia (Figure 7.1 c) by approximately 2-3 days, or 15-20%. Quantification of the acceleration of healing via one-equation mathematical modelling and curve fitting, as was used for fracture healing, was inappropriate because the leucocyte and neutrophil count trends beyond the peak values were unclear and the difficulty of fitting to the multiple inflexion points across the timeline. It may have been possible to fit the datasets to piecewise functions, which consist of multiple sub-functions across sub-domains of the function, however the F-test is ill-suited for comparing these functions. Counting of leucocytes and neutrophils and staining of peripheral blood smears was performed in conjunction with A.I. Espirito Santo for more accurate cell counts and efficient processing of samples.

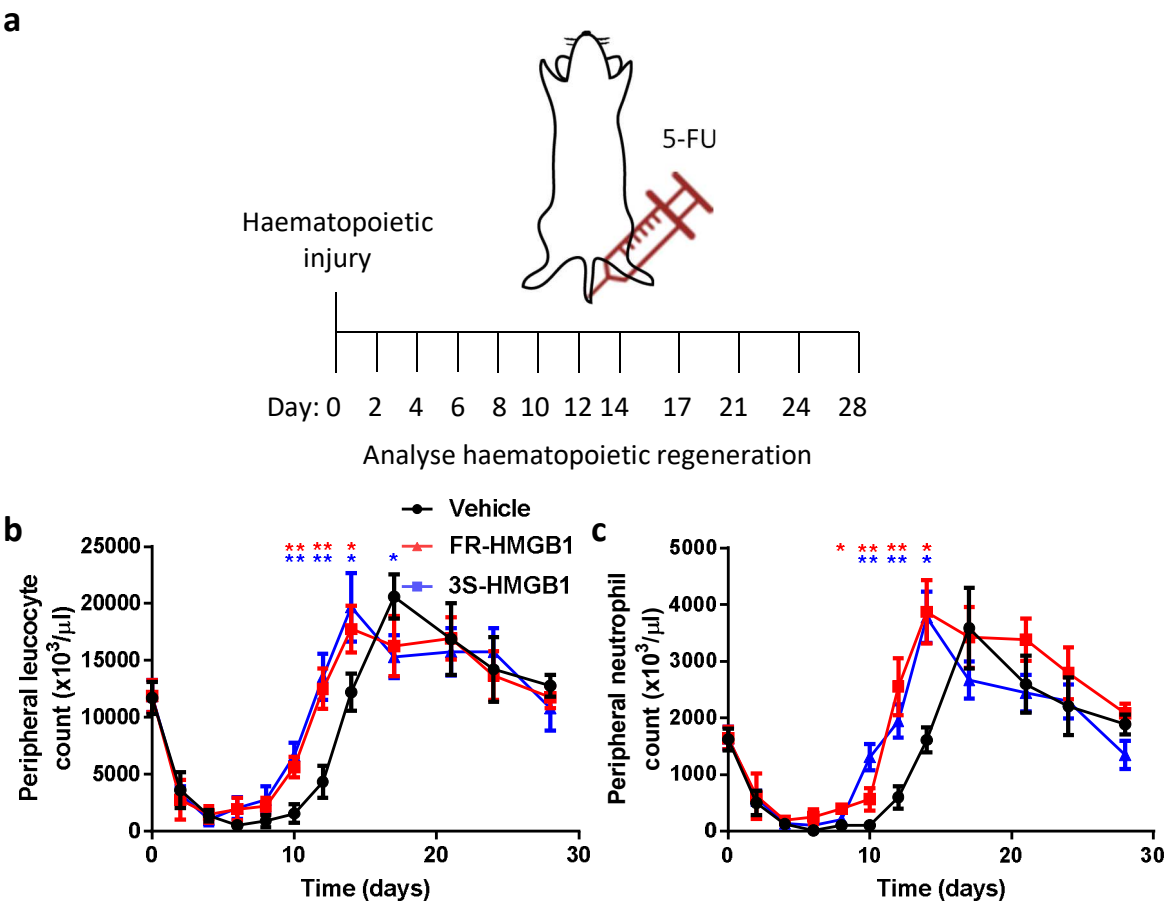

Figure 7.1 Effect of exogenous HMGB1 on haematopoietic regeneration. (a) Schematic of myeloablation haematopoietic injury model with 5-FU and subsequent analysis time points. (b) Peripheral leucocyte and (c) neutrophil counts showing that systemic administration of FR or 3S-HMGB1 accelerates haematopoietic recovery following 5-FU myeloablation (n = 8 for FR and 3S-HMGB1, 9 for vehicle controls). 5-FU = 5-fluouracil.

7.3.2. Effect of exogenous HMGB1 on muscle regeneration

Local chemical injury with an intramuscular injection of barium chloride ($BaCl_2$) is a well-established model of muscle injury[122] that was previously used in the injury-G_{Alert} study to assess muscle regeneration[117]. The primary read out of the model used by the injury-GAlert paper was muscle fibre cross-sectional area because this relates to the functional capacity of the muscle belly[117,122]. Therefore, I assessed whether local administration of HMGB1 would lead to accelerated recovery following muscle injury with $BaCl_2$ (Figure 7.2 a). Measurements of muscle fibre cross sectional area showed that mice treated locally FR and 3S-HMGB1 displayed accelerated muscle regeneration (Figure 7.2 b, c). Muscles were sectioned and stained by the institute's Histology Core, and quantification of muscle fibre cross sectional area was performed in conjunction with A.I. Espirito Santo for more accurate measurements and efficient processing of samples.

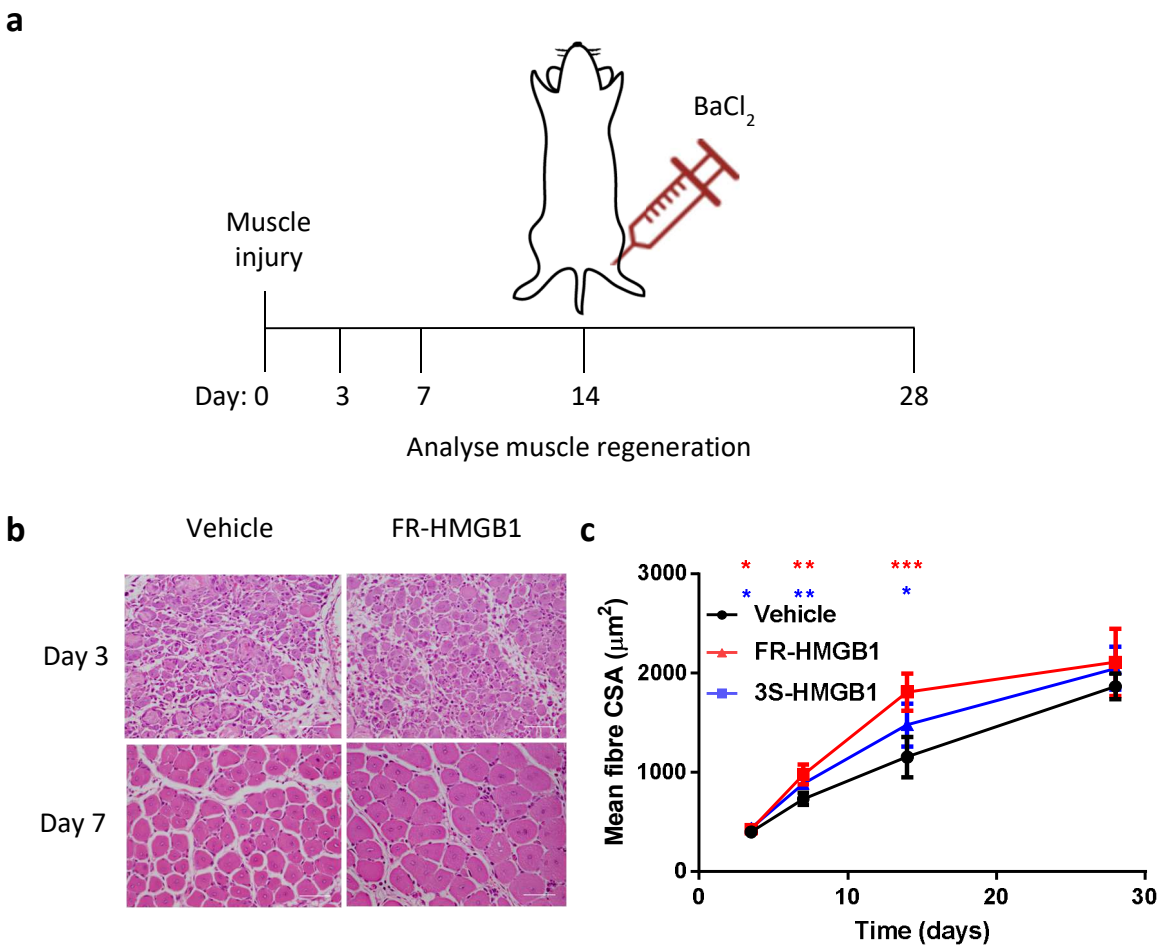

Figure 7.2 Effect of exogenous HMGB1 on muscle regeneration. (a) Schematic of chemical muscle injury model with $BaCl_2$, and subsequent analysis time points. (b) Representative muscle histology, and (b) mean muscle fibre cross sectional area showing that systemic administration of FR or 3S-HMGB1 accelerates muscle regeneration following $BaCl_2$ chemical injury (n = 4 for each condition and time point).

7.3.3. Effect of exogenous HMGB1 pre-treatment on fracture healing

The literature indicated that stem cells remained in G_{Alert} for 3-4 weeks post-injury[117], which is consistent with my finding that HMGB1-treated cells having a sustained and dynamic increased propensity to cycle, and with the original reports of accelerated healing as long as 2-4 weeks after the priming injury[159,160]. Therefore, I assessed whether animals pre-treated with HMGB1 two weeks prior to fracture exhibited accelerated fracture healing (Figure 7.3 a). Treatment with FR or 3S-HMGB1 accelerated healing, which was apparent on *in vivo* microCT radiographs (Figure 7.3 b) and evidenced by left shifts of the callus volume and the callus bone mineral density curves (Figure 7.3 c). The acceleration of healing was quantified as 18.3% and 20.6%, respectively (Figure 7.3 c). This was confirmed with functional testing of the femurs at day 28, which showed that mice pre-treated systemically with FR or 3S-HMGB1 had femurs with significantly higher mechanical strength compared to vehicle controls (Figure 7.3 d).

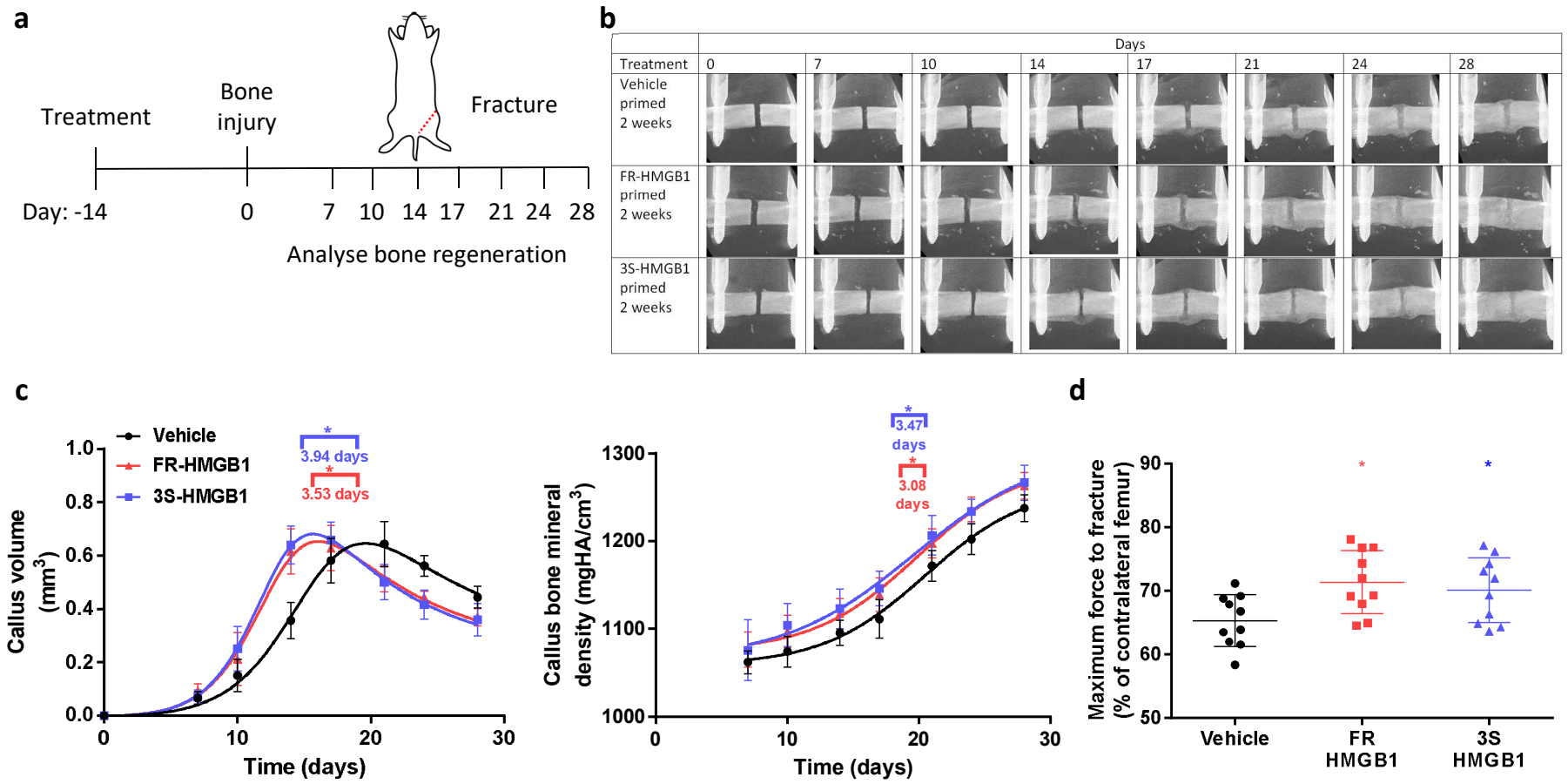

Figure 7.3 Effect of exogenous HMGB1 pre-treatment on fracture healing. (a) Schematic of fracture model and analyses with HMGB1 pre-treatment. (b) Representative *in vivo* microCT radiographs, (c) callus volumes, callus bone mineral densities, and (d) mechanical strength of femurs pre-treated with FR and 3S-HMGB1 two weeks prior to fracture showing accelerated fracture healing compared to vehicle controls (n = 10 for each condition).

7.3.4. Effect of exogenous HMGB1 pre-treatment on haematopoietic and muscle regeneration

Based on the finding that systemic HMGB1 pre-treatment accelerated fracture healing, I assessed whether systemic administration of HMGB1 2 weeks prior to 5-FU haematopoietic injury or $BaCl_2$-induced muscle injury resulted in accelerated haematopoietic or muscle regeneration, respectively (Figure 7.4 a). Serial peripheral blood microsampling and cell counting revealed that FR and 3S-HMGB1 pre-treated mice had a shorter period of leucopaenia and neutropaenia by approximately 2 days, or 15% (Figure 7.4 b). Similarly, mice pre-treated with FR or 3S-HMGB1 showed accelerated regeneration of muscle tissue as shown by measurements of muscle fibre cross sectional area (Figure 7.4 c).

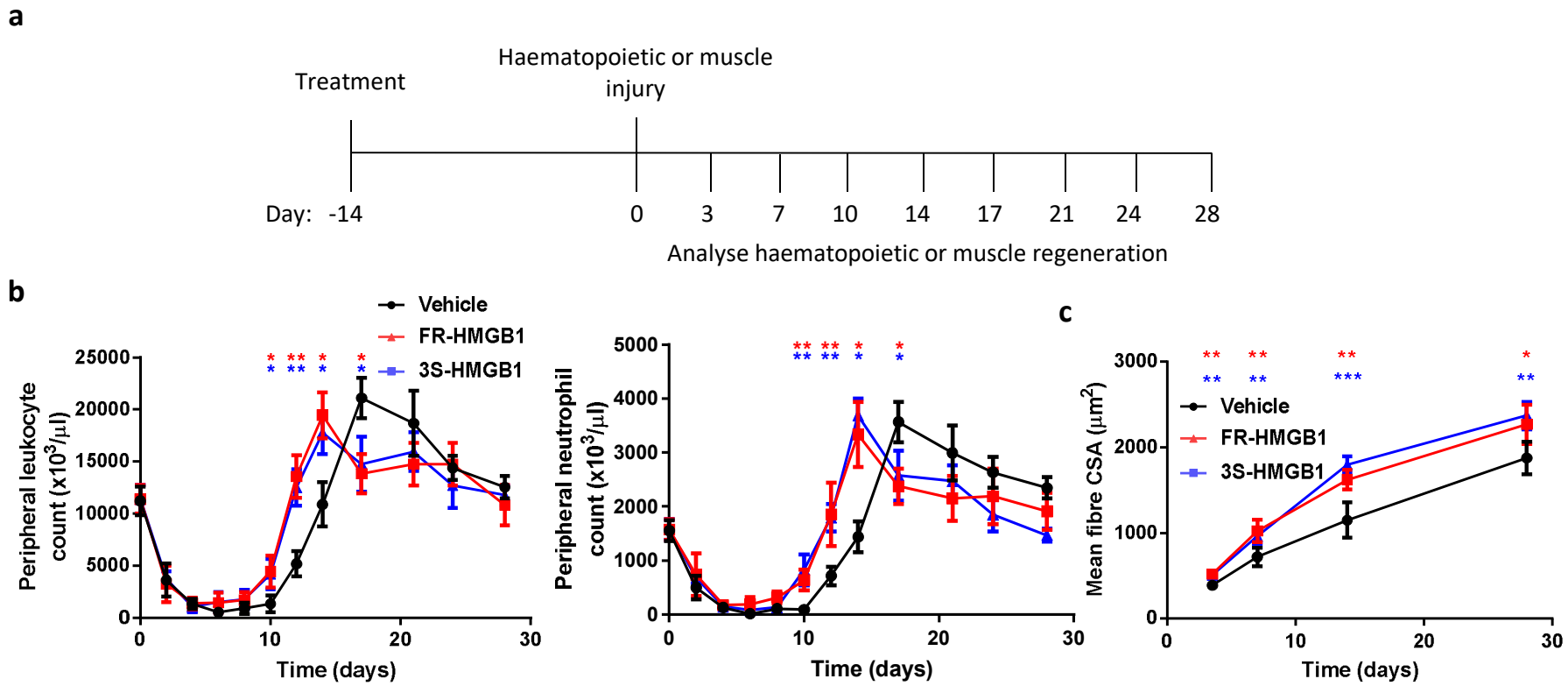

Figure 7.4 Effect of exogenous HMGB1 pre-treatment on haematopoietic and muscle regeneration. (a) Schematic of haematopoietic and muscle injury model and analyses following pre-treatment with HMGB1. (b) Peripheral leucocyte and neutrophil counts and (c) mean muscle fibre cross sectional area showing that systemic administration of FR or 3S-HMGB1 two weeks before injury accelerates haematopoietic regeneration following myeloablative 5-FU injury (n = 8 for FR and 3S-HMGB1, 9 for vehicle controls), and muscle regeneration following chemical $BaCl_2$ muscle injury, respectively (n = 5 for each condition and time point).

7.4. Discussion

The effects of exogenous FR or 3S-HMGB1 treatment on haematopoietic or muscular regeneration are unknown. With the findings in the previous chapters that HMGB1 transitions mSSCs to G_{Alert} and accelerated fracture healing, and transitions mHSCs and mMuSCs to G_{Alert}, and the prior report that the injury-G_{Alert} pathway led to accelerated muscle regeneration[117], the reasonable extrapolation was that exogenous HMGB1 may also accelerate haematopoietic and muscular regeneration. Furthermore, results in the prior chapters have shown that HMGB1 treatment leads to mSSCs having a sustained and dynamic increased propensity to cycle, which was consistent with prior reports that stem cells can remain in G_{Alert} for an extended period[117], and that injury-priming an animal as long as 2-4 weeks prior to the subsequent injury results in accelerated healing[159,160]. Therefore, it was possible that HMGB1-priming an animal 2 weeks prior to fracture, haematopoietic or muscle injury would accelerate regeneration of those respective tissues.

Utilising the well-established 5-FU myeloablation model of haematopoietic injury and peripheral blood counts to assess recovery[120,121], it was clear that both FR and 3S-HMGB1 treatments accelerated the recovery of leucocytes and neutrophils, and reduced the period of neutropaenia. This has translational relevance because the duration of neutropaenia is directly related to the risk of infection, with each day of neutropaenia approximately doubling the risk of a febrile neutropaenia episode. Febrile neutropaenia is a medical emergency with a mortality rate of 6.8-9.5%[168], so an acceleration of haematopoietic recovery following chemotherapy would make chemotherapy safer for patients.

The chemical $BaCl_2$ model of muscle injury is well-established for studying muscle healing and repair[122]. It was previously shown that $BaCl_2$-induced muscle injury transitioned mMuSCs to G_{Alert}, and the model was used to show that injury-priming animals led to an acceleration of muscle regeneration. Therefore, I selected this model to assess whether FR and 3S-HMGB1 treatment would

lead to accelerated muscle regeneration. Histological measurements of muscle fibre cross sectional area showed that they did accelerate muscle regeneration.

Subsequently both these injury models and the optimised fracture model were used to determine whether pre-treatment with HMGB1 two weeks before injury would accelerate healing. Pre-treatment with either FR or 3S-HMGB1 did not cause ectopic tissue formation prior to the fracture, and accelerated fracture healing as determined by *in vivo* microCT and mechanical strength testing. Both forms of HMGB1 also accelerated haematopoietic and muscle regeneration following injuries. It should be noted that whilst efficacy of pre-treatment compared to treatment at the time of injury was not performed, it appears for the fracture healing model that treatment at the time was more effective. This would be consistent with the previous finding that cells gradually transition back from G_{Alert} to G_0 over a 4 week period[117]. The pre-treatment data also support the concept that HMGB1 leads to accelerated regeneration and healing in multiple tissues by transitioning resident $CXCR4^+$ stem cells to G_{Alert} rather than through an alternative mechanism, such as enhanced chemotaxis.

In summary, the work described in this chapter establishes HMGB1 as a mediator that accelerates the regeneration of multiple tissues, including bone, blood and muscle. Moreover, it identifies HMGB1-G_{Alert} as a pathway which causes a dynamic and adaptive multi-tissue regenerative response to existing or future injury and activation signals.

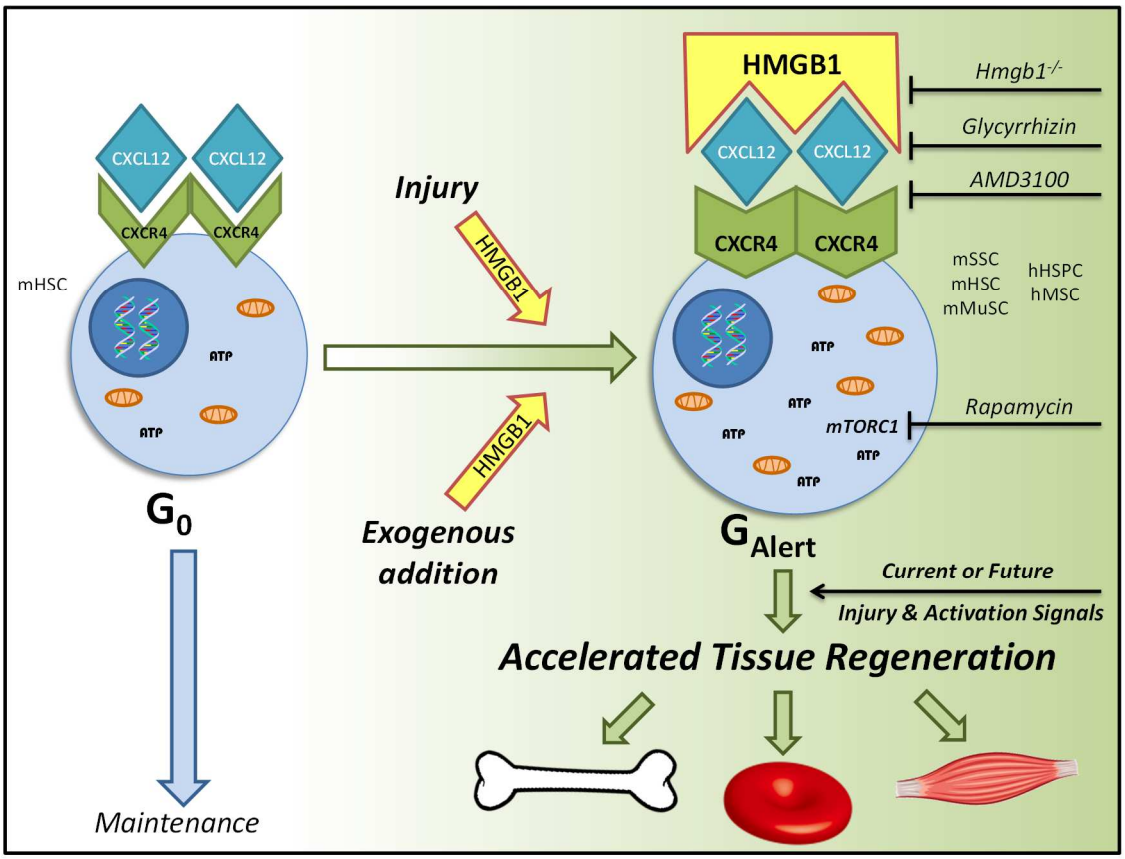

Figure 7.5 Schematic of findings from this chapter. HMGB1 accelerates bone, haematopoietic and muscle tissue regeneration, even if administered two weeks prior to injury.

Chapter 8. General discussion

8.1. Final discussion

The role of alarmins in tissue healing is unknown. Fracture healing is an ideal process for studying tissue regeneration and healing because fractured bones have a well-established regenerative capacity and under normal circumstances heal completely. Additionally, the fracture healing course in mice and humans are physiologically similar[45] with both undergoing the stages of inflammation, callus formation, and remodelling, so deeper *in vivo* investigations with small animal models are translationally relevant. From a decade of investigating the biology of fracture healing, the group had shown that early immune cells, such as neutrophils[109], play a key role in regulating fracture healing, and the initial release of low levels of pro-inflammatory signals, such as TNF[108], are important for subsequent downstream repair. As alarmins are amongst the earliest mediators released on tissue injury and trigger the initial inflammatory cascade[128], it was hypothesised that alarmins may play an important role in fracture healing. Subsequently a candidate approach focussing on the alarmins S100A8/A9, and HMGB1 was based on both being associated with regulating skeletal cells, and in particular osteogenic differentiation[62,84].

With the group's and the field's emphasis on ensuring translational relevance of basic life science studies[175], this project began by studying alarmins in human clinical samples and their effects on primary human cells. Measurements of plasma levels of S100A8/A9 and HMGB1 showed that levels of both alarmins were elevated systemically post-fracture in patients. Then to evaluate the relative contribution of each alarmin to the fracture process I conducted a series of experiments to assess their direct or indirect effect on the osteogenic differentiation of hMSCs, which are known to be involved in fracture healing. These assays showed the direct addition of the alarmins did not affect osteogenic differentiation, and in the presence of monocytes or their products, S100A8, S100A9, and DS-HMGB1 inhibited osteogenic differentiation. Next, based on the likely temporal *in vivo* scenario of hMSCs being exposed to alarmins prior to potent osteogenic signals, hMSCs were pre-treated with alarmins before incubation with osteogenic media. Only pre-treatment of hMSCs with FR or 3S-HMGB1, which did not induce pro-inflammatory cytokine production, increased their osteogenic

differentiation. Collectively these data suggest that FR-HMGB1 plays a role in human fracture healing, by priming hMSCs for subsequent exposure to osteogenic mediators.

In order to understand the *in vivo* relevance of the *in vitro* findings I required a robust fracture model that could be followed over a time course. A murine femoral fracture model stabilised with an external fixator was selected and carefully optimised due to its high suitability for serial *in vivo* microCT measurements, and mechanical strength testing. Both these parameters are necessary to study the acceleration of fracture healing[133], and mathematical models were generated to quantify the acceleration of fracture healing. The model was further validated by measuring the plasma levels of S100A8/A9 and HMGB1 post-fracture and they were found to be elevated, in line with my human clinical data. Next, exogenous administration of FR or 3S-HMGB1 was found to accelerate fracture healing by approximately 20% and 30% respectively, and a dose-response was established for 3S-HMGB1. The similar results seen with FR or 3S-HMGB1 indicated that the acceleration of healing effects were due to FR-HMGB1 with no contribution from DS-HMGB1. In the clinical setting, both FR and 3S-HMGB1 may be targets for accelerating fracture healing, and 3S-HMGB1 may be preferred due to its definite inability to promote excessive inflammation.

Following the gain of function, seen in terms of accelerated fracture healing from exogenous administration of HMGB1, it was essential to conduct loss of function tests to determine the significance of endogenous HMGB1 to the fracture healing process. Inducible whole body *Hmgb1*$^{-/-}$ mice were generated as germ line deletion of HMGB1 is perinatally lethal[138]. Challenging these mice with the fracture model revealed that genetic deletion of HMGB1 led to significantly delayed and impaired fracture healing. This showed that endogenous HMGB1 plays a key role in maintaining the quality and rate of fracture healing *in vivo*. This finding is consistent with the impaired and delayed healing observed in mice in a cardiotoxin muscle injury model where HMGB1 was partially deleted (*Hmgb1*$^{+/-}$)[140].

Based on the finding that HMGB1 modulates the rate of fracture healing, it was important to identify the molecular pathway through which it acted. Whist the various redox forms of HMGB1 had been reported to interact with many molecules and receptors, the fully reduced form of HMGB1 has been conclusively shown to form a heterocomplex with CXCL12, which in turn binds to the receptor, CXCR4[86,88]. CXCL12 mediates chemotaxis by binding to CXCR4, and the HMGB1-CXCL12 heterocomplex has been shown to further enhance the chemotaxis of leucocytes, by inducing a different conformational change in CXCR4 compared to CXCL12 alone[88]. Therefore, it was possible that HMGB1 was modulating the rate of fracture healing by interacting with CXCL12 and CXCR4 to enhance the migration of callus-contributing cells to the fracture site. Levels of the HMGB1-CXCL12 heterocomplex levels were found to be elevated post-fracture in the plasma of patients and mice. Using small molecule inhibitors of the HMGB1-CXCL12 and CXCL12-CXCR4 interactions confirmed that HMGB1 was modulating the rate of fracture healing by interacting with CXCL12 and CXCR4 *in vivo*. Notably, the fracture healing of *Hmgb1*$^{-/-}$ mice was markedly delayed and of poorer quality than glycyrrhizin treated mice, which suggests that the loss of the important intracellular interactions and functions of HMGB1, which include organising and bending DNA and regulating transcription, contributed substantially to fracture healing. Whilst outside the focus of this thesis, rescue experiments would further delineate between the relative contributions of intracellular and extracellular HMGB1 to fracture healing.

Of the various cells that have been reported to contribute to the formation of callus, I focussed on the recently identified and characterised murine skeletal stem cell, because it had been definitively proven with modern genetic lineage tracing and immunophenotypic cell isolation techniques to be a major contributor to the formation of callus[101]. Flow cytometry and cell migration assays showed that the mSSCs expressed functional CXCR4. This indicated that HMGB1 via CXCL12 and CXCR4 may directly act on mSSCs to potentially enhance the migration of these cells to the fracture site, and thereby accelerate fracture healing. If this were true, then solely upregulating CXCL12-mediated migration should have been sufficient to accelerate fracture healing. However, exogenous addition

of CXCL12 alone only resulted in aberrant fracture healing, suggesting that whilst HMGB1 may directly affect the mSSC, it was likely to involve a cellular mechanism apart from simply enhanced cell migration.

Literature from the stem cell biology field indicates that asides from chemotaxis, the CXCL12-CXCR4 axis is also a major regulator of cell cycling, in particular the enforcement of quiescence of haematopoietic stem cells[152–157]. It is possible that the established conformational change in CXCR4 caused by the HMGB1-CXCL12 heterocomplex, compared to CXCL12 alone, may induce a different signalling cascade to CXCL12, and instead of enforcing quiescence, the HMGB1-CXCL12-CXCR4 axis may influence the cycling of mSSCs in a manner that would lead to accelerated fracture healing. The cycling kinetics of mSSCs is likely to be pertinent to fracture healing because it is linked through the process of asymmetric cell division to the process of osteogenic differentiation, which is a major cellular process that occurs during fracture healing[45].

BrdU pulse labelling assays were utilised to investigate the effects of exogenous FR and 3S-HMGB1 treatment on the cycling of mSSCs in the context of a fracture injury. These assays are well-suited for studying *in vivo* cell cycling in the post-injury context where cell cycling is rapid[158]. They revealed that exogenous FR and 3S-HMGB1 treatment increased the propensity to cycle of mSSCs in the context of a fracture injury. This effect was sustained for a prolonged period, which was not seen with BMP2, a recognised mSSC activator[101]. Furthermore, mSSCs from mice treated with HMGB1 displayed an increasing propensity to cycle over time, which appeared to mirror the well-established gradual upregulation of endogenous osteogenic signals post-fracture[45,127]. Collectively these data shows that compared to the short term and static effect of a recognised mSSC activator, HMGB1 has a markedly different sustained and dynamic effect on the cycling of mSSCs.

Traditionally it was thought that the stem cells were either actively cycling (G1, S, G2, and M phases), or quiescent (G_0). Accordingly, molecules that permitted either were termed stem cell activators or enforcers of quiescence, respectively. Recently, it was described that the quiescent phase is actually

more dynamic and can be separated into two distinct phases, namely G_0 and G_{Alert}[117]. Cells in the G_{Alert} state are not actively cycling, but are poised to efficiently enter the cycle compared to the deeply metabolically quiescent G_0 cells. These fundamental cellular discoveries helped to explain a 40 year old finding that a priming injury resulted in accelerated tissue regeneration of a second distant injury in the same animal[159], because the stem cells distant from the priming injury, including mMuSCs and mHSCs, transition to G_{Alert}. However, even after that landmark paper, the identity of the systemic molecular mediator(s) which transitioned stem cells to G_{Alert} remained unknown, so the translational potential of the G_{Alert} phase could not be harnessed for therapeutic benefit.

The data that I had accrued, including the systemic elevation of HMGB1 levels post injury, increased osteogenic differentiation of HMGB1-primed hMSCs, accelerated fracture healing with exogenous HMGB1 treatment, sustained and dynamic higher propensity to cycle of mSSCs from HMGB1 treated mice, and the functional expression of CXCR4 on mSSCs akin to mHSCs and mMuSCs, all suggested that HMGB1 is a possible stem cell 'alerter'. Therefore, I hypothesised that HMGB1 may accelerate fracture healing by transitioning mSSCs to the G_{Alert} state, and that HMGB1 may also transition other $CXCR4^+$ stem and progenitor cells to G_{Alert}. The key criteria describing the G_{Alert} state are mTORC1 dependency, increased cell size, mitochondrial DNA and ATP levels, and faster entry to cell cycle[117]. Through *in vivo*, *ex vivo,* and *in vitro* assays it was shown that HMGB1 satisfied all these criteria and was a systemic mediator which transitioned mSSCs, mHSCs, mMuSCs, hHSPCs, and hMSCs to G_{Alert}.

It has previously been suggested that a ligand which activated c-Met might be involved in transitioning cells to $G_{Aler}{}^{117}{}_t$, because the genetic ablation of c-Met signalling prevented mMuSCs transitioning to G_{Alert}. The HMGB1-CXCL12-CXCR4-G_{Alert} pathway is consistent with this finding because even pharmacologically disrupting c-Met signalling resulted in a dramatic downregulation of surface expression of CXCR4. At the time of writing, a report has just been released which shows that pre-treatment with HGF-A, an enzyme which converts inactive pro-HGF to HGF, a c-Met ligand, accelerated muscle regeneration[176]. Therefore, the authors suggested that HGF-A is an alerting

factor. However, it is unclear how HGF-A acts as an alerting factor at the molecular and cellular level, because HGF, the final ligand which interacts with c-Met, has been shown by multiple studies to be a definite mMuSC activator *in vitro*[177] and *in vivo*[178]. Nonetheless the HMGB1-CXCL12-CXCR4-G_{Alert} and HGF-A-HGF-c-Met-G_{Alert} pathways may be complementary, and this would be consistent with other known interactions between c-Met and CXCR4 signalling[163–167].

Having established that HMGB1 transitions mSSCs to G_{Alert} and accelerated fracture healing, and that it also transitions mHSCs and mMuSCs to G_{Alert}, and knowing that injury alerted mMuSC lead to accelerated muscle regeneration, I postulated that exogenous HMGB1 would also accelerate haematopoietic and muscular regeneration. Furthermore, as my data showed that HMGB1 treatment had a lasting effect on the propensity to cycle of mSSCs, consistent with prior reports that stem cells can remain in G_{Alert} for up to 4 weeks[117], and that injury-priming an animal as long as 2-4 weeks prior to the subsequent injury results in accelerated healing[159,160], I additionally hypothesised that HMGB1-priming an animal 2 weeks prior to injury would accelerate tissue regeneration. Utilising the femoral fracture model, and well-established models of haematopoietic and muscle models showed that FR and 3S-HMGB1 accelerated regeneration of both these tissues even if administered 2 weeks prior to the injury. Coupled with the lack of ectopic tissue formation in the steady state environment following pre-treatment with HMGB1, these results indicates that that HMGB1 treatment is a dynamic and adaptive form of multi-tissue regenerative therapy, which takes cues from the steady state or activating regenerative molecular signals present at that time. It is important to note that the nature of this response is markedly different to stem cell activators, which are known to cause *de novo* tissue formation. Indeed, the ectopic *de novo* formation of tissue is the primary reason why some are used clinically, such as BMP2 for spinal fusion.

8.2. Future directions

8.2.1. Intracellular, genetic, and epigenetic regulation of HMGB1-G_{Alert}

The mTORC1 signalling pathway has been reported to be a regulator of the transition to G_{Alert}. As mTORC1 signalling is critical to many cellular processes[179], and the transition to G_{Alert} appears to be highly specific, it is possible that there are other more specific intracellular pathways that regulate the transition to G_{Alert}. These other pathways may be suitable targets for drug development, and if found to be more specific to G_{Alert}, would likely have less off-target effects. In addition, the prolonged cellular effect of HMGB1 suggests that there may be an epigenetic regulator of the HMGB1-G_{Alert} pathway. Targeting this epigenetic regulation may enable the time in the G_{Alert} state to be shortened, prolonged, or even made permanent, according to clinical need. This would be particularly relevant for stem memory T cells[180], a rare subset of T cells that are long-lived, self-renewing, express CXCR4, and regulate the long-term adaptive immune response. The HMGB1-G_{Alert} pathway may potentiate the effects of these cells with diverse potential clinical applications, from boosting the duration of protection from vaccines, rejuvenating the adaptive immunity of aged and other immunocompromised persons, and enhancing the efficacy of cancer immunotherapies.

8.2.2. Crystal structure of HMGB1-CXCL12-CXCR4 and CXCL12-CXCR4

Whilst it has been reported that the HMGB1-CXCL12 heterocomplex causes a different conformational change in CXCR4[88], compared to CXCL12 alone, it is unknown exactly what this change is. Understanding the crystal structure of CXCL12-CXCR4 and HMGB1-CXCL12-CXCR4 would give insight into the downstream signalling that regulates the G_{Alert} transition. It would also permit the structural modelling and testing of small molecules that would cause the G_{Alert} transition by interacting with CXCR4 or CXCL12 in a similar manner as the HMGB1-CXCL12 heterocomplex or HMGB1, respectively. Production of these small molecules, or truncations of HMGB1, would likely be cheaper and simpler than the large scale GMP production of purified HMGB1 proteins, due to its N-terminus having a high affinity for LPS, and its C-terminus being toxic to bacteria. In addition, the

crystal structure of CXCL12-CXCR4 would add immensely to the fields of virology, stem cell biology, cancer biology, and developmental biology due to the CXCL12-CXCR4 axis mediating multiple effects.

8.2.3. Further disease contexts

At first, it may be surprising that HMGB1 is able to accelerate the regeneration of diverse tissues such bone, muscle, and blood, which are solid, soft, and liquid tissues, respectively. However, all three tissues share common elements, namely that the major cells which contribute to their repair express CXCR4, and are capable of transitioning to G_{Alert}. Amongst the several tissues which have cells that express CXCR4, a promising and interesting target would be the liver and the hepatocyte. Even though the hepatocyte is a fully differentiated cell, it behaves as a quiescent cell *in vivo*[181], has a known substantial regenerative contribution to the liver, and abundantly expresses CXCR4. If HMGB1 were to transition hepatocytes to G_{Alert} and accelerate hepatic regeneration, this would conceptually expand the HMGB1-G_{Alert} pathway beyond mesodermal stem and progenitor cells to include fully differentiated endodermal cells too. This would have significant translational implications for the management of liver diseases, which are a major health burden[182,183]. The translational relevance of haematopoietic and muscular regeneration may be further investigated in models of radiotherapy, bone marrow and haematopoietic stem cell transplant models, and orthotopic tumour models to represent human haematopoietic stem cell transplantations and cancer cachexia conditions.

Asides from upregulating the HMGB1-G_{Alert} pathway for applications in regenerative medicine, it would be interesting to assess if inhibiting this pathway may be useful for preventing unwanted tissue growth. In particular, it is well-known that cancers can recur many years after the primary tumour has been put into remission. Although it is unknown why this occurs, one event that has been long-noted to shortly precede the sudden growth of dormant distant micrometastases is trauma or surgery[184]. It is possible that those injuries release HMGB1 which transitions the dormant cancer cells[185], including cancer stem cells[186,187], and circulating tumour cells[188], to G_{Alert} and they are

then responsive to their surrounding growth signals. Therefore, inhibition of the HMGB1-G_{Alert} pathway may reduce the incidence of cancer recurrence and metastasis, which is the leading cause of death from cancer.

8.3. Concluding statement

In conclusion, I have identified a molecular and cellular pathway that accelerates the physiological regenerative response in a dynamic and adaptive manner to current or future injuries, findings that have broad relevance to the fields of both stem cell biology and regenerative medicine. I demonstrate here that HMGB1 accelerates healing of multiple tissues by forming a heterocomplex with CXCL12, which then binds to CXCR4, to transition stem cells to G_{Alert}. I propose a model in which a highly-conserved injury signal, HMGB1, acts via a well-established maintenance signalling pathway, CXC12-CXCR4, to ultimately promote tissue regeneration (Figure 7.5). As a therapeutic target with broad clinical applicability, FR or 3S-HMGB1 could be administered as a single dose either locally or systemically at the time of injury or even up to 2 weeks beforehand. Most importantly this pathway has wide potential therapeutic benefit, as it could conceivably accelerate healing in any tissue that relies on repair from cells that express CXCR4 and can transition to G_{Alert}.

References

1. Kleinrock, M. *et al.* Medicines Use and Spending in the US: A Review of 2015 and Outlook to 2020. *IMS Inst. Healthc. Informatics* (2016).

2. British Pharmacopoeia Commission. *British Pharmacopoeia 2017*. (TSO, 2017).

3. Gratwohl, A. *et al.* One million haemopoietic stem-cell transplants: a retrospective observational study. *Lancet. Haematol.* **2,** e91-100 (2015).

4. Kuter, D. J. *et al.* Efficacy of romiplostim in patients with chronic immune thrombocytopenic purpura: a double-blind randomised controlled trial. *Lancet* **371,** 395–403 (2008).

5. Townsley, D. M. *et al.* Eltrombopag Added to Standard Immunosuppression for Aplastic Anemia. *N. Engl. J. Med.* **376,** 1540–1550 (2017).

6. Scheinberg, P. *et al.* Horse versus Rabbit Antithymocyte Globulin in Acquired Aplastic Anemia. *N. Engl. J. Med.* **365,** 430–438 (2011).

7. Toy, E. L. *et al.* Comparison of Infection-Related Hospitalization Risk and Associated Costs among Patients Receiving Sargramostim (Leukine®), Filgrastim (Neupogen®), and Pegfilgrastim (Neulasta®) for Chemotherapy-Induced Neutropenia. *Blood* **112,** (2015).

8. Safdar, A. Difficulties with fungal infections in acute myelogenous leukemia patients: immune enhancement strategies. *Oncologist* **12 Suppl 2,** 2–6 (2007).

9. Crawford, J. *et al.* Reduction by Granulocyte Colony-Stimulating Factor of Fever and Neutropenia Induced by Chemotherapy in Patients with Small-Cell Lung Cancer. *N. Engl. J. Med.* **325,** 164–170 (1991).

10. Anasetti, C. *et al.* Peripheral-Blood Stem Cells versus Bone Marrow from Unrelated Donors. *N. Engl. J. Med.* **367,** 1487–1496 (2012).

11. Greil, C. *et al.* Successful peripheral blood stem cell mobilization with a cost-efficient single

fixed-dose plerixafor schedule in poor mobilizers. *Leuk. Lymphoma* **58,** 1849–1858 (2017).

12. Singh, P. & Suresh, D. K. Clinical evaluation of GEM 21S(®) and a collagen membrane with a coronally advanced flap as a root coverage procedure in the treatment of gingival recession defects: A comparative study. *J. Indian Soc. Periodontol.* **16,** 577–83 (2012).

13. Fang, R. C. & Galiano, R. D. A review of becaplermin gel in the treatment of diabetic neuropathic foot ulcers. *Biologics* **2,** 1–12 (2008).

14. Jones, A. L. *et al.* Recombinant Human BMP-2 and Allograft Compared with Autogenous Bone Graft for Reconstruction of Diaphyseal Tibial Fractures with Cortical Defects. A Randomized, Controlled Trial. *J. Bone Jt. Surg.* **88,** 1431 (2006).

15. Zhang, H. *et al.* A Meta Analysis of Lumbar Spinal Fusion Surgery Using Bone Morphogenetic Proteins and Autologous Iliac Crest Bone Graft. *PLoS One* **9,** e97049 (2014).

16. Conway, J. D., Shabtai, L., Bauernschub, A. & Specht, S. C. BMP-7 Versus BMP-2 for the Treatment of Long Bone Nonunion. *Orthopedics* **37,** e1049–e1057 (2014).

17. Robinson, Y. *et al.* Evidence supporting the use of bone morphogenetic proteins for spinal fusion surgery. *Expert Rev. Med. Devices* **5,** 75–84 (2008).

18. Gluckman, E. *et al.* Outcome of Cord-Blood Transplantation from Related and Unrelated Donors. *N. Engl. J. Med.* **337,** 373–381 (1997).

19. Laughlin, M. J. *et al.* Outcomes after Transplantation of Cord Blood or Bone Marrow from Unrelated Donors in Adults with Leukemia. *N. Engl. J. Med.* **351,** 2265–2275 (2004).

20. Eapen, M. *et al.* Outcomes of transplantation of unrelated donor umbilical cord blood and bone marrow in children with acute leukaemia: a comparison study. *Lancet (London, England)* **369,** 1947–54 (2007).

21. Schmidt, C. Gintuit cell therapy approval signals shift at US regulator. *Nat. Biotechnol.* **30,** 479–479 (2012).

22. Zaulyanov, L. & Kirsner, R. S. A review of a bi-layered living cell treatment (Apligraf) in the treatment of venous leg ulcers and diabetic foot ulcers. *Clin. Interv. Aging* **2,** 93–8 (2007).

23. Fraser, J. K. *et al.* The Celution(®) System: Automated Processing of Adipose-Derived Regenerative Cells in a Functionally Closed System. *Adv. wound care* **3,** 38–45 (2014).

24. Hart, C. E., Loewen-Rodriguez, A. & Lessem, J. Dermagraft: Use in the Treatment of Chronic Wounds. *Adv. wound care* **1,** 138–141 (2012).

25. Munavalli, G. S., Smith, S., Maslowski, J. M. & Weiss, R. A. Successful treatment of depressed, distensible acne scars using autologous fibroblasts: a multi-site, prospective, double blind, placebo-controlled clinical trial. *Dermatol. Surg.* **39,** 1226–36 (2013).

26. Manfredini, M., Zerbinati, F., Gildone, A. & Faccini, R. Autologous chondrocyte implantation: a comparison between an open periosteal-covered and an arthroscopic matrix-guided technique. *Acta Orthop. Belg.* **73,** 207–18 (2007).

27. Bone and Joint Initiative USA. *The Burden of Musculosketal Diseases in the United States: Prevalence, Societal and Economic Cost*. (United States Bone and Joint Initiative, 2014).

28. Moran, C. J. *et al.* Translation of science to surgery. *Bone Joint J.* **92–B,** (2010).

29. Donaldson, L. J., Reckless, I. P., Scholes, S., Mindell, J. S. & Shelton, N. J. The epidemiology of fractures in England. *J. Epidemiol. Community Health* **62,** 174–80 (2008).

30. Marti, R. & Kloen, P. *Concepts and Cases in Nonunion Treatment*. (Thieme, AOTrauma, 2011).

31. Court-Brown, C. M., Bugler, K. E., Clement, N. D., Duckworth, A. D. & McQueen, M. M. The epidemiology of open fractures in adults. A 15-year review. *Injury* **43,** 891–7 (2012).

32. Court-Brown, C. M., Rimmer, S., Prakash, U. & McQueen, M. M. The epidemiology of open long bone fractures. *Injury* **29,** 529–34 (1998).

33. Harris, A. M. *et al.* Complications Following Limb-Threatening Lower Extremity Trauma. *J. Orthop. Trauma* **23,** 1–6 (2009).

34. Keating, J. F., Blachut, P. A., O'Brien, P. J. & Court-Brown, C. M. Reamed nailing of Gustilo grade-IIIB tibial fractures. *J. Bone Joint Surg. Br.* **82,** 1113–6 (2000).

35. Gopal, S., Giannoudis, P. V, Murray, A., Matthews, S. J. & Smith, R. M. The functional outcome of severe, open tibial fractures managed with early fixation and flap coverage. *J. Bone Joint Surg. Br.* **86,** 861–7 (2004).

36. Kanakaris, N. K. & Giannoudis, P. V. The health economics of the treatment of long-bone non-unions. *Injury* **38S,** S77–S84 (2007).

37. Smith, P., Ariti, C. & Bardsley, M. *Focus on hip fracture: Trends in emergency admissions for fractured neck of femur, 2001 to 2011*. (Nuffield Trust & Health Foundation, 2013).

38. Cummings, S. R. & Melton, L. J. Epidemiology and outcomes of osteoporotic fractures. *Lancet* **359,** 1761–7 (2002).

39. Siu, A. L. *et al.* Early ambulation after hip fracture: effects on function and mortality. *Arch. Intern. Med.* **166,** 766–71 (2006).

40. von Rüden, C. & Augat, P. Failure of fracture fixation in osteoporotic bone. *Injury* **47,** S3–S10 (2016).

41. Dittmer, D. K. & Teasell, R. Complications of immobilization and bed rest. Part 1: Musculoskeletal and cardiovascular complications. *Can. Fam. Physician* **39,** 1428–32, 1435–7 (1993).

42. Teasell, R. & Dittmer, D. K. Complications of immobilization and bed rest. Part 2: Other complications. *Can. Fam. Physician* **39,** 1440–2, 1445–6 (1993).

43. Lane, J. M. BMPs: why are they not in everyday use? *J. Bone Joint Surg. Am.* **83–A Suppl,** S161-3 (2001).

44. Garrison, K. R. *et al.* Bone morphogenetic protein (BMP) for fracture healing in adults. *Cochrane database Syst. Rev.* CD006950 (2010). doi:10.1002/14651858.CD006950.pub2

45. Einhorn, T. A. & Gerstenfeld, L. C. Fracture healing: mechanisms and interventions. *Nat. Rev. Rheumatol.* **11,** 45–54 (2015).

46. Kolar, P., Gaber, T., Perka, C., Duda, G. N. & Buttgereit, F. Human early fracture hematoma is characterized by inflammation and hypoxia. *Clin. Orthop. Relat. Res.* **469,** 3118–26 (2011).

47. Kolar, P. *et al.* The early fracture hematoma and its potential role in fracture healing. *Tissue Eng. Part B. Rev.* **16,** 427–34 (2010).

48. Chung, R., Cool, J. C., Scherer, M. A., Foster, B. K. & Xian, C. J. Roles of neutrophil-mediated inflammatory response in the bony repair of injured growth plate cartilage in young rats. *J. Leukoc. Biol.* **80,** 1272–80 (2006).

49. Chan, J. Upregulation of early inflammation to enhance fracture repair. (2014).

50. Xing, Z. *et al.* Multiple roles for CCR2 during fracture healing. *Dis. Model. Mech.* **3,** 451–8

51. Wu, A. C., Raggatt, L. J., Alexander, K. A. & Pettit, A. R. Unraveling macrophage contributions to bone repair. *Bonekey Rep.* **2,** 373 (2013).

52. Nicolaidou, V. Monocytes Promote Osteogenic Differentiation of Mesenchymal Stem Cells. (Imperial College London, 2011).

53. Nicolaidou, V. *et al.* Monocytes induce STAT3 activation in human mesenchymal stem cells to promote osteoblast formation. *PLoS One* **7,** e39871 (2012).

54. Wong, M. M. Effects of Cell Death and Phagocytosis on Mesenchymal Stem Cell Function. (Imperial College London, 2009).

55. Bianchi, M. E. DAMPs, PAMPs and alarmins: all we need to know about danger. *J. Leukoc. Biol.* **81,** 1–5 (2007).

56. Oppenheim, J. J., Tewary, P., de la Rosa, G. & Yang, D. Alarmins initiate host defense. *Adv. Exp. Med. Biol.* **601,** 185–94 (2007).

57. Matzinger, P. The danger model: a renewed sense of self. *Science* **296,** 301–5 (2002).

58. Oppenheim, J. J. & Yang, D. Alarmins: chemotactic activators of immune responses. *Curr. Opin. Immunol.* **17,** 359–65 (2005).

59. Bianchi, M. E. & Manfredi, A. A. Immunology. Dangers in and out. *Science* **323,** 1683–4 (2009).

60. Schiopu, A. & Cotoi, O. S. S100A8 and S100A9: DAMPs at the crossroads between innate immunity, traditional risk factors, and cardiovascular disease. *Mediators Inflamm.* **2013,** 828354 (2013).

61. Edgeworth, J., Gorman, M., Bennett, R., Freemont, P. & Hogg, N. Identification of p8,14 as a highly abundant heterodimeric calcium binding protein complex of myeloid cells. *J. Biol. Chem.* **266,** 7706–13 (1991).

62. Zreiqat, H., Howlett, C. R., Gronthos, S., Hume, D. & Geczy, C. L. S100A8/S100A9 and their association with cartilage and bone. *J. Mol. Histol.* **38,** 381–91 (2007).

63. Grevers, L. C. *et al.* S100A8 enhances osteoclastic bone resorption in vitro through activation of Toll-like receptor 4: implications for bone destruction in murine antigen-induced arthritis.

Arthritis Rheum. **63,** 1365–75 (2011).

64. Scaffidi, P., Misteli, T. & Bianchi, M. E. Release of chromatin protein HMGB1 by necrotic cells triggers inflammation. *Nature* **418,** 191–5 (2002).

65. Gardella, S. *et al.* The nuclear protein HMGB1 is secreted by monocytes via a non-classical, vesicle-mediated secretory pathway. *EMBO Rep.* **3,** 995–1001 (2002).

66. Bonaldi, T. *et al.* Monocytic cells hyperacetylate chromatin protein HMGB1 to redirect it towards secretion. *EMBO J.* **22,** 5551–60 (2003).

67. Semino, C. *et al.* The maturation potential of NK cell clones toward autologous dendritic cells correlates with HMGB1 secretion. *J. Leukoc. Biol.* **81,** 92–9 (2007).

68. Degryse, B. *et al.* The high mobility group (HMG) boxes of the nuclear protein HMG1 induce chemotaxis and cytoskeleton reorganization in rat smooth muscle cells. *J. Cell Biol.* **152,** 1197–206 (2001).

69. Straino, S. *et al.* High-mobility group box 1 protein in human and murine skin: involvement in wound healing. *J. Invest. Dermatol.* **128,** 1545–53 (2008).

70. Limana, F. *et al.* Exogenous high-mobility group box 1 protein induces myocardial regeneration after infarction via enhanced cardiac C-kit+ cell proliferation and differentiation. *Circ. Res.* **97,** e73-83 (2005).

71. Charoonpatrapong, K. *et al.* HMGB1 expression and release by bone cells. *J. Cell. Physiol.* **207,** 480–90 (2006).

72. Yang, J. *et al.* HMGB1 is a bone-active cytokine. *J. Cell. Physiol.* **214,** 730–9 (2008).

73. Bidwell, J. P., Yang, J. & Robling, A. G. Is HMGB1 an osteocyte alarmin? *J. Cell. Biochem.* **103,** 1671–80 (2008).

74. Palumbo, R. *et al.* Extracellular HMGB1, a signal of tissue damage, induces mesoangioblast migration and proliferation. *J. Cell Biol.* **164,** 441–9 (2004).

75. Mitola, S. *et al.* Cutting edge: extracellular high mobility group box-1 protein is a proangiogenic cytokine. *J. Immunol.* **176,** 12–5 (2006).

76. Schlueter, C. *et al.* Angiogenetic signaling through hypoxia: HMGB1: an angiogenetic switch molecule. *Am. J. Pathol.* **166,** 1259–63 (2005).

77. Yang, S., Xu, L., Yang, T. & Wang, F. High-mobility group box-1 and its role in angiogenesis. *J. Leukoc. Biol.* **95,** 563–74 (2014).

78. Sachdev, U. *et al.* High mobility group box 1 promotes endothelial cell angiogenic behavior in vitro and improves muscle perfusion in vivo in response to ischemic injury. *J. Vasc. Surg.* **55,** 180–191 (2012).

79. Merenmies, J., Pihlaskari, R., Laitinen, J., Wartiovaara, J. & Rauvala, H. 30-kDa heparin-binding protein of brain (amphoterin) involved in neurite outgrowth. Amino acid sequence and localization in the filopodia of the advancing plasma membrane. *J. Biol. Chem.* **266,** 16722–9 (1991).

80. Salmivirta, M., Rauvala, H., Elenius, K. & Jalkanen, M. Neurite growth-promoting protein (amphoterin, p30) binds syndecan. *Exp. Cell Res.* **200,** 444–51 (1992).

81. Taniguchi, N. *et al.* Stage-specific secretion of HMGB1 in cartilage regulates endochondral ossification. *Mol. Cell. Biol.* **27,** 5650–63 (2007).

82. Yamoah, K. *et al.* High-mobility group box proteins modulate tumor necrosis factor-alpha expression in osteoclastogenesis via a novel deoxyribonucleic acid sequence. *Mol. Endocrinol.* **22,** 1141–53 (2008).

83. Zhou, Z. *et al.* HMGB1 regulates RANKL-induced osteoclastogenesis in a manner dependent on RAGE. *J. Bone Miner. Res.* **23,** 1084–96 (2008).

84. Meng, E. *et al.* High mobility group box 1 protein inhibits the proliferation of human mesenchymal stem cells and promotes their migration and differentiation along osteoblastic pathway. *Stem Cells Dev.* **17,** 805–13 (2008).

85. Lotze, M. T. & Tracey, K. J. High-mobility group box 1 protein (HMGB1): nuclear weapon in the immune arsenal. *Nat. Rev. Immunol.* **5,** 331–42 (2005).

86. Venereau, E. *et al.* Mutually exclusive redox forms of HMGB1 promote cell recruitment or proinflammatory cytokine release. *J. Exp. Med.* **209,** 1519–28 (2012).

87. Magna, M. & Pisetsky, D. S. The Role of HMGB1 in the Pathogenesis of Inflammatory and Autoimmune Diseases. *Mol. Med.* **20,** 138–46 (2014).

88. Schiraldi, M. *et al.* HMGB1 promotes recruitment of inflammatory cells to damaged tissues by forming a complex with CXCL12 and signaling via CXCR4. *J. Exp. Med.* **209,** 551–63 (2012).

89. Seaberg, R. M. & van der Kooy, D. Stem and progenitor cells: the premature desertion of rigorous definitions. *Trends Neurosci.* **26,** 125–131 (2003).

90. Guimarães-Camboa, N. *et al.* Pericytes of Multiple Organs Do Not Behave as Mesenchymal Stem Cells In Vivo. *Cell Stem Cell* **20,** 345–359.e5 (2017).

91. Fayaz, H. C. *et al.* The role of stem cells in fracture healing and nonunion. *Int. Orthop.* **35,** 1587–97 (2011).

92. Wang, X. *et al.* Role of mesenchymal stem cells in bone regeneration and fracture repair: a review. *Int. Orthop.* **37,** 2491–8 (2013).

93. Gomez-Barrena, E. *et al.* Bone fracture healing: Cell therapy in delayed unions and

nonunions. *Bone* **70,** 93–101 (2015).

94. Fischer, U. M. *et al.* Pulmonary Passage is a Major Obstacle for Intravenous Stem Cell Delivery: The Pulmonary First-Pass Effect. *Stem Cells Dev.* **18,** 683–692 (2009).

95. Eggenhofer, E., Luk, F., Dahlke, M. H. & Hoogduijn, M. J. The life and fate of mesenchymal stem cells. *Front. Immunol.* **5,** 148 (2014).

96. Loebinger, M. R., Eddaoudi, A., Davies, D. & Janes, S. M. Mesenchymal Stem Cell Delivery of TRAIL Can Eliminate Metastatic Cancer. *Cancer Res.* **69,** 4134–4142 (2009).

97. Sage, E. K., Thakrar, R. M. & Janes, S. M. Genetically modified mesenchymal stromal cells in cancer therapy. *Cytotherapy* **18,** 1435–1445 (2016).

98. Ross, D. T. *et al.* Systematic variation in gene expression patterns in human cancer cell lines. *Nat. Genet.* **24,** 227–35 (2000).

99. Masters, J. R. W. Human cancer cell lines: fact and fantasy. *Nat. Rev. Mol. Cell Biol.* **1,** 233–236 (2000).

100. Birgersdotter, A., Sandberg, R. & Ernberg, I. Gene expression perturbation in vitro—A growing case for three-dimensional (3D) culture systems. *Semin. Cancer Biol.* **15,** 405–412 (2005).

101. Chan, C. K. F. *et al.* Identification and Specification of the Mouse Skeletal Stem Cell. *Cell* **160,** 285–298 (2015).

102. Worthley, D. L. *et al.* Gremlin 1 identifies a skeletal stem cell with bone, cartilage, and reticular stromal potential. *Cell* **160,** 269–84 (2015).

103. Kassem, M. & Bianco, P. Skeletal Stem Cells in Space and Time. *Cell* **160,** 17–19 (2015).

104. Tevlin, R. *et al.* Pharmacological rescue of diabetic skeletal stem cell niches. *Sci. Transl. Med.*

9, eaag2809 (2017).

105. Chan, C. K. F. *et al.* Clonal precursor of bone, cartilage, and hematopoietic niche stromal cells. *Proc. Natl. Acad. Sci. U. S. A.* **110,** 12643–8 (2013).

106. Marecic, O. *et al.* Identification and characterization of an injury-induced skeletal progenitor. *Proc. Natl. Acad. Sci. U. S. A.* **112,** 9920–5 (2015).

107. Harry, L. E. *et al.* Comparison of the healing of open tibial fractures covered with either muscle or fasciocutaneous tissue in a murine model. *J. Orthop. Res.* **26,** 1238–1244 (2008).

108. Glass, G. E. *et al.* TNF-alpha promotes fracture repair by augmenting the recruitment and differentiation of muscle-derived stromal cells. *Proc. Natl. Acad. Sci. U. S. A.* **108,** 1585–90 (2011).

109. Chan, J. K. *et al.* Low-dose TNF augments fracture healing in normal and osteoporotic bone by up-regulating the innate immune response. *EMBO Mol. Med.* **7,** 547–561 (2015).

110. Rontgen, V. *et al.* Fracture healing in mice under controlled rigid and flexible conditions using an adjustable external fixator. *J. Orthop. Res.* **28,** 1456–1462 (2010).

111. Zwingenberger, S. *et al.* Establishment of a femoral critical-size bone defect model in immunodeficient mice. *J. Surg. Res.* **181,** e7–e14 (2013).

112. Morgan, E. F. *et al.* Micro-computed tomography assessment of fracture healing: relationships among callus structure, composition, and mechanical function. *Bone* **44,** 335–44 (2009).

113. O'Neill, K. R. *et al.* Micro-computed tomography assessment of the progression of fracture healing in mice. *Bone* **50,** 1357–1367 (2012).

114. Liu, L., Cheung, T. H., Charville, G. W. & Rando, T. A. Isolation of skeletal muscle stem cells by

fluorescence-activated cell sorting. *Nat. Protoc.* **10,** 1612–1624 (2015).

115. Wilson, A. *et al.* Hematopoietic Stem Cells Reversibly Switch from Dormancy to Self-Renewal during Homeostasis and Repair. *Cell* **135,** 1118–1129 (2008).

116. Peytour, Y. *et al.* Obtaining of CD34+ cells from healthy blood donors: development of a rapid and efficient procedure using leukoreduction filters. *Transfusion* **50,** 2152–2157 (2010).

117. Rodgers, J. T. *et al.* mTORC1 controls the adaptive transition of quiescent stem cells from G0 to G(Alert). *Nature* **510,** 393–6 (2014).

118. Szade, K., Zukowska, M., Jozkowicz, A. & Dulak, J. Measuring ATP Concentration in a Small Number of Murine Hematopoietic Stem Cells. in *Methods in molecular biology (Clifton, N.J.)* **1516,** 205–217 (2016).

119. Schindelin, J. *et al.* Fiji: an open-source platform for biological-image analysis. *Nat. Methods* **9,** 676–682 (2012).

120. Moore, M. A. & Warren, D. J. Synergy of interleukin 1 and granulocyte colony-stimulating factor: in vivo stimulation of stem-cell recovery and hematopoietic regeneration following 5-fluorouracil treatment of mice. *Proc. Natl. Acad. Sci. U. S. A.* **84,** 7134–8 (1987).

121. Busch, K. *et al.* Fundamental properties of unperturbed haematopoiesis from stem cells in vivo. *Nature* **518,** 542–6 (2015).

122. Hardy, D. *et al.* Comparative Study of Injury Models for Studying Muscle Regeneration in Mice. *PLoS One* **11,** e0147198 (2016).

123. Yang, H. *et al.* Redox modification of cysteine residues regulates the cytokine activity of high mobility group box-1 (HMGB1). *Mol. Med.* **18,** 250–9 (2012).

124. Zhou, L. *et al.* Impact of human granulocyte and monocyte isolation procedures on functional

studies. *Clin. Vaccine Immunol.* **19,** 1065–74 (2012).

125. Delirezh, N., Shojaeefar, E., Parvin, P. & Asadi, B. Comparison the effects of two monocyte isolation methods, plastic adherence and magnetic activated cell sorting methods, on phagocytic activity of generated dendritic cells. *Cell J.* **15,** 218–23 (2013).

126. Prins, H.-J. *et al.* In vitro induction of alkaline phosphatase levels predicts in vivo bone forming capacity of human bone marrow stromal cells. *Stem Cell Res.* **12,** 428–440 (2014).

127. Cho, T.-J., Gerstenfeld, L. C. & Einhorn, T. A. Differential Temporal Expression of Members of the Transforming Growth Factor β Superfamily During Murine Fracture Healing. *J. Bone Miner. Res.* **17,** 513–520 (2002).

128. Chan, J. K. *et al.* Alarmins: awaiting a clinical response. *J. Clin. Invest.* **122,** 2711–9 (2012).

129. Li, Q., Yu, B. & Yang, P. Hypoxia-induced HMGB1 in would tissues promotes the osteoblast cell proliferation via activating ERK/JNK signaling. *Int. J. Clin. Exp. Med.* **8,** 15087–97 (2015).

130. Granero-Moltó, F. *et al.* Regenerative effects of transplanted mesenchymal stem cells in fracture healing. *Stem Cells* **27,** 1887–98 (2009).

131. Undale, A. *et al.* Induction of fracture repair by mesenchymal cells derived from human embryonic stem cells or bone marrow. *J. Orthop. Res.* **29,** 1804–11 (2011).

132. Reinke, S. *et al.* Terminally Differentiated CD8+ T Cells Negatively Affect Bone Regeneration in Humans. *Sci. Transl. Med.* **5,** (2013).

133. Histing, T. *et al.* Small animal bone healing models: Standards, tips, and pitfalls results of a consensus meeting. *Bone* **49,** 591–599 (2011).

134. Gregor, T. *et al.* Correlating Micro-CT Imaging with Quantitative Histology. in *Injury and Skeletal Biomechanics* (InTech, 2012). doi:10.5772/48680

135. Particelli, F. *et al.* A comparison between micro-CT and histology for the evaluation of cortical bone: effect of polymethylmethacrylate embedding on structural parameters. *J. Microsc.* **245,** 302–310 (2012).

136. Giannoudis, P. V, Einhorn, T. a & Marsh, D. Fracture healing: the diamond concept. *Injury* **38 Suppl 4,** S3-6 (2007).

137. Terrando, N. *et al.* Tumor necrosis factor-alpha triggers a cytokine cascade yielding postoperative cognitive decline. *Proc. Natl. Acad. Sci. U. S. A.* **107,** 20518–22 (2010).

138. Yanai, H. *et al.* Conditional ablation of HMGB1 in mice reveals its protective function against endotoxemia and bacterial infection. *Proc. Natl. Acad. Sci. U. S. A.* **110,** 20699–704 (2013).

139. Ventura, A. *et al.* Restoration of p53 function leads to tumour regression in vivo. *Nature* **445,** 661–665 (2007).

140. Dormoy-Raclet, V. *et al.* HuR and miR-1192 regulate myogenesis by modulating the translation of HMGB1 mRNA. *Nat. Commun.* **4,** 2388 (2013).

141. Mollica, L. *et al.* Glycyrrhizin binds to high-mobility group box 1 protein and inhibits its cytokine activities. *Chem. Biol.* **14,** 431–41 (2007).

142. De Clercq, E. The AMD3100 story: The path to the discovery of a stem cell mobilizer (Mozobil). *Biochem. Pharmacol.* **77,** 1655–1664 (2009).

143. Kawakami, Y. *et al.* SDF-1/CXCR4 Axis in Tie2-Lineage Cells Including Endothelial Progenitor Cells Contributes to Bone Fracture Healing. *J. Bone Miner. Res.* **30,** 95–105 (2015).

144. Morrison, S. J. & Kimble, J. Asymmetric and symmetric stem-cell divisions in development and cancer. *Nature* **441,** 1068–1074 (2006).

145. Knoblich, J. A. Mechanisms of Asymmetric Stem Cell Division. *Cell* **132,** 583–597 (2008).

146. Lechler, T. & Fuchs, E. Asymmetric cell divisions promote stratification and differentiation of mammalian skin. *Nature* **437,** 275–80 (2005).

147. Morrison, S. J., Wright, D. E. & Weissman, I. L. Cyclophosphamide/granulocyte colony-stimulating factor induces hematopoietic stem cells to proliferate prior to mobilization. *Proc. Natl. Acad. Sci. U. S. A.* **94,** 1908–13 (1997).

148. Clayton, E. *et al.* A single type of progenitor cell maintains normal epidermis. *Nature* **446,** 185–189 (2007).

149. Mascré, G. *et al.* Distinct contribution of stem and progenitor cells to epidermal maintenance. *Nature* **489,** 257–262 (2012).

150. Lim, X. *et al.* Interfollicular Epidermal Stem Cells Self-Renew via Autocrine Wnt Signaling. *Science (80-.).* **342,** 1226–1230 (2013).

151. Yang, J., Plikus, M. V & Komarova, N. L. The Role of Symmetric Stem Cell Divisions in Tissue Homeostasis. *PLoS Comput. Biol.* **11,** e1004629 (2015).

152. Peled, A. *et al.* Dependence of human stem cell engraftment and repopulation of NOD/SCID mice on CXCR4. *Science (80-.).* **283,** 845–8 (1999).

153. Sugiyama, T., Kohara, H., Noda, M. & Nagasawa, T. Maintenance of the Hematopoietic Stem Cell Pool by CXCL12-CXCR4 Chemokine Signaling in Bone Marrow Stromal Cell Niches. *Immunity* **25,** 977–988 (2006).

154. Nie, Y., Han, Y.-C. & Zou, Y.-R. CXCR4 is required for the quiescence of primitive hematopoietic cells. *J. Exp. Med.* **205,** 777–83 (2008).

155. Tzeng, Y.-S. *et al.* Loss of Cxcl12/Sdf-1 in adult mice decreases the quiescent state of hematopoietic stem/progenitor cells and alters the pattern of hematopoietic regeneration

after myelosuppression. *Blood* **117,** 429–439 (2011).

156. Ding, L. & Morrison, S. J. Haematopoietic stem cells and early lymphoid progenitors occupy distinct bone marrow niches. *Nature* **495,** 231–235 (2013).

157. Greenbaum, A. *et al.* CXCL12 in early mesenchymal progenitors is required for haematopoietic stem-cell maintenance. *Nature* **495,** 227–30 (2013).

158. Rocheteau, P., Gayraud-Morel, B., Siegl-Cachedenier, I., Blasco, M. A. & Tajbakhsh, S. A Subpopulation of Adult Skeletal Muscle Stem Cells Retains All Template DNA Strands after Cell Division. *Cell* **148,** 112–125 (2012).

159. Joseph, J. & Dyson, M. The effect of abdominal wounding on the rate of tissue regeneration. *Experientia* **26,** 66–67 (1970).

160. Davis, T. A., Longcor, J. D., Hicok, K. C. & Lennon, G. G. Prior injury accelerates subsequent wound closure in a mouse model of regeneration. *Cell Tissue Res.* **320,** 417–426 (2005).

161. Maesner, C. C., Almada, A. E. & Wagers, A. J. Established cell surface markers efficiently isolate highly overlapping populations of skeletal muscle satellite cells by fluorescence-activated cell sorting. *Skelet. Muscle* **6,** 35 (2016).

162. Holstein, J. H. *et al.* Rapamycin affects early fracture healing in mice. *Br. J. Pharmacol.* **154,** 1055–1062 (2008).

163. Vasyutina, E. *et al.* CXCR4 and Gab1 cooperate to control the development of migrating muscle progenitor cells. *Genes Dev.* **19,** 2187–98 (2005).

164. Webster, M. T. *et al.* c-MET Regulates Myoblast Motility and Myocyte Fusion during Adult Skeletal Muscle Regeneration. *PLoS One* **8,** e81757 (2013).

165. Holland, J. D. *et al.* Combined Wnt/β-Catenin, Met, and CXCL12/CXCR4 Signals Characterize

Basal Breast Cancer and Predict Disease Outcome. *Cell Rep.* **5,** 1214–1227 (2013).

166. Huang, S. *et al.* HGF-Induced PKCζ Activation Increases Functional CXCR4 Expression in Human Breast Cancer Cells. *PLoS One* **7,** e29124 (2012).

167. Kollet, O. *et al.* HGF, SDF-1, and MMP-9 are involved in stress-induced human CD34+ stem cell recruitment to the liver. *J. Clin. Invest.* **112,** 160–169 (2003).

168. Lyman, G. H. *et al.* Risk of mortality in patients with cancer who experience febrile neutropenia. *Cancer* **116,** 5555–5563 (2010).

169. Wood, A. J. J., Lieschke, G. J. & Burgess, A. W. Granulocyte Colony-Stimulating Factor and Granulocyte-Macrophage Colony-Stimulating Factor. *N. Engl. J. Med.* **327,** 28–35 (1992).

170. Lok, C. Cachexia: The last illness. *Nature* **528,** 182–183 (2015).

171. Argilés, J. M., Busquets, S., Stemmler, B. & López-Soriano, F. J. Cancer cachexia: understanding the molecular basis. *Nat. Rev. Cancer* **14,** 754–762 (2014).

172. Tisdale, M. J. Cachexia in cancer patients. *Nat. Rev. Cancer* **2,** 862–871 (2002).

173. Lee, P., Regenbogen, S. & Gawande, A. A. How many surgical procedures will Americans experience in an average lifetime?: Evidence from three states. in *How many surgical procedures will Americans experience in an average lifetime?: Evidence from three states* (55th Annual Meeting of the Massachusetts Chapter of the American College of Surgeons, 2008).

174. Longley, D. B., Harkin, D. P. & Johnston, P. G. 5-Fluorouracil: mechanisms of action and clinical strategies. *Nat. Rev. Cancer* **3,** 330–338 (2003).

175. Duda, G. N. *et al.* Changing the Mindset in Life Sciences Toward Translation: A Consensus. *Sci. Transl. Med.* **6,** 264cm12-264cm12 (2014).

176. Rodgers, J. T., Schroeder, M. D., Ma, C. & Rando, T. A. HGFA Is an Injury-Regulated Systemic Factor that Induces the Transition of Stem Cells into G Alert. *Cell Rep.* **19,** 479–486 (2017).

177. Allen, R. E., Sheehan, S. M., Taylor, R. G., Kendall, T. L. & Rice, G. M. Hepatocyte growth factor activates quiescent skeletal muscle satellite cells in vitro. *J. Cell. Physiol.* **165,** 307–312 (1995).

178. Tatsumi, R., Anderson, J. E., Nevoret, C. J., Halevy, O. & Allen, R. E. HGF/SF Is Present in Normal Adult Skeletal Muscle and Is Capable of Activating Satellite Cells. *Dev. Biol.* **194,** 114–128 (1998).

179. Saxton, R. A. & Sabatini, D. M. mTOR Signaling in Growth, Metabolism, and Disease. *Cell* **169,** 361–371 (2017).

180. Gattinoni, L., Speiser, D. E., Lichterfeld, M. & Bonini, C. T memory stem cells in health and disease. *Nat. Med.* **23,** 18–27 (2017).

181. Cheung, T. H. & Rando, T. A. Molecular regulation of stem cell quiescence. *Nat. Rev. Mol. Cell Biol.* **14,** 329–40 (2013).

182. Murray, C. J. L. & Lopez, A. D. Measuring the Global Burden of Disease. *N. Engl. J. Med.* **369,** 448–457 (2013).

183. Ndugga, N. *et al.* Disparities between research attention and burden in liver diseases: implications on uneven advances in pharmacological therapies in Europe and the USA. *BMJ Open* **7,** e013620 (2017).

184. Demicheli, R., Retsky, M. W., Hrushesky, W. J. M., Baum, M. & Gukas, I. D. The effects of surgery on tumor growth: a century of investigations. *Ann. Oncol.* **19,** 1821–1828 (2008).

185. Sosa, M. S., Bragado, P. & Aguirre-Ghiso, J. A. Mechanisms of disseminated cancer cell dormancy: an awakening field. *Nat. Rev. Cancer* **14,** 611–622 (2014).

186. Meacham, C. E. & Morrison, S. J. Tumour heterogeneity and cancer cell plasticity. *Nature* **501,** 328–337 (2013).

187. Eide, C. A. & Druker, B. J. Understanding cancer from the stem cells up. *Nat. Med.* **23,** 656–657 (2017).

188. Massagué, J. & Obenauf, A. C. Metastatic colonization by circulating tumour cells. *Nature* **529,** 298–306 (2016).